PMFSEL REPORT NO. 96-2
February, 1996

CORROSION PERFORMANCE OF A SECOND-GENERATION HIGH RATIO ZINC SILICATE COATING IN A REINFORCED CONCRETE ENVIRONMENT

by

Jeffrey J. Mitchell, Enrique Vaca-Cortes,
James O. Jirsa, and Ramon L. Carrasquillo

REPORT ON SECOND PHASE OF RESEARCH
SPONSORED BY

INORGANIC COATINGS, INC.

PHIL M. FERGUSON STRUCTURAL ENGINEERING LABORATORY
Department of Civil Engineering / Bureau of Engineering Research
The University of Texas at Austin

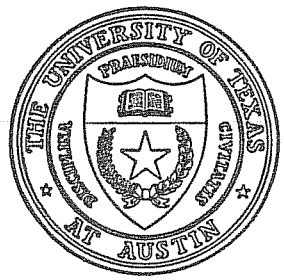

PMFSEL REPORT NO. 96-2
February, 1996

CORROSION PERFORMANCE OF A SECOND-GENERATION HIGH RATIO ZINC SILICATE COATING IN A REINFORCED CONCRETE ENVIRONMENT

by

Jeffrey J. Mitchell, Enrique Vaca-Cortes,
James O. Jirsa, and Ramon L. Carrasquillo

REPORT ON SECOND PHASE OF RESEARCH SPONSORED BY

INORGANIC COATINGS, INC.

PHIL M. FERGUSON STRUCTURAL ENGINEERING LABORATORY
Department of Civil Engineering / Bureau of Engineering Research
The University of Texas at Austin

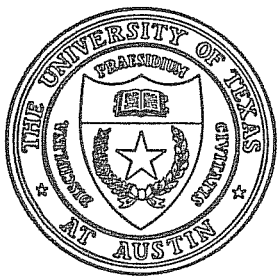

PMFSEL REPORT NO. 96-2
February, 1996

CORROSION PERFORMANCE OF A SECOND-GENERATION HIGH RATIO ZINC SILICATE COATING IN A REINFORCED CONCRETE ENVIRONMENT

by

Jeffrey J. Mitchell, Enrique Vaca-Cortes,
James O. Jirsa, and Ramon L. Carrasquillo

REPORT ON SECOND PHASE OF RESEARCH
SPONSORED BY

INORGANIC COATINGS, INC.

PHIL M. FERGUSON STRUCTURAL ENGINEERING LABORATORY
Department of Civil Engineering / Bureau of Engineering Research
The University of Texas at Austin

ABSTRACT

The macrocell method was used to evaluate a high ratio zinc silicate coating for corrosion performance on concrete reinforcing steel. Twenty-seven macrocells were constructed and subjected to cyclical chloride exposure for two years. The variables investigated were the effects of coating damage, the effects of coating the cathode steel, and two repair techniques. For comparison, galvanized steel was used in six of the specimens, and epoxy-coated steel was used in three specimens.

It was found that the zinc silicate coating provided good corrosion protection throughout the period of exposure when the coating was applied to all the steel in the specimens. Substantial levels of corrosion were observed when only one layer of the steel was coated. The zinc silicate coating performed well, especially when any damage to the coating was repaired prior to placement of the concrete.

TABLE OF CONTENTS

LIST OF FIGURES

LIST OF TABLES

CHAPTER ONE

INTRODUCTION

1.1 BACKGROUND

The problem of steel corrosion in concrete is a significant issue facing the construction industry today. The corrosion of reinforcing bars affects an enormous number of bridges, roadways, and parking garages in northern regions, as well as many coastal structures. In one study,[26] twenty-two bridge decks were visually inspected, and 40% of the decks containing untreated reinforcing bars were in the initial stages of deterioration. In another investigation,[3] 249 bridges were inspected. Twenty-five percent of the decks showed potholes and fracture patterns indicative of corrosion. None of the 249 bridges had been through more than four winter seasons. Clearly, corrosion is a major problem in reinforced concrete structures and merits extensive attention.

Corrosion damage manifests itself in the form of progressive deterioration. As the steel corrodes, chemical products are produced that take up more than twice the volume of the original material. The volume increase around the bars creates expansive pressures on the order of 5000 psi. Cracks then begin to form in the concrete, allowing additional corrosive agents to gain access to the steel and accelerating deterioration. Fracture planes form, rust-colored stains appear on the surface of the concrete, larger pieces of concrete begin to spall away, and the structures become unserviceable. These problems are alarmingly acute in places where deicing salts are applied to roadways and in marine environments (particularly in the splash zones).

Although there are numerous corrosion mechanisms that may occur, the overall process can be summarized quite simply. There must be a liquid environment, a material to be corroded, and a catalyst that consumes electrons. In the case of steel in concrete, water, oxygen, steel, and chloride ions usually provide the necessary ingredients. In a typical corrosion cell, water, oxygen and chloride ions diffuse into the concrete to the depth of the reinforcing steel. The chloride ions depassivate the steel, iron atoms dissolve into solution, electrons are liberated, oxygen consumes the electrons by forming OH^-, and the dissolved iron ions recombine to form corrosion produces such as Fe_3O_4 and Fe_2O_3. This process requires that water, steel, oxygen, and chloride ions all be present in the concrete; the corrosion of steel in concrete will almost never take place in the absence of any one of these materials, unless carbonation or cracking produces a change in the pH of the pore water.

A number of different corrosion protection systems have been developed to curtail the corrosion of steel in concrete. Traditional protection schemes include the use of high-quality concrete and adequate cover, the installation of water and ion barriers, impressed cathodic current, and the coating of the reinforcing steel. The work reported here focuses on sacrificial coatings for reinforcing steel.

One type of coating system uses an electrochemically active metal — typically zinc — to coat the steel. The zinc coatings both provide a barrier against water and chlorides, and galvanically protect the steel surface. Zinc is used primarily for economic reasons; zinc is cheaper than magnesium and other

sacrificial metals. Zinc also remains passive to lower pHs than steel, and is several times more resistant than steel to corrosion in the presence of chlorides.

Zinc may either be applied to steel in the form of hot-dip galvanizing, or in the form of a zinc-based paint. Considerable research has been done in the last 50 years in the development of zinc-based paints. The latest zinc coatings, the high ratio inorganic zinc silicates, are an outgrowth of NASA technology, devised to protect rocket launchers from corrosion.

The high ratio zinc silicates are water-based and self-curing, combining the simplicity of one coat with the environmental benefits of water-based solvent, instead of a VOC-based solvent (volatile organic compound).[19] The zinc silicates function by binding metallic zinc to the steel surface in an inorganic polymer matrix. After curing, the coating is hard, insoluble, and can be recoated. The presence of zinc in the coating provides a measure of galvanic protection for the steel. Exposure tests have demonstrated this protection over the last 14 years in severe chloride environments.

It remains to be demonstrated, however, that the high ratio zinc silicate coatings will perform well in a high pH, resistive, concrete environment. This report deals with research conducted at The University of Texas at Austin to investigate the use of high ratio zinc silicates in reinforced concrete for the control of reinforcing steel corrosion.

1.2 OBJECTIVES

A series of experiments were designed to examine the corrosion behavior of a specific high ratio zinc silicate coating in a concrete environment. Previous tests carried out at The University of Texas at Austin found that a "first-generation" zinc silicate coating did not provide effective corrosion protection.[12] The goal of the present experiments is to determine whether a reformulated (second-generation) coating shows an improvement over the previous coating, and whether the improvement is substantial enough to make the new formulation a viable product for reducing the corrosion of steel in concrete.

1.3 SCOPE

The experiments reported here closely followed the same procedures used to evaluate the first formulation. The macrocell method was used to monitor corrosion behavior in a forced corrosion environment. The macrocells consisted of blocks of concrete cast with fixed amounts of steel in top and bottom mats. Instrumentation was set up to weekly monitor the potential differences between the steel layers.

Salt solution was ponded on the top of the macrocells in 14-day, wet/dry cycles. The top steel became exposed to chlorides in solution and was forced to become the anode in an electrochemical corrosion cell. Electrons liberated at the anode traveled through a conductor to the bottom layer of steel, producing the corrosion currents that were monitored.

Separate concrete chloride cells were also constructed and subjected to the same exposure cycle in order to monitor the diffusion of chloride ions into the concrete. Drilled samples of concrete dust were taken from specified depths on a monthly basis and analyzed for chloride concentration.

Nine different coating combinations were used on the steel. The primary coating variables investigated were the effects of damage to high ratio zinc silicate coating prior to concrete placement, the

effectiveness of two different repair techniques, and the effects of using coated, rather than uncoated cathodes.

1.4 Analysis of Results

The macrocells provided three types of data for analysis. First, the potential difference readings were used to calculate instantaneous corrosion current and charge flux magnitudes. Corrosion current vs. time plots were developed to illustrate the theoretical corrosion activity in the macrocells throughout the experiment, and charge flux vs. time plots were created to show the theoretical cumulative damage levels.

Second, the theoretical data were compared with visual observation of the corrosion damage. Macrocells were opened on two occasions, permitting corrosion damage levels and locations to be photographed and described.

Finally, chloride concentration depth profiles from the chloride cells were examined over time and compared to concentration profiles obtained from the macrocells during the autopsies. These data allowed the penetration of the chlorides into the concrete to be monitored for magnitude and consistency.

CHAPTER 2

CORROSION OF STEEL IN CONCRETE

2.1 MECHANISM OF GENERAL CORROSION

Corrosion is an electrochemical process requiring two reactions - the anodic and cathodic reactions. These two reactions are sequential, but both must be present for the process of corrosion to be sustained.

The anodic reaction provides the electrons needed in the electrochemical process. A metal atom dissolves into solution as a positive ion, liberating one or more electrons. These electrons then travel through the material by conduction to the location of the cathodic reaction. The distance of travel for the electrons may be extremely small (on the order of microns), or comparatively large (on the order of meters).

At the cathode, a second reaction takes place that consumes the electrons provided by the anodic reaction. An aqueous, ionic species combines with electrons on the surface of the conductor to form a new compound.

There are many possible forms of anodic and cathodic reactions. The anodic reaction is the simplest: metal atoms dissolve into solution. In the case of iron and steel, it is the iron atom that participates in this reaction. The reaction is given below:

$$Fe \Leftrightarrow Fe^{++} + 2e^{-} \qquad (1)$$

Or, more generally, for the case of any metal, M:

$$M \Leftrightarrow M^{+n} + ne^{-} \qquad (2)$$

The cathodic reaction can take a variety of forms. For example, in acidic environments, H^{+} ions in solution combine with free electrons to form hydrogen gas. In other environments, metal ions or metal ion complexes with high valence charges combine with electrons to form ions with lower valences. In the case of steel or iron in aqueous environments, dissolved oxygen and water molecules may also combine with free electrons to form OH^{-} ions in the reaction: [10]

$$O_2 + 4e^{-} + 2H_2O \Leftrightarrow 4OH^{-} \qquad (3)$$

Figure 2.1 illustrates this iron-oxygen-water chain of reactions, in which the iron corrodes to form Fe^{++} and the liberated electrons combine with water to produce OH^{-}. Hydroxide ions and aqueous iron ions are therefore the products of the anodic and cathodic reactions.

It is important to note that oxygen does not participate in the anodic reaction - oxygen is required only at the cathode to participate in the reduction described by formula 3. In fact, the presence of oxygen at the anode can obstruct corrosion by retarding the dissolution rate of iron by forming surface oxides. [9]

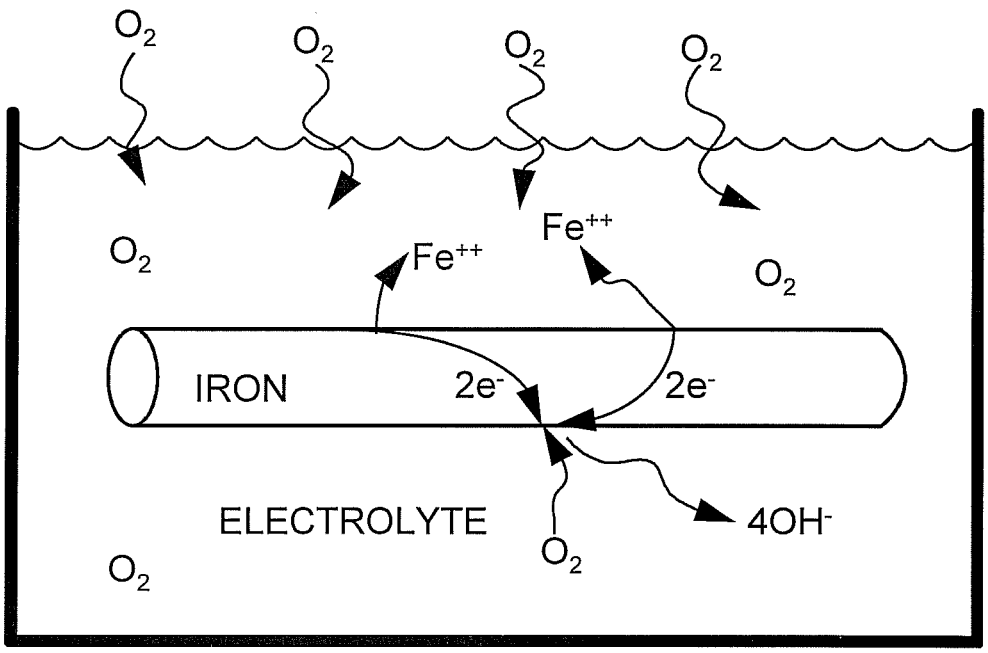

Figure 2- 1 Anodic and cathodic reactions in the general corrosion of iron

In addition to the anodic and cathodic reactions, subsequent reactions may take place involving the aqueous iron ions, producing the corrosion products commonly associated with rust. A possible chain of reactions is:

$$2Fe^{+2} + 4OH^{-} \Leftrightarrow 2Fe(OH)_2 \quad (4)$$

$$2Fe(OH)_2 \Leftrightarrow H_2O + 1/2O_2 \Leftrightarrow 2Fe(OH)_3 \quad (5)$$

Three more factors must also be included in the discussion of general corrosion: the electrolyte, material resistance, and potential difference. First, there must be an electrolyte linking the anode and the cathode in order to sustain corrosion. The electrolyte provides the environment for the corrosion process by acting as the medium for ionic diffusion. Metal ions require a fluid environment for dissolution, and ionic corrosion products produced at the cathode must be able diffuse back toward the anode. The electrolyte therefore provides the corrosion medium and the necessary link between the cathode and the anode.

The effectiveness of the electrolyte as a corrosion-facilitator is a strong function of the number of ions in solution. As ionic concentrations increase, corrosion rates also tend to increase. This effect stems from the fact that more corrosive species tend to be present in high concentration environments, and ionic diffusion rates are increased. As a corollary to this phenomenon, the high concentration electrolytes have lower electrical resistance, further aiding corrosion.

The resistivity of the corroding material is also of great importance. The anodic and cathodic reactions do not take place in isolation; electrons produced at the anode must have a way to get to the site of the cathodic reaction. There must therefore be a path of electrical conductance between the anode and the

cathode. If there is no link between the reaction sites, corrosion will not take place. For this reason, it is generally observed that substances that corrode are low-resistance materials.

A final piece in the puzzle of general corrosion is electrical potential. Electrical "force" is required to move the electrons generated at the anode to the cathode. This "force" is provided by a potential difference between the anode and cathode, with the anode at a greater negative potential. Potential differences may be caused by interaction between the environment and the material, metallurgical factors, or applied currents. [11]

To summarize, several key ingredients must be present for general corrosion to occur. There must be corroding material capable of supplying electrons, a substance that desires to consume electrons, an electrolyte that brings the "electron-hungry" substance into contact with the corroding material, and a path of electric conductance between anodic and cathodic sites. In the case of steel and iron corrosion in aqueous environments, equations 1 and 3 describe the typical anodic and cathodic reactions. Equations 4 and 5 describe subsequent reactions that produce the commonly observed iron corrosion products.

2.2 The Effects of Passivation

The corrosion of many metals is also influenced by a phenomenon known as material passivation. Metals such as titanium, stainless steel, iron and carbon steels react to form surface oxides that retard or prevent the dissociation of metal ions into solution. Passivation takes place under environmental conditions that vary from metal to metal.

In the case of steel and iron, passivation occurs when a surface oxide of gamma iron forms. This passive layer is invisible and its composition has not been established exactly, except that it involves oxygen. [9] Steel will not corrode while its passive layer remains intact. An important property of this passive layer is its instability in most environments except those of high pH. Steel and iron will depassivate in solutions of pH less than 10 or 11.

Most commonly encountered aqueous environments have fairly neutral pH's of about 7. Under such conditions, steel will not passivate. However, the pH in moist concrete is typically about 13, due to the presence of calcium hydroxide ($Ca(OH)_2$), a by-product of hydration. Under normal conditions, therefore, steel will not corrode inside concrete. This environmentally-produced corrosion protection has been observed to be effective, except under certain circumstances.

Steel will only corrode in concrete environments if the pH is lowered below the 10.0 threshold, or if the passive layer is broken down in some other way. Carbonation will lower the pH of concrete pore water past the 10.0 limit, but the process takes considerable time. It is rare to see carbonation effects present in good quality, uncracked concrete below a depth of 1/2 in. [5] Cracking and insufficient cover can make carbonation a threat.

Steel may also depassivate in high pH environments in the presence of bromide ions. The most commonly found bromide ion in concrete environments is chloride, and chloride does pose a very real threat to the integrity of many reinforced concrete structures.

2.3 The Chloride Effect: Corrosion of Steel in Concrete

The chloride ion is a very common substance in many reinforced concrete environments. The most common source of solid chloride is salt (NaCl). In this form, chlorides come into contact with concrete

through deicing applications, contaminated mix water, marine environments, and contaminated aggregates. Chloride ions are also introduced through the use of some accelerating admixtures, such as calcium chloride, and concrete bleaching operations.

In order to promote corrosion, free chloride ions must be present in moist concrete at the level of the reinforcing steel. Aqueous chloride ions may come into contact with the reinforcing steel as water saturates concrete that already contains chloride, or as dissolved chloride ions diffuse through the concrete mass. The diffusion of chloride ions from the outside of the concrete to the interior is the most common mechanism resulting in chloride exposure.

Chloride ions do the most damage when they enter reinforced concrete after hydration has stopped and the concrete has hardened. The process of hydration can remove up to approximately 7 g/l of chloride from fresh concrete. [17] This removal takes place as aqueous chlorides react with tricalcium aluminate (C_3A), a compound in portland cement. However, the reaction between C_3A and chlorides is affected by several factors, and it is generally not wise to rely on hydration to remove significant amounts of chlorides. This is especially true when the chlorides are present after hydration has slowed.

Corrosion begins once free chloride and water are present at the surface of the steel in critical amounts. The precise mechanism of chloride-induced corrosion, however, is not known. There are at least five different theories as to why chlorides induce corrosion. One body of research indicates that chloride ions promote corrosion by forming compounds that liberate iron ions from the steel surface. The small chloride ions are able to diffuse through the protective passive layer and combine with the steel to form chloride complexes. [9] One possible reaction is:

$$Fe^{+3} + 6Cl^- \Leftrightarrow FeCl_6^- \qquad (6)$$

The chloride-iron compounds produced then react with the abundant hydroxide ions in solution to produce the common steel corrosion product, $Fe(OH)_2$. The predicted reaction is given below in equation 7:

$$FeCl_6^{-3} + 2OH^- \Leftrightarrow Fe(OH)_2 + 6Cl^- \qquad (7)$$

Note that in the above reaction, the chloride ions are released to participate further in the corrosion process.

According to a second theory, [9,15] corrosion is accelerated as the chloride-iron complexes hydrolyze to form hydrochloric acid. This theory is substantiated by the claim that pH's of 3.0 have been measured immediately adjacent to severely corroding reinforcing steel. Some researchers [9] dismiss this claim, however, insisting that the substantial buffer of hydroxide ions in the concrete pore water will neutralize any H^+ ions produced by hydrolysis.

The final corrosion products produced by chloride corrosion vary with environment. Where sufficient oxygen is available, the common, rust-colored iron oxides may be expected. In low-oxygen environments, however, dark green and dark gray/black corrosion products have been observed on bare steel anode sites.[1, 12] It is postulated these products are chloride-iron complexes that fail to form iron oxide due to the lack of oxygen. The dark green products often turn rust-colored in a matter of minutes when exposed to the atmosphere.

Regardless of the exact mechanism and by-products, it is universally accepted that chloride ions induce the corrosion of steel in concrete. When steel is exposed to aqueous chloride ions, the electrical potential of the steel becomes more negative, and anode sites are established.

It is important to note that water and chloride are not the only ingredients required for corrosion to occur. The water and chloride establish the anodes, but oxygen (or some other electron-consumer) and water must be present at the cathodes, and electrical and ionic conductivity must exist between the two sites. Chlorides simply act as catalysts where conditions for corrosion are favorable.

Figure 2.2, below, illustrates an example of a chloride-induced corrosion macrocell. Chlorides and water penetrate to the level of the top steel and establish the anode. Water saturates the concrete to the depth of the lower mat of steel, where oxygen is more available. Steel stirrups link the anodic top steel to the cathodic bottom steel, providing a pathway for the electrons. This scenario is common in bridge decks and other reinforced concrete surfaces exposed to deicing salts.

Microcell corrosion may also be induced by aqueous chlorides. In the case of microcells, variations in chloride ion concentrations place one area of steel in a higher electrical potential than an adjacent piece of steel. If sufficient oxygen is present, corrosion will proceed locally. Pitting corrosion is an example of local microcell action. Differentials in chloride ion concentrations thus become very important - often more important than the absolute magnitude of the overall chloride ion concentration. [1]

The corrosion of steel in concrete is often self-accelerating, leading to progressive deterioration. The products of steel corrosion occupy more than 2 times the volume of the original materials. This increase in volume can create internal expansive pressures of approximately 5000 psi, causing the concrete to crack. Cracks in the concrete then allow more water, chlorides, and oxygen to reach the level of the

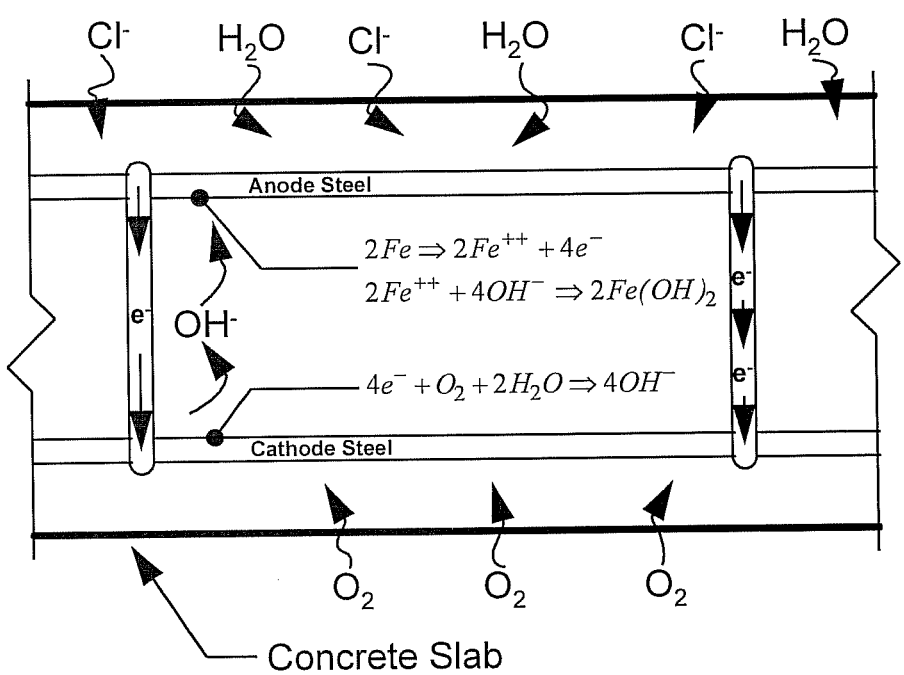

Figure 2- 2 Chloride-induced macrocell corrosion

steel, and the corrosion rate increases. It is very common to find severe reinforcing steel corrosion - particularly pitting - at the site of cracks.

As corrosion progresses, cracks become wider and more numerous. Corrosion products are forced to the surface and unsightly staining of the concrete may be observed. In the later stages of corrosion, pieces of concrete may spall away from the surface. This is often referred to as "potholing". Costly repairs then become necessary. In some instances, the structures may need to be demolished.

The problem of chlorides in reinforced concrete structures is therefore a significant one. Chlorides promote corrosion and have been instrumental in the damage and decay of many concrete structures. Billions of dollars in corrosion damage have already been realized, and more is likely in the future. It is the goal of many researchers to find a way to prevent chlorides from taking part in the process of steel corrosion in concrete environments.

2.4 GALVANIC CORROSION

The topic of galvanic corrosion is worthy of discussion because it provides a theoretical basis for at least one solution to the problem of steel corrosion in concrete.

Galvanic corrosion is the name given to the phenomenon of coupled corrosion. Conductive materials may be classified in terms of their potentials with respect to a standard hydrogen electrode, or their standard emf. Metals may additionally be classified in terms of their potentials in other environments, such as seawater. When two metals are dissimilar, as determined by their location in the emf or comparable series, and are connected electrically and placed in a conductive, corrosive environment, it is generally observed that one metal experiences accelerated corrosion, while the other metal experiences less corrosion than if placed in the same environment, alone and uncoupled. [10] This change in corrosion behavior is a direct result of the potential difference that exists between the two metals in the corrosive environment. The metal with the more negative potential becomes the anode, and the metal with the less negative potential with respect to the standard electrode becomes the cathode. In some cases, the cathode, or protected metal, may demonstrate little or no corrosion.

Several points must be emphasized with respect to galvanic corrosion. A good electrical contact must exist between the two coupled metals, the environment must be a conductive solution, and both metals must be in contact with the environment. If the electrical contact between the metals is poor, or if the environment is highly resistive, galvanic action will not take place as strongly. [25] Also, if only one of the metals is subjected to the environment, that metal will corrode as if it were uncoupled in that environment.

Additionally, galvanic couples are environment-specific. Two metals that show definite galvanic action in one environment may show little or no galvanic corrosion in other environments. In some cases, the relationship between the metals may even reverse; a metal that is cathodic to another metal in one environment may become anodic to the same metal in another environment. This behavior is directly a function of the relative potentials of the coupled metals in the specific surroundings.[10]

Finally, the presence of a passive layer on the metal may complicate analysis. Certain metals may become more passive when subjected to higher corrosion potentials. This is not the case with steel in most environments, however.

The concept of galvanic corrosion has been used in a number of protection schemes for steel, with galvanizing as probably the most common technique. In galvanizing, steel is dipped in molten zinc, forming an outer coating of zinc and zinc alloys on the steel. Zinc coatings protect the steel by providing both a barrier and galvanic protection; where a break occurs in the zinc and both zinc and steel become exposed to corrosive attack, the zinc corrodes preferentially to the steel. Galvanic action takes place because zinc is more electrochemically active than steel in most environments. Figure 2.3, below, illustrates the concept of galvanic protection. As shown, the corrosion rate of the zinc in the vicinity of a break in the coating accelerates, protecting the iron even in the absence of the barrier.

2.5 Corrosion Protection for Steel in Concrete

A number of different approaches to preventing steel corrosion in concrete have been developed and refined in recent years. The most significant of these schemes include exposure reduction, the use of corrosion inhibitors, cathodic protection, and the use of reinforcing steel coatings. Each of these methods will be briefly described below.

2.5.1 Exposure Reduction

Exposure reduction is the simplest (and some would say, most effective) method of corrosion reduction. By preventing chlorides, water, and oxygen from reaching the reinforcing steel, corrosion becomes impossible. Exposure reduction can first be achieved by placing the concrete in an environment free from dangerous substances. This is not a practical option, however, as concrete placed outside will become exposed to water and oxygen, and structures located in marine or snow-belt areas will be exposed to chloride ions. The only remaining possibility consists of preventing the harmful materials from diffusing into the concrete.

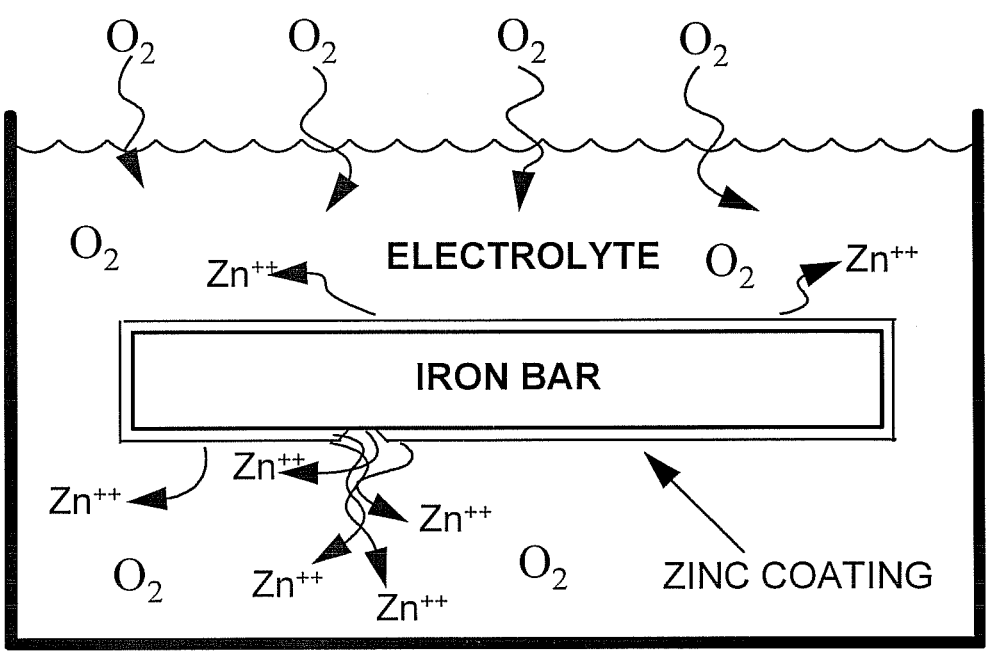

Figure 2- 3 Sacrificial action in a galvanic couple

Concrete permeability and adequate cover are the key variables in preventing this diffusion. Concrete with lower water permeability will obviously show lower chloride diffusion rates. Oxygen and ionic diffusion rates will similarly be retarded. Increased cover over the reinforcing steel will always provide additional corrosion resistance.

Concretes with lower permeability also show substantially higher electrical resistivity than more permeable concretes. This reduces the speed at which corrosion may take place, regardless of the chloride ion concentration. Indeed, some engineers claim that increasing concrete resistivity and excluding oxygen are the most significant and trustworthy methods of corrosion prevention. [1,11]

There are a number of ways to obtain low permeability concrete. The simplest involves using good concrete; properly placed, well consolidated, and correctly finished concrete designed with a low water/cement ratio (.45 or less) and cured properly will have a low permeability.

Other methods of reducing permeability involve the use of admixtures or special materials. Latex modifiers, polymer compounds, and silica fume are examples of concrete additives that lower the permeability. The use of special additives may be too costly, however.

Finally, impermeable membranes may be placed within the concrete between the reinforcing steel and the source of corrosive agents. Sealing compounds may also be applied to exposed surfaces. Both of these methods have shown some success in selectively lowering concrete permeability and delaying the onset of corrosion. [3]

All of the above methods have shown some practical success. The water/cement ratio is probably the most widely-acknowledged method in permeability reduction. None of these methods, however, can completely prevent corrosion once the chlorides, oxygen, and water become present in the concrete in sufficient amounts.

2.5.2 Corrosion Inhibitors

Corrosion inhibitors provide a method (in theory) to stop the corrosion process even though all necessary ingredients for corrosion are present. An inhibitor is a substance that acts as a "reverse catalyst" that slows or stops the corrosion rate. Most inhibitors are proprietary and empirically developed, so little is known about the exact mechanisms and reactions involved. It is known, though, that inhibitors tend to function in one of several modes.

The first class of inhibitors function by adsorption. These inhibitors first diffuse into and bond with the surface of the metal subject to corrosion. The adsorbed inhibitors then function as a form of applied passivation by obstructing the anodic and cathodic reactions. Adsorption inhibitors account for the majority of corrosion inhibitors used. [10]

A second class of inhibitors contain hydrogen-evolution poisons. These inhibitors function by specifically targeting the hydrogen reduction reaction:

$$2H^+ + 2e^- \Leftrightarrow H_2 \qquad (8)$$

The hydrogen poisons reduce the corrosion rate by retarding the cathodic reaction found in acidic environments. These inhibitors are not useful in basic environments such as concrete, where oxygen reduction provides the cathodic reaction.

A final class of corrosion inhibitors is the oxidizers. Oxidizers prevent the corrosion of metals (such as steel) that exhibit active/passive transitions. These inhibitors perform by stabilizing the passive layer, retarding the anodic corrosion reaction.

In general, the use of corrosion inhibitors has seen only limited success. Inhibitors are designed to target very specific reactions, in a very specific range of concentrations. When additional reactions come into play, or when the concentration of corrosive agents changes, corrosion inhibitors quickly lose their effectiveness. In addition, a number of inhibitors are toxic, and can be used only with great care where the consequences of contamination are severe. Corrosion inhibitors therefore present, at best, only a partial solution to the problem of corrosion in concrete.

2.5.3 Cathodic Protection

Cathodic protection, in various forms, has been used for quite some time. This method of corrosion protection works by extinguishing the potential differences that drive the corrosion process. Cathodic protection applies an equal and opposite potential, in the form of impressed electrical current, between the anode and cathode in the corrosion cell. When the potential difference is thus externally forced to zero, corrosion stops. Corrosion cannot occur when cathodic protection is properly applied and maintained.

The current demand in most typical cathodic protection applications is not very large. A fraction of a milliampere is usually all that is required per square foot of concrete surface. Protection for 10,000 square feet of concrete would draw about as much power as a 150 watt light bulb. [15]

A number of different methods can be used to implement cathodic protection in reinforced concrete. Conductors may be installed on the surface of a concrete slab, under concrete overlays, or on the surface of the reinforcing steel. Alternatively, conductive concrete overlays may be used to conduct the impressed current.

DC potentials opposite in sign to the anticipated corrosion cells are then applied to the concrete from a dedicated power supply unit. All cathodic protection schemes involve the use of a controlled current through the concrete mass.

Although often very effective, cathodic protection does present several problems. First, cathodic protection is not possible unless the anodes and cathodes can be absolutely identified. If current of the incorrect sign or magnitude is applied, the steel corrosion can be accelerated, with disastrous results. Cathodic protection is therefore only possible where macrocell corrosion is anticipated.

Second, cathodic protection schemes may cause peripheral corrosion problems. Metal appurtenances, ducts, and conduits may be induced to corrode by stray DC currents. Steel in contact with the concrete must be carefully isolated.

Cathodic protection is therefore not the solution to every concrete corrosion problem. It has been used successfully, though, in a number of applications, including many bridge decks.

2.5.4 Direct Coating of Reinforcing steel

A final corrosion protection scheme for steel in concrete involves directly coating the reinforcing steel. Two types of coatings are currently used: simple barrier coatings, and sacrificial coatings Epoxy barrier coatings are produced by fusion-bonding an epoxy-based powder with the surface of the steel. The epoxy coating forms a barrier that prevents water and chloride ions from reaching the surface of the reinforcing steel. As barriers, epoxy coatings are only beneficial when the integrity of the coating remains good. Breaks in the epoxy caused by handling or poor application processes allow corrosion to take place in localized areas. Furthermore, such localized corrosion can become very severe due to small anode/cathode area ratios.

This shortcoming is exaggerated by the fact that epoxy coatings are comparatively soft, and damage is virtually inevitable. When epoxy coatings were first used, proponents predicted corrosion protection in excess of 20 years. Current estimates indicate corrosion protection of 10 years or less. While the corrosion benefits of epoxy coating cannot be denied, lower-than-expected field performance and problems with bond strength have caused a number of users investigate other protection options.

Galvanic coatings, on the other hand, provide both a barrier to corrosive substances and galvanic protection for local areas where the coating wears or chips away. When both the steel and the coating become exposed to the corrosive medium, the galvanic coating will preferentially corrode, while the steel remains protected.

Galvanic coatings are more complicated than the simple barrier coatings. As sacrificial anodes, the coatings must be designed and tested for each exposure environment, as reversals and ineffectiveness in galvanic behavior may take place from environment to environment. Additionally, some highly resistive exposure environments do not lend themselves well to galvanic action of any sort. [25]

Although quite a deal of research has been conducted on the use of galvanic coatings in concrete, conflicting results have been reported. [4, 13, 25] In some cases, galvanic coatings have been seen to perform well, while in others, little benefits have been realized. The galvanic coatings therefore represent an enigmatic solution to the problem of steel corrosion in concrete.

Within the class of galvanic coatings, two options are emerging as feasible concrete protection systems. The first is traditional galvanizing, which involves coating steel with molten zinc. A coating system of pure zinc and zinc-rich alloys is produced in this approach. A second, more recent galvanic coating involves the use of zinc-rich paints. In this system, zinc is bound in an inorganic polymer matrix to the surface of the steel. This zinc-rich matrix forms the coating. The following chapter will investigate some of the theoretical considerations that pertain to the use of zinc in concrete. This discussion will form the framework for subsequent experimental analysis.

CHAPTER 3

THE USE OF ZINC FOR CORROSION CONTROL IN CONCRETE

3.1 ZINC CORROSION PROPERTIES

Without a doubt, zinc is the most common material used in metallic coatings for steel. Zinc has is used extensively, in part, due to its inherent corrosion resistance. Zinc remains passive in most environments of pH 6-13; a pH range which encompasses most environmental situations. In contrast, steel remains electrochemically active and subject to severe corrosion up to a pH of 11.5. Steel is therefore much more prone to corrosion than zinc in most situations.

It is important to note, however, that the high pH found in concrete (12-13.5) should favor steel more than zinc. In fact, under ideal conditions, steel should not corrode at all in concrete environments. This pattern has not been observed to be the case. Zinc is 2.5-5 times more resistant to chloride than steel, and in concrete environments where steel has been observed to corrode, zinc will often demonstrate better corrosion performance.[27] It must be reiterated, though, that a concrete environment is not ideal for zinc, and zinc will corrode.

Corroding zinc is usually not as harmful to reinforced concrete as corroding steel. Zinc oxide, zinc hydroxide, and calcium hydrozincate are typical zinc corrosion products in alkaline concrete environments, and produce an approximate 50% expansion, in contrast to the 200% expansion developed by corroding steel. [13] Zinc corrosion therefore produces lower expansive stresses and causes less cracking in the concrete.

An important exception to this rule occurs in high concentration chloride environments. In locations where abundant free chloride ions are available, zinc hydroxychloride II ($Zn_5[OH]_8Cl_2*H_2O$) has been observed to form. This compound produces an expansion on the order of 350%, creating much greater internal stresses than most iron oxides. [13] A number of surprising corrosion failures in concrete of zinc-protected steel have been attributed to the formation of zinc hydroxychloride II.

The primary benefit of zinc, however, does not come from its inherent corrosion resistance. Many metals and alloys, such as nickel, tin, titanium, and platinum, are more corrosion resistant than zinc. It is the electrochemical relationship between zinc and steel that makes zinc unique among the corrosion resistant metals. Zinc will sacrificially protect steel when a galvanic couple is established. Zinc is the most economically feasible metal to offer such a galvanic relationship with steel.

The nature of the galvanic relationship between steel and zinc changes from environment to environment. It is therefore necessary to study this couple very specifically inside concrete in order to evaluate its corrosion protection effectiveness. One recent study has been conducted on zinc-coated steel in concrete, and a three-stage corrosion progression has been proposed. [27] The stages are described below.

INITIATION: In the initiation stage, the zinc in the coating becomes passivated. The outer layers of zinc react with the alkaline concrete environment to produce protective oxides such as zinc oxide, zinc hydroxide, and calcium hydrozincate. These passivating reactions require a minimum amount of zinc to be present in the coating, consuming approximately 10 microns of pure zinc. Once passivated, the zinc coating undergoes very little corrosion. Corrosion is therefore effectively prevented, unless the environment is disturbed in some way.

PROTECTION: The protection stage begins when the zinc passivation either breaks down or fails to develop. If not enough zinc is present in the coating, the initiation stage may be bypassed altogether, and the protection stage will take place first. Protection will otherwise begin if the chloride concentration reaches a threshold level (2 - 5 times the threshold for steel), the pore water pH drops below 6 or increases above 13.3, or breaks in the zinc coating promote galvanic action. During protection, the zinc dissolves unchecked. The rate of corrosion is usually lower than steel for the same chloride concentration. The protection stage continues until environmental changes allow the zinc to repassivate (initiation stage), or all the zinc becomes corroded.

PROPAGATION: The propagation stage takes over after all the zinc has been exhausted. The steel corrodes as if there were no protective zinc coating. Cracking and failure of the concrete will usually take place quickly after the start of propagation.

It is worth noting that 4-5 times longer is required for galvanized steel to reach the propagation stage than for uncoated steel to reach severe corrosion in identical exposure conditions. Therefore, definite benefits are possible with zinc corrosion protection in concrete.

3.2 METHODS OF APPLICATION

Galvanizing is the oldest method of applying zinc coatings to steel. In galvanizing, prepared pieces of steel are dipped in a molten bath of pure zinc at temperatures of approximately 450° C. The zinc metallurgically bonds to the surface of the steel, creating a multi-layer coating of pure zinc and zinc-rich alloys. Galvanized coatings adhere very well to the steel and are tough and abrasion resistant. A drawback of galvanized coatings is that they are expensive and are restricted to steel sizes and shapes that can be dipped in a zinc bath. Galvanizing is not practical with vary large or irregular pieces of steel.

Plating and electrogalvanizing are alternate methods for applying pure metallic zinc to steel surfaces using externally applied voltage. The cold plating processes result in thinner coatings, and are typically used either in conjunction with other coatings, or on parts that may be damaged by high temperatures. [20]

A final method of zinc application that has developed more recently is the use of zinc-rich paints. As mentioned previously, zinc paints bind particles of zinc to the steel in a polymer matrix. Zinc-rich paints may be heat-cured, post-cured, or self-curing. Below is a discussion of the historical development of inorganic zinc coatings. Particular attention will be given to a specific new class of zinc-rich paint: the inorganic, high-ratio zinc silicates.

3.3 INORGANIC ZINC COATINGS

3.3.1 Historical Development

Inorganic zinc coatings were first developed and used in Australia in the 1930's by Nightingale, who mixed zinc dust in an alkaline sodium silicate solution, applied the mixed solution to a steel surface with

a brush, and baked the coated steel in an oven. [20] The baking process cured the coating, changing its mechanical and chemical properties. Variations of this heat-cured inorganic coating were used in Australia throughout the 1940's with remarkable success. Several applications performed satisfactorily for 50 years, greatly exceeding the original 20-year guarantee.

The baked coatings, however, were not practical for large applications such as ship hulls, storage tanks, and structural steel, due to size constraints. The next step was the development of an inorganic zinc coating that could be cold-cured through the application of a curing solution. In 1952, a successful post-cured coating was developed that used a zinc and sodium silicate organic base with a dibutyl amine phosphate curing solution. This coating represented a revolution in corrosion protection because it possessed good mechanical properties, it functioned well as corrosion protection, and the coating could be applied to steel of any shape and size. [18]

While an improvement over the early heat-cured coatings, the post-cured coatings still required a two step application process, followed by a washing operation to remove the post-cure solution from the surface. A less time and material-intensive process was desired. The next logical step was to produce a self-curing coating that could be applied in one process. Several classes of self-curing inorganic zinc coatings have been developed and put into use.

One group of self-cure coatings is the alkali silicates. The alkali silicates are water-based, utilizing alkali inorganic zinc silicate. These coatings cure by water evaporation. Unfortunately, the alkali silicates cure slowly and tend to crack while drying.[24] These coatings therefore represent a less than completely satisfactory solution to the self-cure problem.

More success was found with the ethyl silicates, which use ethyl silicate as a binder for the zinc particles. The ethyl silicate and zinc are applied with an organic solvent, as opposed to water in the case of the alkali silicates. The ethyl silicate coatings demonstrate better mechanical properties than the alkali silicates, with faster curing times and much less tendency to crack while curing. The organic solvents, however, pose environmental problems, especially in light of recent legislation limiting the use of volatile organic compounds (VOC's). [19]

The most recent development in self-cure inorganic zinc coatings are the high-ratio zinc silicates, developed by NASA in the late 1970's for the protection of rocket launchers. This new class of coatings is water based, yet demonstrates the mechanical properties of the ethyl silicates. The high ratio zinc silicates therefore combine the strengths of both the alkali silicates and the ethyl silicates.

The high ratio zinc silicates have shown considerable promise in the years since their release in the early 1980's. They have performed well in a number of severe marine environment applications, and have provoked interest in the use of these coatings in other situations. In particular, the high ratio zinc silicates have been proposed as a corrosion protection system for reinforcing steel in concrete.

3.3.2 High Ratio Zinc Silicate Coatings

The high ratio zinc silicates function fundamentally in the same way as the older alkali and ethyl silicates. A silica/alkali metal compound is added to a liquid medium (in this case water), where chemical reactions produce a polymer of silicic acid. When particulate zinc is added to this mixture, the zinc reacts with exposed OH groups to form a new silicon-oxygen-zinc polymer. It is this polymer that binds the zinc and forms the coating as the water evaporates and the material cures. [20]

The high ratio zincs differ from earlier self-cure formulations, however, in that they use an improved silica/alkali binding compound. The high ratio silicates make use of a potassium silicate that has been post-processed and refined to increase the ratio of silica to potassium. The refined potassium silicates have a silica-to-potassium ratio of 5.3:1 (or higher), in contrast to the 3.2:1 ratio used in older formulations. [18] This higher silica content produces more reactive OH groups when the potassium silicate hydrolyzes with the water. As a result, the zinc reacts more rapidly, and the eventual coating possesses better corrosion and mechanical properties than the older self-cure coatings.

As barriers, the high ratio zinc silicates present somewhat of a technological breakthrough. The zinc silicate matrix becomes harder and more durable over time as a result of chemical reactions produced by normal exposure. Moisture and carbon dioxide in the air form carbonic acid within the coating. The carbonic acid ionizes the zinc particles, allowing the zinc to react further with the zinc silicate. This ongoing reaction makes the coating more dense and metal-like, and improves adhesion to the metal substrate. [20] In addition, the ionized zinc also forms zinc carbonate and zinc hydroxide in the pore spaces of the coating, sealing the coating and reducing porosity. The high ratio zinc silicate coatings therefore tend to become more tough and durable in response to exposure, rather than deteriorate.

The zinc silicate matrix gives this class of coatings a distinct advantage over pure metallic coatings, such as galvanizing. The zinc silicate matrix is chemically inert and unreactive in most environments. [20] Under severe exposure, the matrix slows down the corrosion of the zinc particles, giving the coating a longer life than pure metallic zinc.

Extensive atmospheric testing has been done on the high ratio zinc silicates in recent years. Below is a list of advantages found. [24]

1. Rapid cure, with water resistance obtained in approximately 2 hours.
2. Excellent resistance to mudcracking during cure with coating thickness' in excess of 3 mils.
3. Exceptional hardness obtained in 2 hours.
4. Good adhesion to properly prepared steel surfaces.
5. Easy application with a variety of spray equipment.
6. Easy cleanup with water; environmentally friendly.
7. Exceptional atmospheric corrosion protection without topcoating.
8. Simple repair/recoating procedures.
9. Low maintenance requirements.
10. Lower cost than multi-coat organic coatings

A criticism of the high ratio zinc silicates is that the coatings cannot be applied in excess of 8 mil layers without problems occurring during cure. If the outer layer of the coating is allowed to dry faster than the interior, drying stresses may produce a pattern of cracks known as mudcracking. [24] It was also found that formation of an exterior crust may leave the underlying coating uncured and vulnerable to damage.

Curing conditions are also important. In cool, humid environments, the water in the coating evaporates more slowly and the coatings take longer to cure.

Finally, the coatings were found to take a significant time (4-6 months) to reach peak hardness and complete zinc saturation. Adequate hardness for handling may be obtained within hours, however.

Although these problems must be considered, they do not obscure the fact that the high ratio zinc silicates have performed very well in a number of applications, both in terms of corrosion protection and economics. The high ratio zinc silicate coatings therefore show considerable promise.

3.3.3 The Use of the High Ratio Zinc Silicates in Concrete

The high ratio zinc silicates have been proven very effective in atmospheric corrosion protection. However, much less testing has been done to date in concrete environments, and early testing did not yield promising results. Experiments conducted previously at the University of Texas at Austin [12] found that when placed in concrete, the high ratio zinc silicates failed to provide galvanic protection for reinforcing steel.

It was postulated this failure resulted from bonding between the coating and the concrete. During autopsies, the coating was observed to bond to the concrete and pull away from the steel. If the concrete-coating bond did in fact interfere with the contact between the coating and the steel, this could very well have been the reason for the failures.

Other possible explanations include a lack of protective oxide formation in the zinc, and adverse pH effects. The first-generation of high ratio zinc silicates clearly did not perform adequately in a concrete environment.

A second-generation of high ratio zinc silicate has since been developed that does not bond to preferentially to concrete. The new coating is the subject of the current tests. It has been suggested that the different concrete-coating bond characteristics will result in improved corrosion performance.

3.4 CONCLUDING CONSIDERATIONS: ZINC IN CONCRETE

From the above discussion, it may be concluded that concrete is a complicated environment for zinc. Zinc has demonstrated widespread success in atmospheric exposure, but there are key differences between atmospheric and concrete exposure. In concrete, the pH is typically much higher than in the atmosphere, and zinc is sensitive to very high pH. In addition, there is much less oxygen present in concrete. This lack of oxygen at the anodes could prevent the formation of necessary protective zinc oxides within concrete, leading to possible rapid, and in some cases very expansive, corrosion of the zinc. Every proposed zinc-based protection system should therefore be tested fully within concrete before field implementation.

In spite of these causes for skepticism, some zinc coatings have shown considerable success where they have already been used in concrete. In a number of situations where both zinc-coated (galvanized) and uncoated reinforcing steel have been used in severe exposure, the zinc-coated bars have performed well, in marked contrast to the uncoated bars. One 21-year-old bridge in a marine environment showed little or no corrosion of the galvanized reinforcing steel. In fact, it was estimated that 60-70% of the original coating still remained. [4]

Galvanizing remains an expensive option, though, costing approximately $0.25 more per pound of steel than epoxy coatings. The high ratio zinc silicates, on the other hand, have proven to be very competitive in cost with other coating systems. [7]

When competitive pricing is combined with the fact that high ratio zinc silicate coatings are less sensitive to mechanical damage than non-galvanic systems, the zinc silicates should present an attractive option for concrete applications if testing proves them to be effective that environment.

CHAPTER 4

EXPERIMENTAL THEORY AND PROCEDURES

4.1 THE MACROCELL METHOD

4.1.1 Macrocell Theory

As mentioned, a macrocell is a corrosion cell where the anode and the cathode are separated; the anode steel is distinct from the cathode steel. Macrocell corrosion is forced corrosion resulting from a difference in potential between two areas of steel. Conductance between the two locations provides a link between the anode and cathode and allows corrosion to take place.

Microcell corrosion, in contrast, progresses with the anode and cathode in close proximity, often on the same piece of steel. The corroded area of steel will incorporate both the anode and apparently the cathode, at the same location. In reality, the anode and the cathode are separated, but the distance is very small. Pitting corrosion is an example of microcell action. In a pit, the tip of the pit forms the anode and the mouth of the pit acts as the cathode.

In this experiment, macrocells were constructed to study the corrosion behavior of a specific high ratio zinc silicate coating. The macrocells were fabricated by casting two layers of steel into blocks of concrete. The top layer of steel, or anode, was comprised of a single piece of reinforcing steel, bent into a "U" shape. The bottom layer of steel was placed 5 inches below the top steel, and was comprised of 3 straight pieces of reinforcing steel. Both layers of steel protruded from the front face of the concrete blocks. The bottom steel was connected electrically by welding a length of bar across the protruding ends.

To complete the macrocells, 4-sided acrylic dikes were fixed to the top of the macrocells with silicon adhesive, and a conductor of known resistance was used to connect the top and bottom mats of steel.

A data acquisition system was connected to the conductor, and was used to monitor the potential difference between the top and bottom mats of steel. Figure 4.1 illustrates the key components of the macrocells.

To promote corrosion, a 3.5 NaCl solution was ponded on top of the macrocells in 14-day wet, 14-day dry exposure cycles. The wet and dry cycles produced a more severe exposure condition than constant ponding due to the higher levels of oxygen maintained in the concrete. Evaporation of the salt solution was minimized by covering the dikes with pieces of 1/4" plywood.

During exposure, as the water and salt penetrated the concrete to the top steel, the potential of the top steel became altered and the anodic reactions took place. Metal ions dissolved, liberating electrons. The electrons traveled from the top steel, through the conductor, to the bottom layer of steel where the cathodic reactions took place and completed the macrocell. Figure 4.2 illustrates this corrosion process.

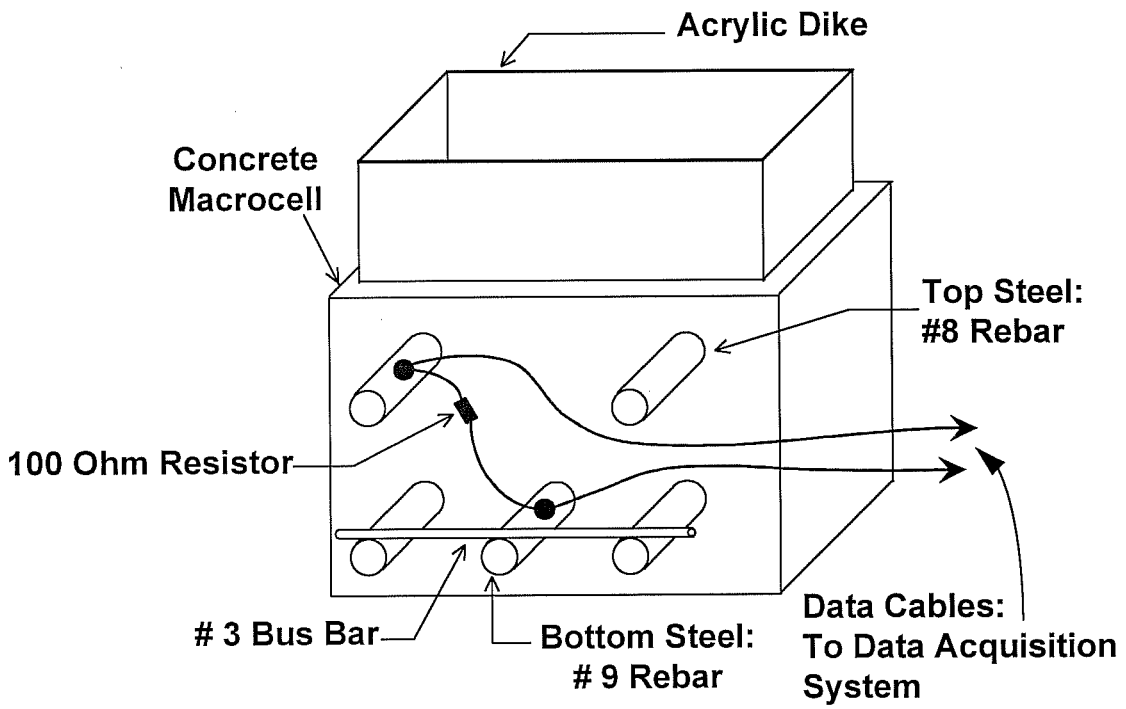

Figure 4- 1 Key macrocell components

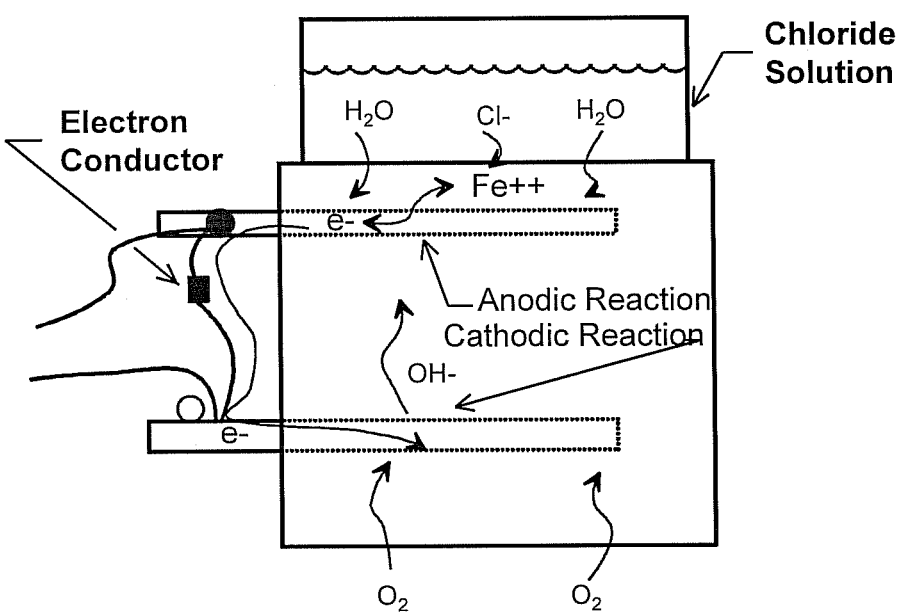

Figure 4- 2 Macrocell corrosion in test set-up

The data acquisition system was used to take instantaneous potential difference readings between the top and bottom mats of steel at weekly intervals. From the potential difference and the known resistance of the conductor, the instantaneous current readings were computed according to Eq. 1, below:

$$i = V / R \tag{1}$$

The current is the result of the electron flow between the top and bottom mats of steel and therefore is considered to represent a measure of the corrosion activity at a given time. The corrosion current values were integrated over time using the trapezoidal method to estimate the total charge flow over the life of the experiment. The total charge flow represented the total number of electrons to pass from the top to the bottom mat of steel, and made it possible to predict the total corrosion damage to the anode.

The process where macrocell corrosion is induced, potential differences are measured, and corrosion currents and damage levels are assessed is known as the macrocell method.

4.1.2 Macrocell Specifications

The macrocell specifications were identical to the specifications used in previous research at The University of Texas investigating both epoxy bars and earlier high ratio zinc silicate coatings. [12] Figure 4.3 gives an illustration of the macrocell dimensions and relative placement of the steel.

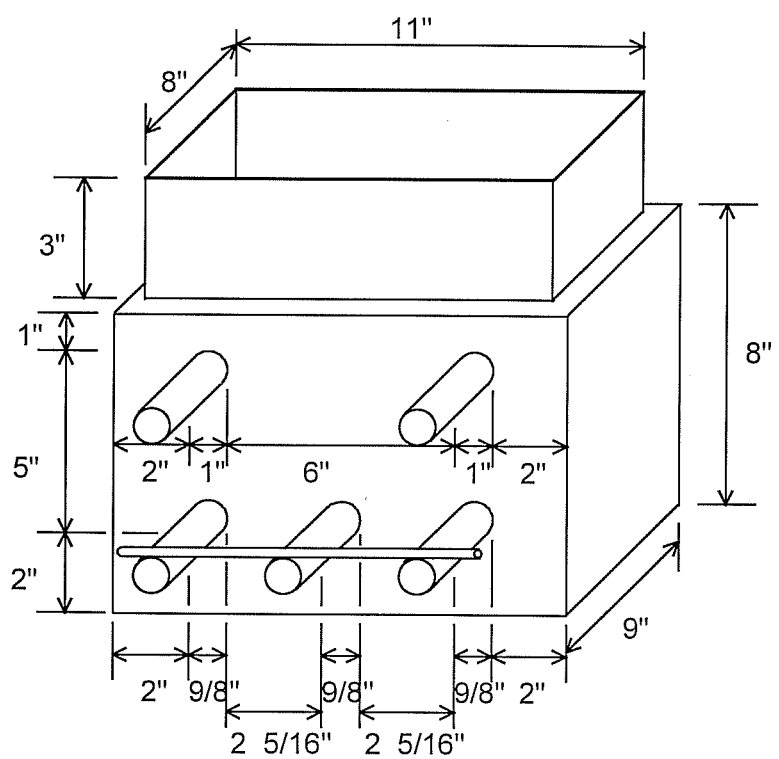

Figure 4- 3 Macrocell dimensions

In previous research, both 1 in. and 2 in. cover over the top mat of steel were considered. The additional inch of cover was found to only delay, rather than prevent, the onset of corrosion. [12] One inch of cover was used in all the macrocells in this study to minimize the time to corrosion.

As in the earlier zinc silicate research, a nominal 3000 psi concrete mix was selected. A low strength, high permeability mix was chosen to maximize the severity of chloride attack. The theoretical mix proportions are given in Table 4.1.

Twenty-one 6"x12" standard cylinders were cast from the mix used in the macrocells. The cylinders were tested periodically for compressive strength. The strength gain curve is presented in Figure 4.4. It can be seen from the curve that the compressive strength corresponded very well with the 3000 psi design specification.

Table 4- 1 *Theoretical mix proportions*

3/4" aggregate	1884 pcy
Sand	1435 pcy
Type II Cement	360 pcy
Water	266 pcy

A chloride permeability test was conducted at approximately 90 days after casting. The test used was the "Rapid Determination of the Chloride Permeability of Concrete", AASHTO designation T 277-83. The concrete was found to pass 11,400 Coulombs of charge in 6 hours. High permeability concrete is defined as permitting over 4000 Coulombs of charge. The concrete therefore had a very high chloride permeability.

Fixed amounts of steel were used in the top and bottom mats. The anodes were all #8 bars bent in a "U" shape, with bend radii at least as severe as the guidelines specified in ACI 318-89. Out-to-out dimensions of the bent top bars varied between 6.25 in. and 8in. Different coating schemes were used on the top bars, according to the variables tested.

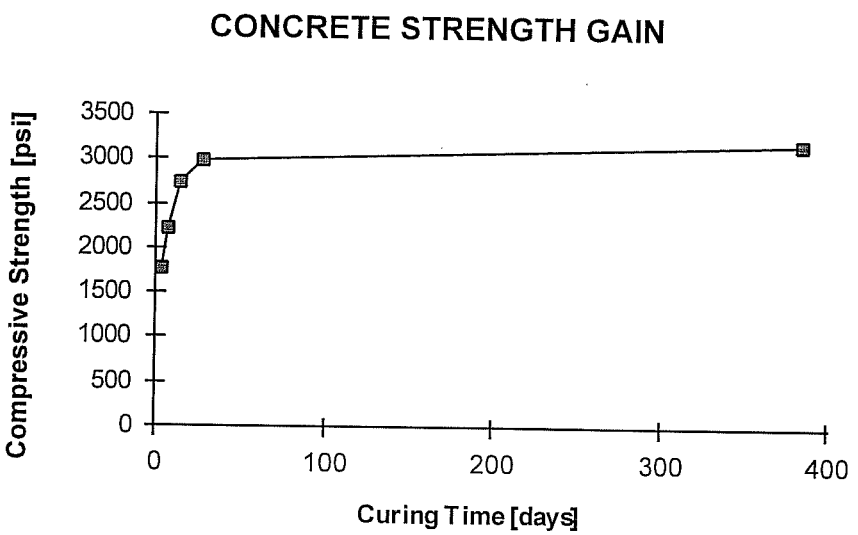

Figure 4- 4 *Strength gain of concrete used in macrocells*

The bottom mats of steel were comprised of three, 12-inch lengths of straight #9 bars. The cathode steel was either coated with the inorganic zinc silicate, or left uncoated. As mentioned, the bottom steel was connected externally by welding a #3 bus bar across the protruding legs. All steel placed in the concrete was given at least 2 inches of cover on all sides except the protruding ends and over the tops of the anode bars. Short lengths of multi-stranded, insulated, copper wire were used to connect the top mats of steel with the bottom mats. One hundred-ohm resistors were inserted in the conductors between the top and bottom steel to provide a measurable resistance to the corrosion currents. Sensors from the data acquisition system were installed at either ends of the conductors.

The dikes used to contain the chloride solution were constructed from 1/16" acrylic. The dimensions of the dikes were specified to allow them to fit within the footprint of the macrocells, standing 3 inches high. The dikes were fixed to the tops of the macrocells with silicon adhesive.

4.2 Experimental Variables

4.2.1 General Description of Tests

Nine groups of macrocells were constructed, with 3 cells in each group, yielding a total of 27 cells. Each group of cells was designed to investigate a specific set of coating variables. The different groups are described in section 4.2.2.

The macrocells were classified according to the coating scheme used on the anode and cathode steel. Six groups of cells contained anodes that had been coated with the second-generation high ratio zinc silicate. The anodes were coated, bent, and recoated, according to the desired condition, by the coating manufacturer. The zinc silicate coatings were either left unrepaired, were wire-brushed and repaired, or were grit-blasted and repaired. All zinc silicate-coated anodes were made from grade 40 steel, with the same deformation pattern and mill markings. The bars were used as supplied by the high ratio zinc silicate producer.

Two groups of cells used anodes that had been hot-dip galvanized. The galvanized bars were used as supplied by the zinc silicate coating producer. All galvanized bars were made from the same grade 60 steel. These bars were different, both in terms of producing mill and steel strength, from the high ratio zinc silicate-coated anodes.

Finally, a single group of macrocells was constructed with epoxy-coated anodes. The epoxy coating was produced from NAP GARD 7-2709 powder, and was applied by a local epoxy coating supplier. The epoxy bars were all grade 60, were bent by the epoxy supplier, and were used "as received".

The bottom, cathode steel was either coated with the high ratio zinc silicate or left uncoated. In the case of the coated bottom steel, the bars were made from grade 60 steel and were used as supplied by the zinc silicate manufacturer. The uncoated cathode bars were made from same-heat, grade 60 steel obtained from a local mill.

Half of the macrocell groups used the black bar cathodes, while the other half used the coated cathodes. The epoxy specimens provided the only exception, using only coated steel for cathodes. It was felt that prior experiments had provided sufficient data on epoxy-coated samples with uncoated cathodes.

4.2.2 Description of Test Groups

As mentioned, 9 groups of macrocells were constructed, each with a different anode/cathode combination. The nine groups are described below.

Group 1: NB1-NB3: The NB group used anodes that had been coated with the high ratio zinc silicate coating, bent, and used "as received". No repair was done to the coating on the top bars. The NB group therefore tested a heavily damaged coating system. Uncoated cathodes were used.

Group 2: NC1-NC3: The NC group used anodes that had been bent and left unrepaired, identical to the top steel in group 1. Zinc silicate-coated bars were used for the bottom steel.

Group 3: WB1-WB3: The WB cells used top steel that was coated, bent, and repaired. The top bars were wire brushed to remove loose flakes of coating prior to repair. The WB group therefore tested one method of repairing the high ratio zinc silicate coating. The bottom bars were left uncoated.

Group 4: WC1-WC3: The top steel in the WC cells was identical to the top steel in the WB cells. The bottom steel was coated with the inorganic zinc coating.

Group 5: SB1-SB3: The SB group used top bars that were coated, bent, grit-blasted to remove loose flakes of coating, and repaired. The SB group therefore tested an alternate method of repairing the zinc silicate coating. Black bars were used for the bottom steel.

Group 6: SC1-SC3: The SC group, like the SB group, used top bars that were coated, bent, grit-blasted, and repaired. The bottom steel was comprised of the inorganic zinc coated bars.

Group 7: EC1-EC3: Macrocells in the EC group used epoxy-coated top steel supplied by a local epoxy coating manufacturer. The coating was made from a recent formulation NAP GARD 7-2709 powder. Zinc silicate-coated bars were used for the bottom steel.

Group 8: GB1-GB3: The GB group used top steel that was hot-dipped in zinc, bent, and used with no repair to the coating. The bars were used as supplied by the zinc silicate manufacturer. Uncoated cathode steel was used.

Group 9: GC1-GC3: The GC cells, like the GB cells, used top bars that were galvanized, bent, and used unrepaired. The bottom steel was coated with the high ratio zinc silicate coating.

4.3 CONDITION OF STEEL PRIOR TO CONCRETE PLACEMENT

Prior to concrete placement, detailed observations were recorded for all steel bars for later comparison.

4.3.1 Unrepaired Zinc Silicate Coating (NB, NC)

The unrepaired, zinc silicate-coated anodes (Groups NB and NC) were the most heavily damaged of the zinc silicate bars. Figure 4.5 shows the condition of unrepaired bars prior to casting the concrete. As can be seen in Figure 4.5, extensive damage to the coating was present around the bend radius. Much of the original zinc silicate flaked off the steel as the bar was deformed in the 180 degree bend, leaving behind a gray residue where the coating once adhered. Patches of coating remained intact around bar deformations. Extensive areas of damage also were found away from the bend where the mandrel had contacted the outer edge of the bar. Mandrel damage extended in a line approximately 7 1/2 inches long, terminating at the start of the bend. Figure 4.6 shows the mandrel damage.

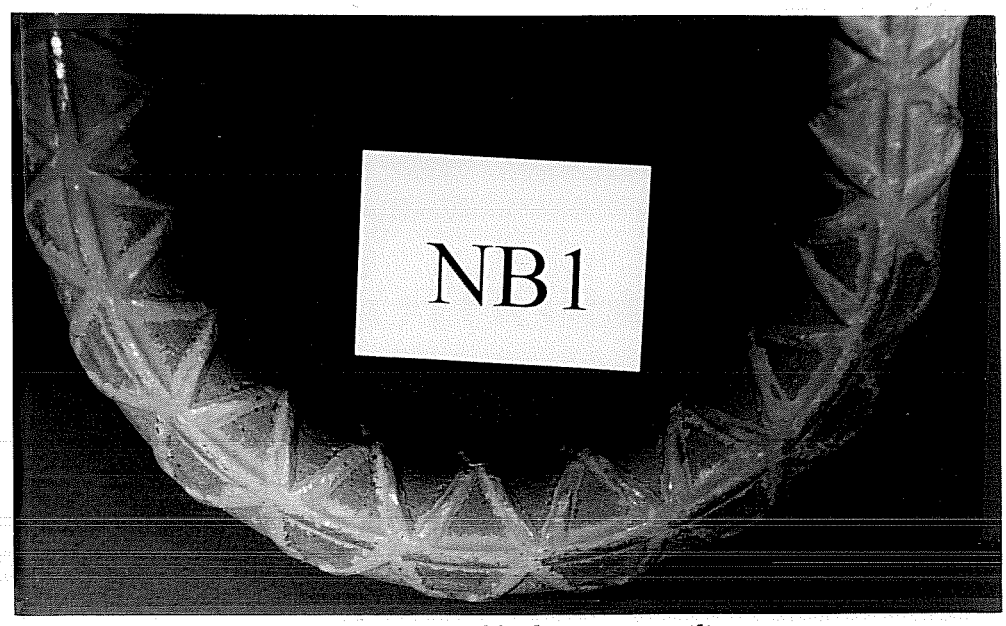

Figure 4- 5 Unrepaired high ratio zinc silicate coatings

Figure 4- 6 Mandrel damage to unrepaired zinc silicate coatings

The unrepaired bars represented a severely distressed coating. Significant corrosion damage may be anticipated if the high ratio zinc silicate coatings do not offer some measure of galvanic protection to the steel.

4.3.2 Wire Brushed and Repaired Zinc Silicate Coatings

The WC and WB groups of macrocells used anodes that had been coated with the high ratio zinc silicate coating, bent in a 180 degree bend, and then wire brushed and repaired by spraying more zinc silicate on the damaged areas. The repaired coatings were in much better condition prior to concrete placement than the unrepaired coatings. Figure 4.7, below, gives an illustration of the wire brushed and repaired zinc silicate coatings.

Small amounts of damage were visible on the repaired coatings, as shown by Figure 4.7. Localized wearing of the coating, primarily on the bar deformations, had taken place during the shipping and handling of the bars. In the case of bar WB3, the mandrel damage had not been completely covered in the repair process. In addition, there was some localized mudcracking to the coating where the zinc silicate had been applied too thickly. The repaired coatings, on the whole, were in very good condition, but they were not completely without damage.

4.3.3 Grit-Blasted and Repaired Zinc Silicate Coatings

Figure 4.8, below, gives an illustration of the SB and SC bar condition. Bars in the SB and SC groups were coated, bent, grit-blasted to remove any loose coating, and repaired. The grit-blasted and repaired bars were very similar in quality to the wire brushed and repaired bars described in 4.3.2.

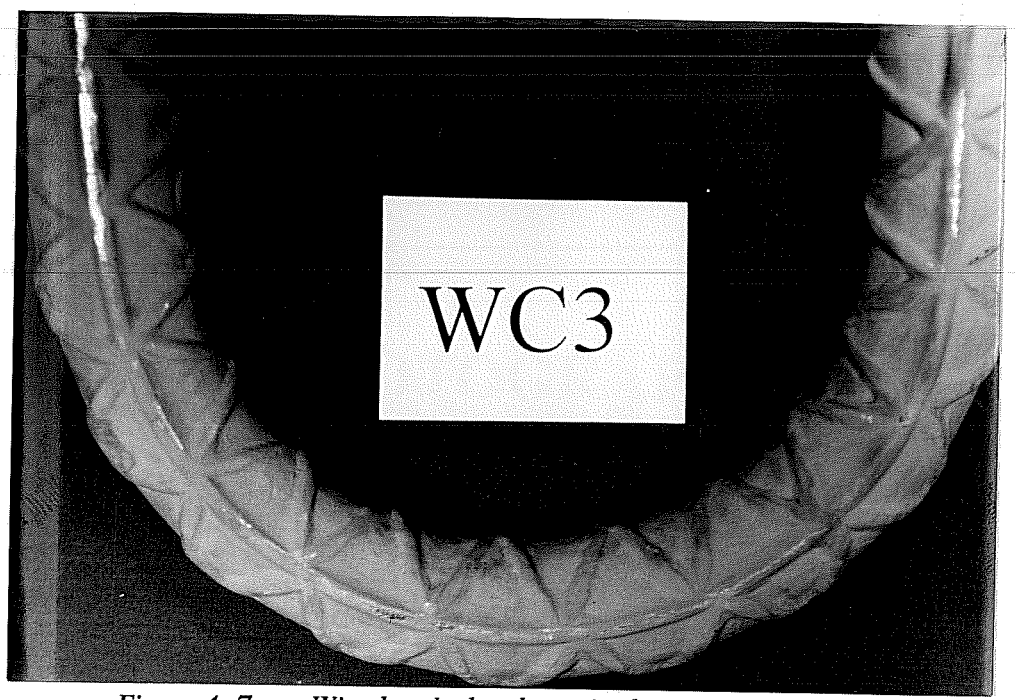

Figure 4- 7 Wire-brushed and repaired zinc silicate coatings

Figure 4- 8 Grit-blasted and repaired zinc silicate coatings

As with the wire brushed bars, the grit-blasted bars showed small localized areas of damage where either wearing had taken place or prior damage had not been completely repaired. Some mudcracking was visible.

4.3.4 Galvanized Bars

The galvanized bars were supplied by the high ratio zinc silicate manufacturer. In every case, the galvanized coating was in very poor condition. The bars had been galvanized prior to bending, and the bending process caused most of the metallic zinc to flake off the bars around the bends. Any zinc that remained on the bends was loosely attached to the bar deformations. Significant mandrel damage had also occurred on the outside of the bend. The areas of steel not covered by the galvanizing was dark brown and in the early stages of corrosion. It was postulated that the steel had not been prepared adequately prior to galvanizing, resulting in a poor coating even before bending damage occurred. Figure 4.9 illustrates the condition of the galvanized coating in the region of the bends.

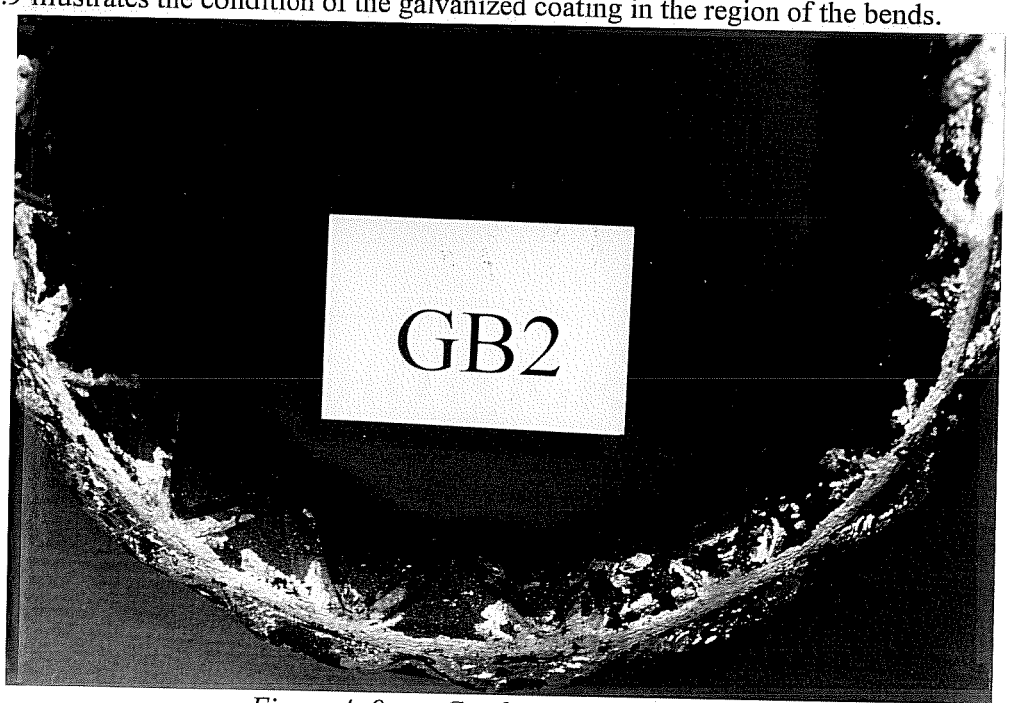

Figure 4- 9 Condition of galvanized steel

The unrepaired galvanized bars were included in the macrocells to provide a comparison to the unrepaired zinc silicate bars. However, the galvanized bars seemed to be in worse condition than the unrepaired zinc silicate bars. The galvanizing did not appear to have been applied with the same care of bar preparation as the zinc silicate coating, and corrosion was evident on the galvanized bars prior to concrete placement. The galvanizing was not felt to be representative of a state-of-the-art galvanized coating.

4.3.5 Epoxy Coated Bars

The epoxy bars were supplied by the epoxy-coated steel supplier and were in excellent condition. Great care had been taken during bending and shipping. There were no visible breaks in the coating except where the bars had been cut. In field situations, epoxy coatings will invariably suffer some damage. The

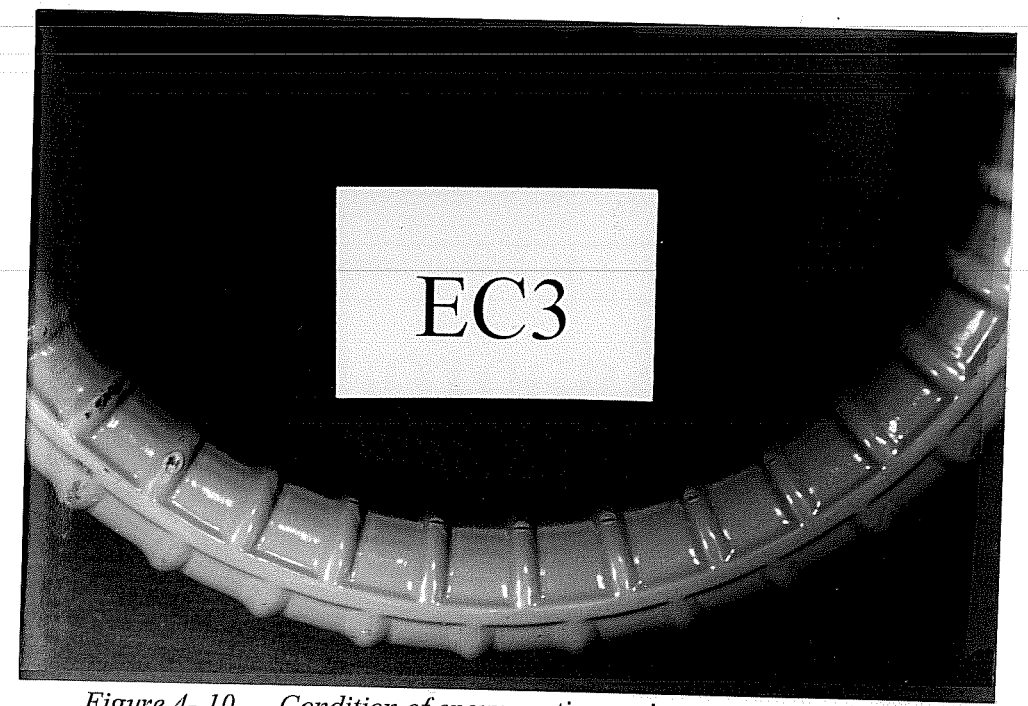

Figure 4- 10 Condition of epoxy coatings prior to concrete placement

coating condition used in these tests was therefore not indicative of field exposure for epoxy coatings. Figure 4.10 shows a photograph of one of the epoxy bars as it was received from the manufacturer.

4.3.6 Bottom Steel

The cathode steel was either uncoated or coated with the high ratio zinc silicate. the coated bars were supplied by the zinc silicate manufacturer and were in good condition. Like the repaired anode bars, the bottom bars had localized areas of damage where the coating had worn away during shipping and handling, but in general, the coating was in very good condition. Figure 4.11 shows a coated bottom bar.

The uncoated bottom bars were cleaned and prepared thoroughly. The bars were wire-brushed to remove all mill scale and then pickled in sulfuric acid several days prior to concrete placement to obtain a uniform electrochemical surface. Figure 4.12 shows an example of a black cathode bar.

4.4 Chloride Specimens and Tests

In addition to the 27 macrocells, 30 7"x7"x6" concrete blocks were cast. Like the macrocells, these blocks were fitted with acrylic dikes and were subjected to the same chloride solution exposure. The chloride cells were used to monitor the progression of chloride ions into the concrete.

At the end of every 28-day exposure cycle, one of the blocks was removed from the experiment and drilled to a depth of three inches. Samples of concrete powder were retained from the holes at quarter-inch intervals. This powder was then analyzed using a Rapid Chloride Test [22] to determine the percent concentration of chloride by weight of concrete. Chloride concentration depth profiles were then plotted for every month of exposure.

Chloride tests were also conducted during the macrocell autopsies. Dust was taken from each of the macrocells investigated at a depth of 1-2 inches immediately prior to both autopsies. At that time, dust was also taken from one of the chloride samples at the same depth range. The chloride concentration

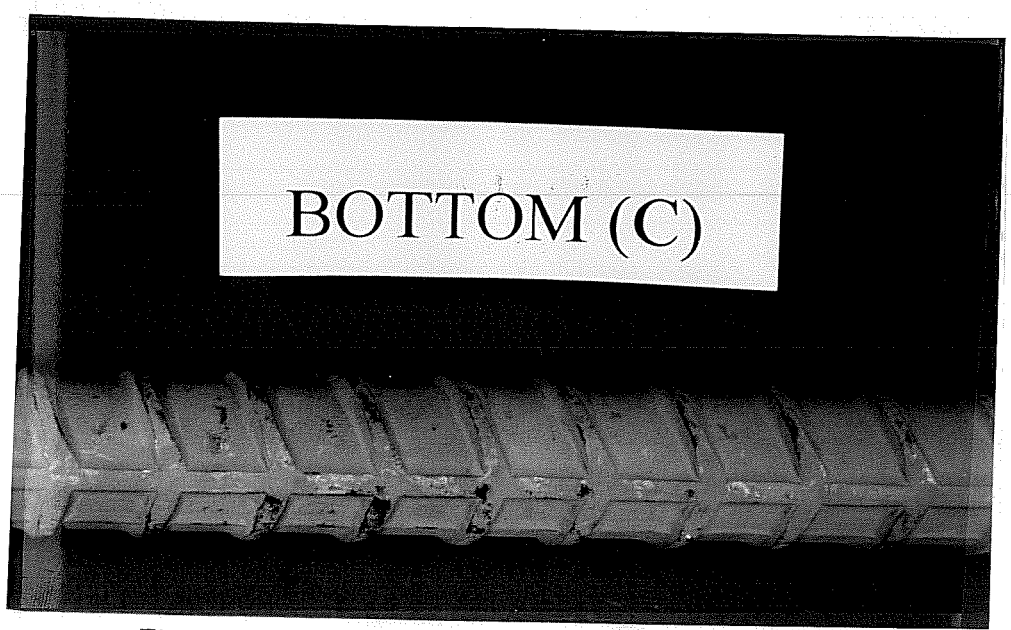

Figure 4- 11 Condition of zinc silicate-coated bottom steel

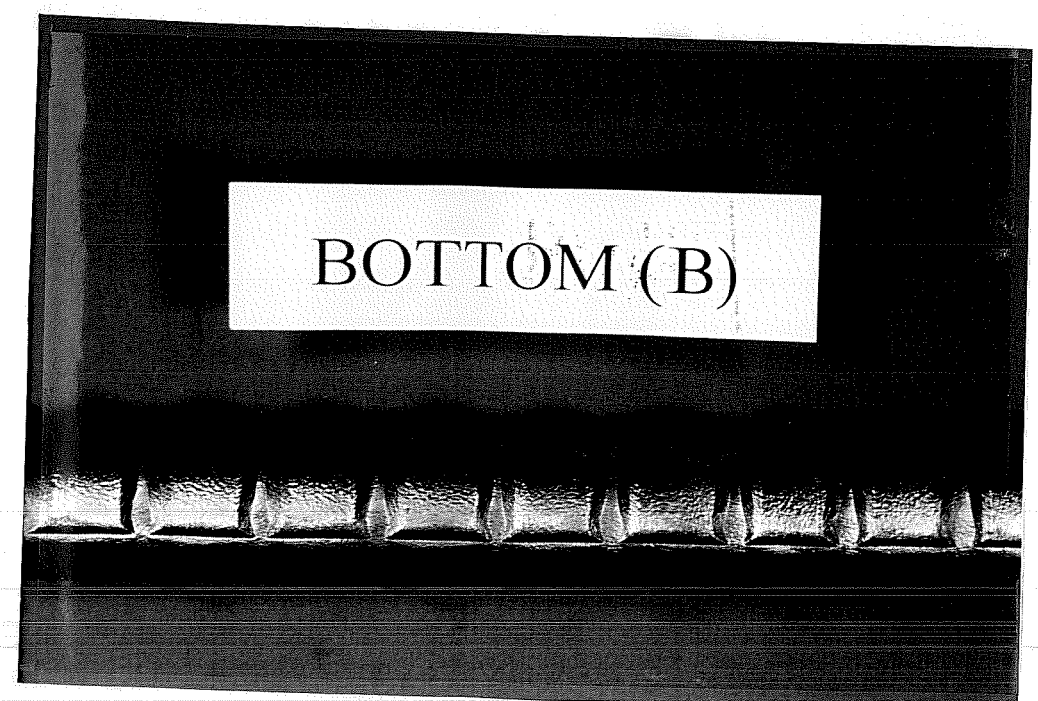

Figure 4- 12 Condition of uncoated cathode bars

estimated by the chloride cell was then compared to the chloride concentration found in the macrocell. This comparison provided a means of assessing the consistency of chloride diffusion in concrete.

In past experiments, significant variability was found in the chloride concentration data. Two macrocells sampled from the same depths at the same time have yielded very different chloride concentration readings. [12] This variability has been attributed to the lack of homogeneity in the concrete.

4.5 Construction of Formwork and Steel Placement

The forms for the macrocells and the chloride cells were constructed from 3/4" form-release plywood. For the macrocells, a single piece of plywood formed the base for a group of cells. Transverse lengths of plywood were fixed to vertical 2"x4" legs, which were in turn fixed to both the base plate and to 2"x4" wales around the base perimeter. Smaller longitudinal pieces of plywood separated the backs of the cells. The macrocell face plates were drilled to accommodate the top and bottom steel, and were screwed in place to the vertical legs after the top steel had been added. Longitudinal wales were also fitted to the outside faces of the macrocells at the level of the top steel. The top wales were used to hold the anode steel in position. Finally, transverse bracing was added to the tops of the vertical legs to increase the rigidity of the formwork. Figure 4.13 shows the formwork upon completion.

The final step in formwork construction was to secure the steel in place against movement. Once positioned, the top steel was anchored with wire ties wrapped around the protruding ends. The bottom steel was held in place by driving wedges under the ends of the bars. Figure 4.14, below, shows the top and bottom steel anchored in position prior to concrete placement.

The chloride cell formwork was constructed similarly to the macrocell formwork. However, due to the smaller size of the chloride cells, the transverse bracing, legs, and top wales were omitted. Figure 4.15 shows the completed chloride cell formwork.

4.6 Concrete Placement

The concrete was placed in one lift using a wheel barrow and shovel. A vibrator was used to consolidate the concrete in each cell. In the macrocells, the vibrator was applied carefully at the back of the cells to avoid shifting the steel or damaging the coatings.

Twenty-one 6"x12" cylinders and four 4"x8" cylinders were cast from the same mix. Standard lifts and consolidation procedures were used in placing the cylinders. The cylinders were later used for strength and permeability tests.

After placement, all cells and cylinders were screeded, trowelled, and hand-finished. The concrete was then covered with plastic and allowed to cure on location. The formwork was stripped approximately 2 weeks after placement. All cylinders, macrocells, and chloride cells were removed from the forms at the same time.

4.7 Sample Preparation

The final modifications were made to the macrocells in a two-week period following removal from formwork. First, short lengths of #3 reinforcing steel were welded across the ends of the cathode bars in each cell. These bus bars provided an electrical connection between the three #9 bars in the bottom mat of steel.

Figure 4- 13 Completed macrocell formwork

Two coats of water sealer were then applied to the side faces of the macrocells and chloride cells. The water sealer was designed to both prevent water leakage from the cells and to simulate an infinite slab with uniform lateral moisture content.

The free ends of the cathode bars were coated with a protective oil to prevent corrosion external to the concrete.

Next, acrylic dikes were attached to the tops of the macrocells and chloride cells. Silicon caulk was used because it adhered well to the concrete and provided a water-tight seal around the base of the dikes.

The last step in preparation was to assemble the conductor and data leads. Equal lengths of double-conductor digital cable were measured and cut for each macrocell. At one end, the digital cable was soldered to the conductor and resistor linking the top and bottom steel. The other end of the digital cable was connected to the computer interface for the data acquisition system. Electrical clamps were placed on the top and bottom bars of each macrocell, and the conductors were attached with spade connectors to the clamps. Finally, the macrocells and chloride cells were arranged on a series of shelves and testing was begun. Figure 4.16 shows the macrocells prior to first exposure.

4.8 Evaluation of Macrocells

Three methods were used to evaluate the corrosion behavior of the coatings. First, the corrosion potential data were used to construct the corrosion current time histories and charge flow plots. These plots indicated the theoretical corrosion damage to the coatings. Higher currents indicated greater corrosion activity, and higher charge flow indicated greater cumulative corrosion damage.

Second, external observations were taken of the macrocells throughout the life of the experiment. Cracks and corrosion products were noted and described as they became evident on the exterior of the cells.

Finally, cells were removed from testing and visual inspections were conducted. The first round of autopsies took place after seven months of exposure, when one third of the cells were taken out of

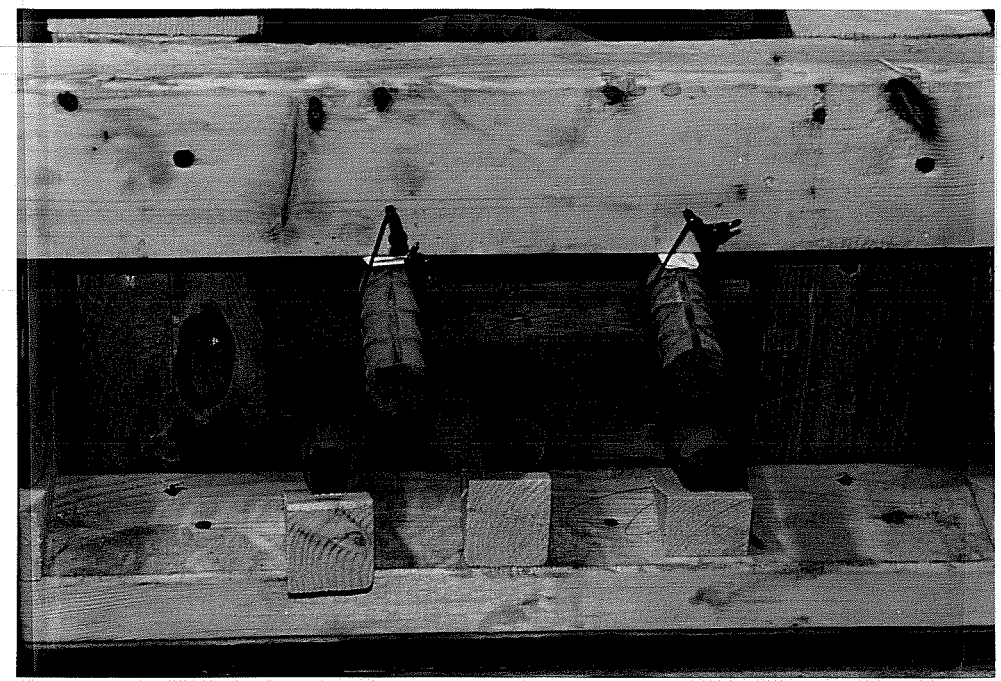

Figure 4- 14 Top and bottom steel anchored in place

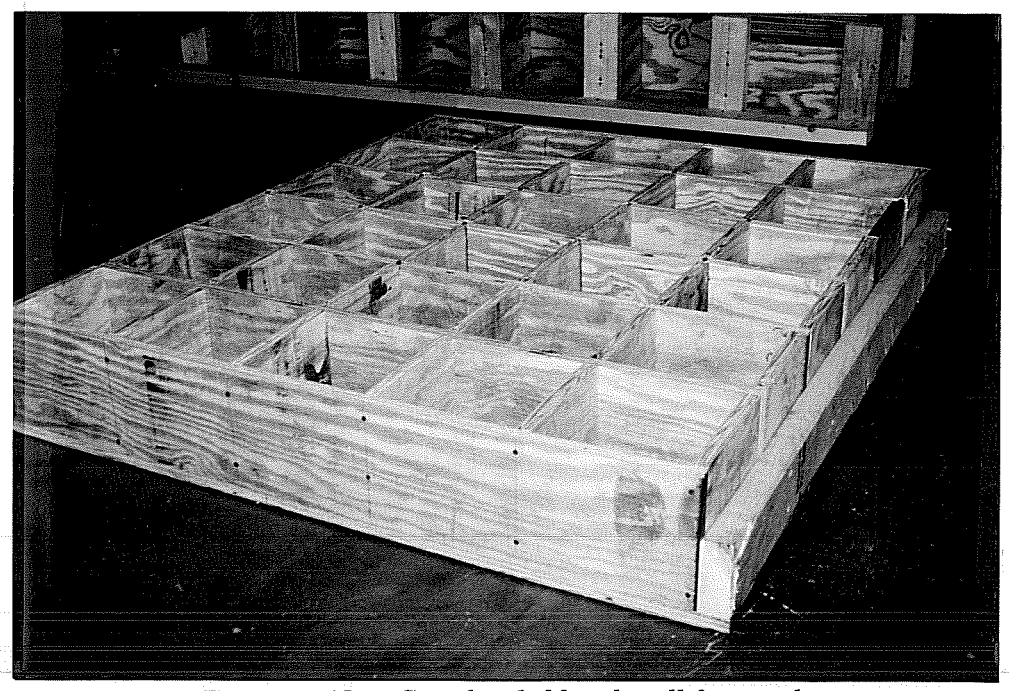

Figure 4- 15 Completed chloride cell formwork

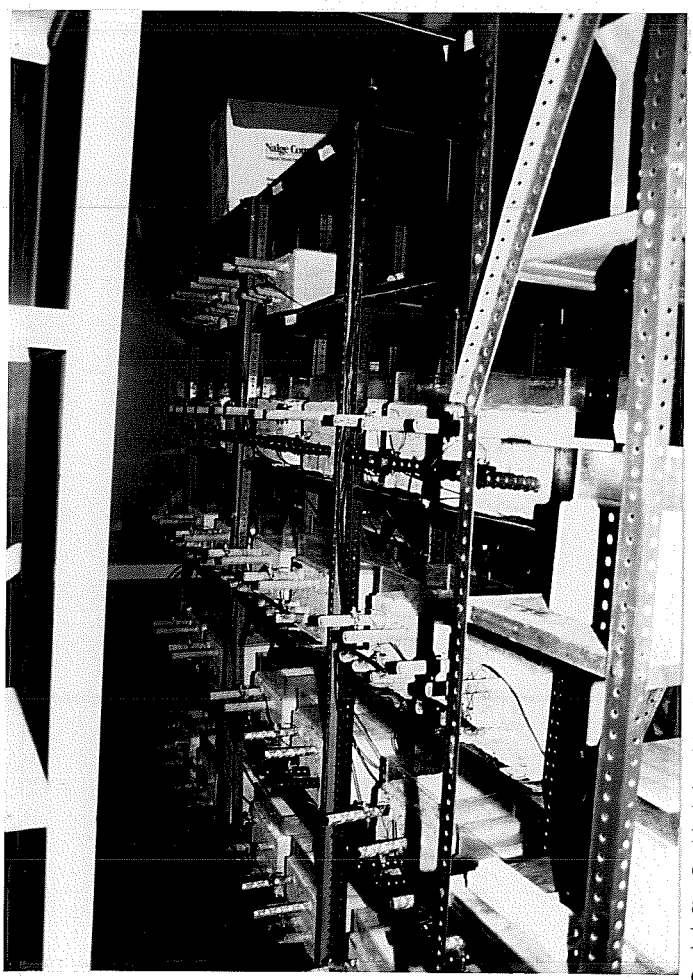

Figure 4- 16 Macrocells prior to first exposure

testing. In each cell group, the median sample as defined by the predicted corrosion damage was selected for the autopsy. This selection process kept the cells with the highest and lowest levels of damage in the experiment. To conduct the visual inspection, the selected cells were removed from the test apparatus and cut with a hand-operated circular concrete saw. Cuts were made around the perimeter of the macrocells at a level 1/4" below the bottom of the top steel. A single cut was made on the top face to a depth of 3/4", terminating 1/4" above the top face of the anode steel. Figure 4.17 shows the saw cuts that were made to the macrocells.

A pry-bar was inserted into the saw cuts and struck with a hammer, separating the top later of concrete and anode steel from the rest of the macrocell. The legs of the top steel were then tapped with the hammer to remove any remaining fragments of concrete.

Each anode bar was examined carefully upon removal from the macrocells. Observations concerning the levels and locations of corrosion, and the corrosion products seen, were recorded. Photographs were also taken of each bar. All observations had to be taken quickly, as the corrosion products tended to react with the atmosphere and change color.

A second round visual inspections was conducted after thirteen months of exposure. The macrocells from each group with the highest corrosion currents and charge flux were inspected at that time. The final inspections in the remaining macrocells were conducted after nearly 24 months of exposure.

4.9 PROCEDURAL MODIFICATIONS

After 8 months of exposure, the front face of 1/2 of the remaining macrocells were coated with an epoxy patching compound. The cells with the highest corrosion current activity in each pair were selected for this treatment. The following were coated: NC3, NB3, WC2, WB2, EC3, SB3, SC1, GB1, GC2. In all cases except NC3, the cells chosen also had the highest cumulative charge flow in each pair.

This modification was performed to more effectively seal the macrocells from oxygen diffusion around the protruding bars. It was found in the first autopsy that corrosion on the zinc silicate-coated bars was concentrated in the first inch within the concrete. It was believed that the corrosion concentrated near the exterior face due to higher concentrations of oxygen. Oxygen participates in the cathodic reaction and in secondary reactions that consume dissolved metal ions.

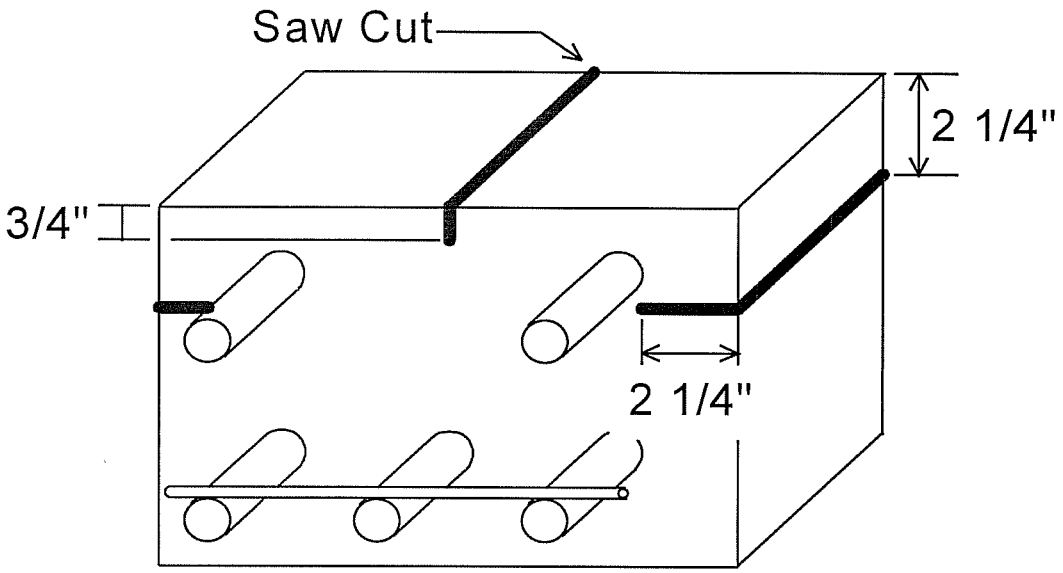

Figure 4- 17 Diagram of cuts made to macrocells

The additional sealing was deemed acceptable because rarely in the field will reinforcing steel protrude from the concrete mass and become exposed to high levels of oxygen.

A second coat of epoxy sealer was applied to the same macrocells after 11 months of exposure. At that time, silicon caulk was also applied to the face of the cells around the anode bar legs to increase the effectiveness of the vapor barrier.

CHAPTER 5

TEST RESULTS

5.1 INTRODUCTION

The first exposure cycle began on September 1, 1993, and continued for twenty-five, 28-day exposure cycles. Data from the nine test groups were taken at weekly intervals during this period. One specimen from each group was removed from testing after 7, 13 and 24 months, and the bars were removed from the concrete for visual inspection. The corrosion current and cumulative charge flow data are presented and discussed, as well as the results from visual inspections. Finally, corrosion products and chloride concentration data are discussed in the final sections of the chapter.

5.2 CORROSION CURRENT DATA

5.2.1 Plots

Figures 5.1-5.9 are presented below, and give the corrosion currents as a function of time for all the macrocell groups. The currents represent the flow of electrons from the top steel to the bottom steel. A high negative current is indicative of significant corrosion.

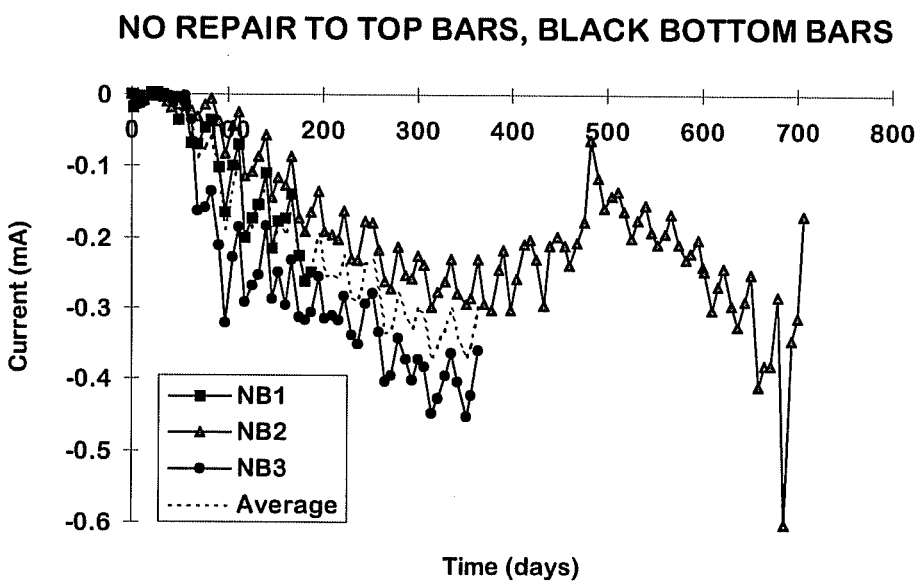

Figure 5- 1 Corrosion currents: Group 1

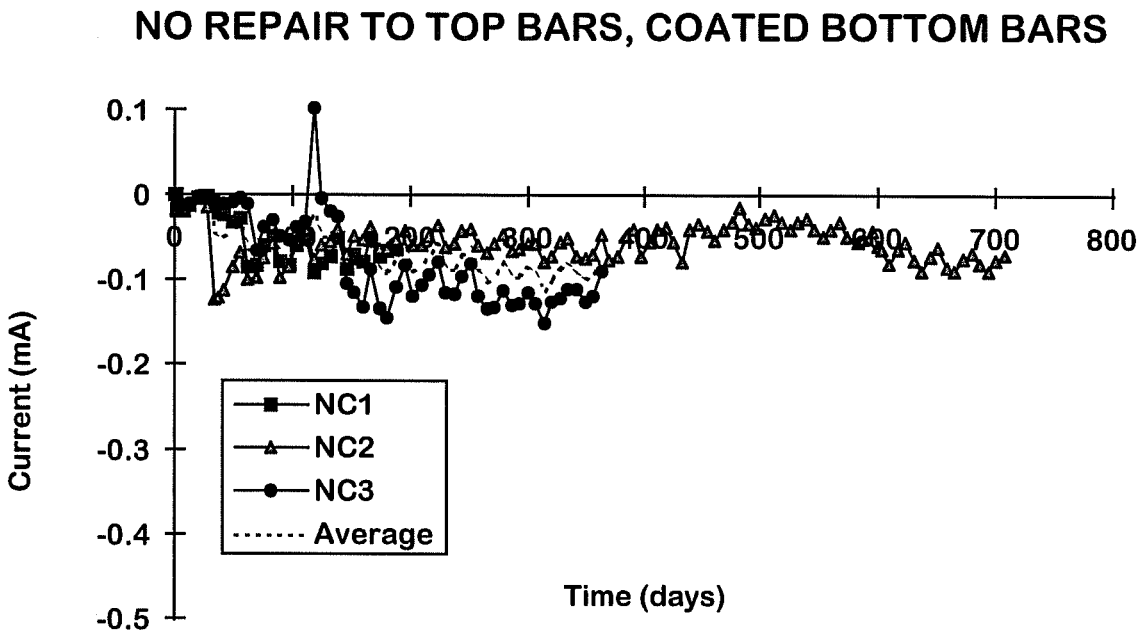

Figure 5- 2 Corrosion currents: Group 2

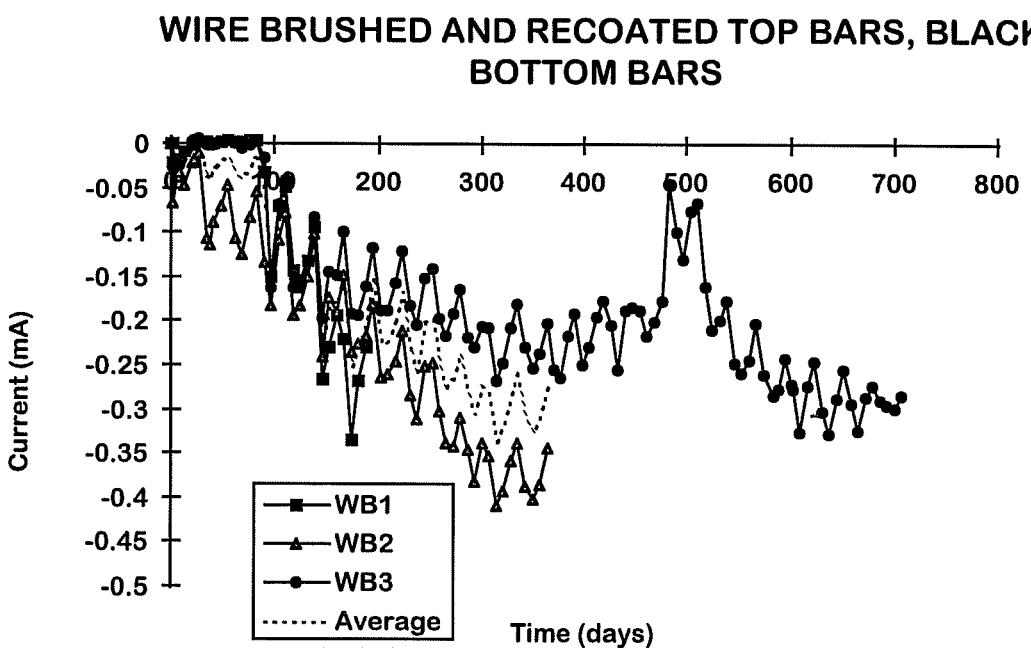

Figure 5- 3 Corrosion currents: Group 3

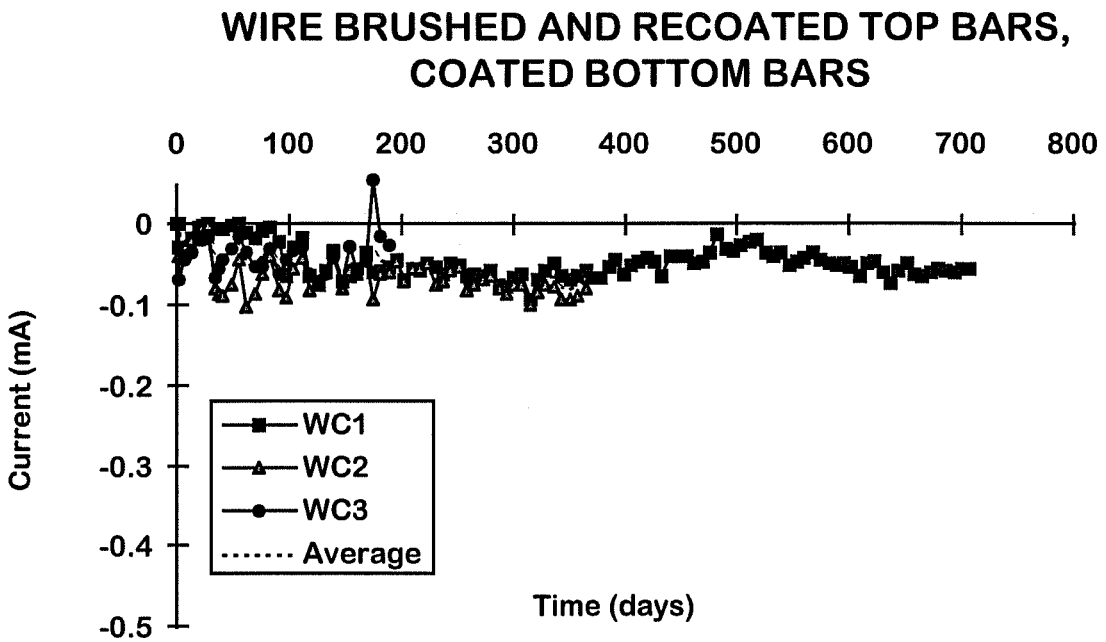

Figure 5- 4 Corroson currents: Group 4

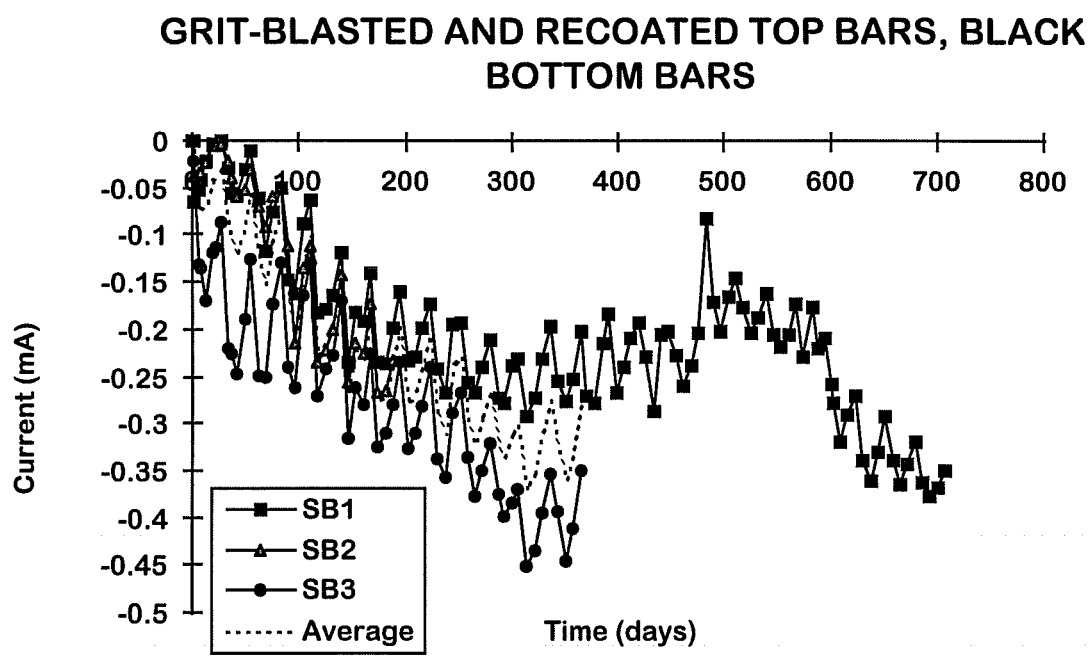

Figure 5- 5 Corrosion currents: Group 5

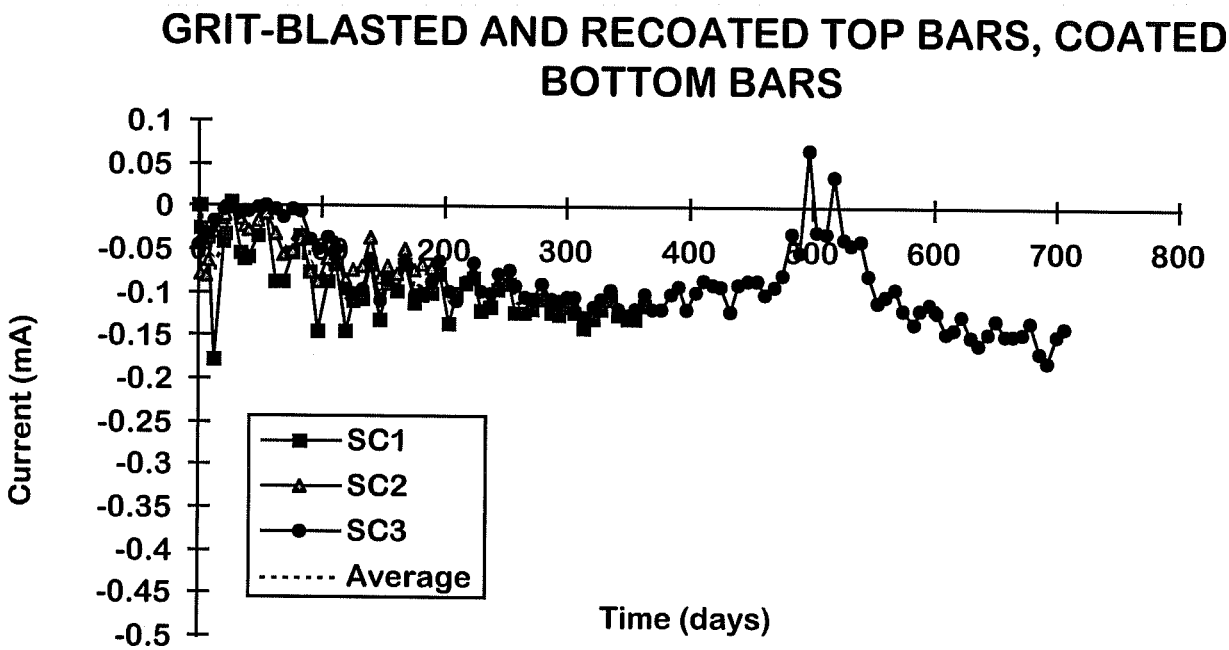

Figure 5- 6 Corrosion currents: Group 6

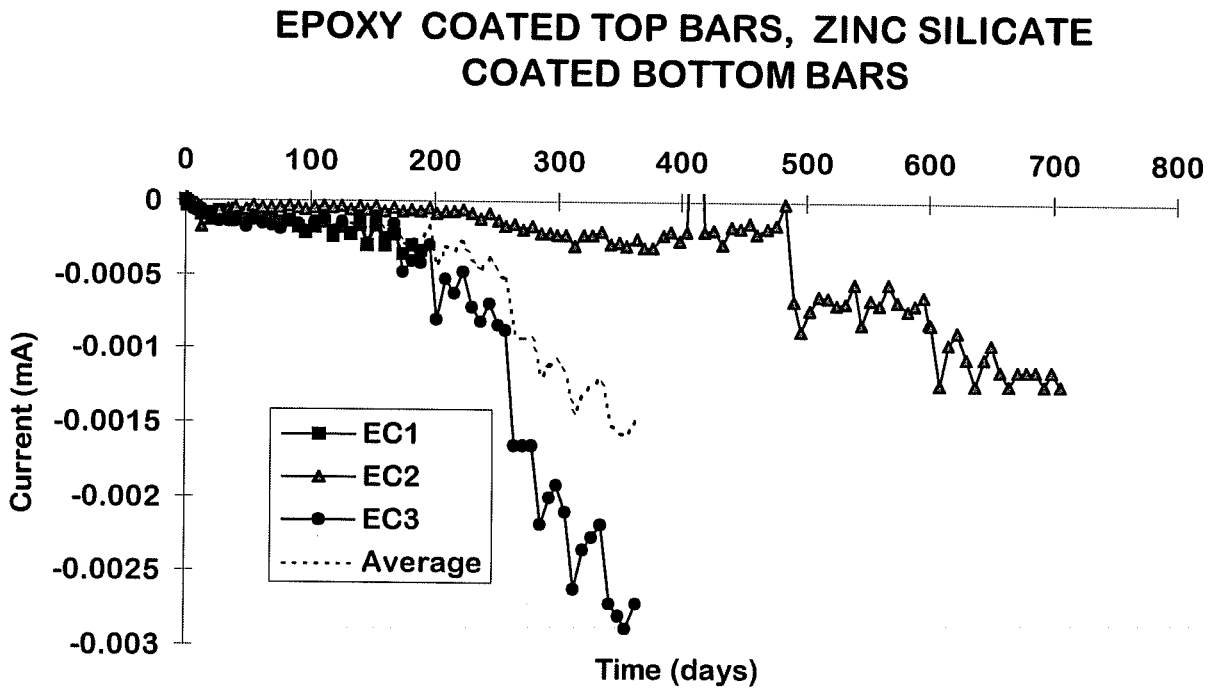

Figure 5- 7 Corrosion currents: Group 7

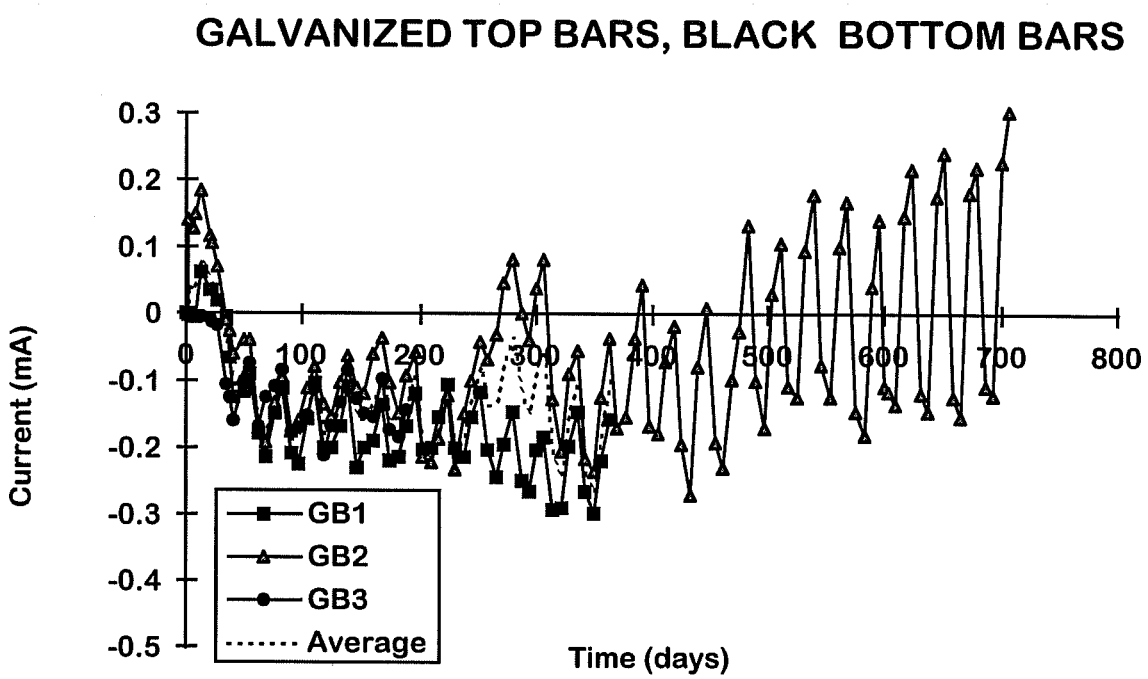

Figure 5- 8 Corrosion currents: Group 8

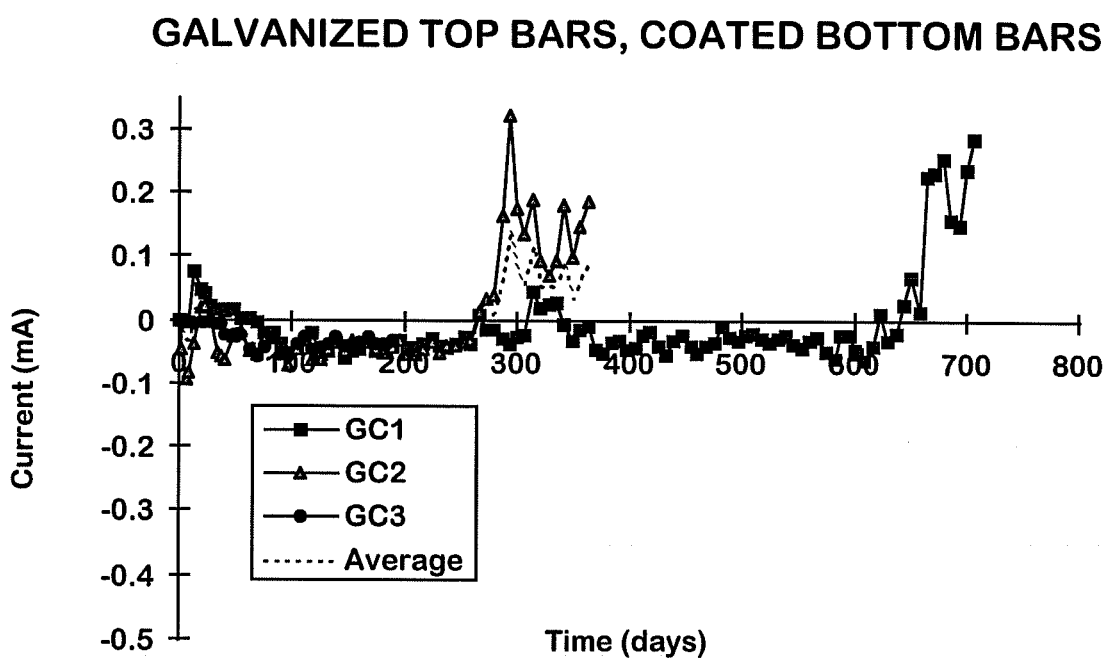

Figure 5- 9 Corrosion currents: Group 9

5.2.2 Analysis of Corrosion Current Data

High Ratio Zinc Silicate-Coated Top Steel: Analysis of the corrosion currents shows the approximate time when corrosion began to take place. In the case of uncoated bars (black), the time to corrosion was approximately 50-100 days. The time to corrosion is indicated in each case by the first significant dip in the graphs.

Both the galvanized and the high ratio zinc coatings are active, in that the coatings themselves are expected to corrode when environmental conditions become sufficiently aggressive. The initiation time for macrocells with black (uncoated) cathodes was similar to that of the black top bars (anodes). However, for macrocells with both anodes and cathodes coated, the initiation time was considerably longer. The initiation time represents the period required for sufficient water and chlorides to diffuse through the one inch of concrete cover, underscoring the benefits of providing more cover.

The corrosion plots clearly delineate the exposure cycles. Once corrosion initiated, the beginning of a wet cycle was marked by a sharp decline in the corrosion current graphs. The values continue to decrease up to the end of the wet cycle, curves increase during the dry portion of the exposure cycle and reach a peak at the end of that period. Subsequent peaks are spaced at 4-week intervals.

Figures 5.1-5.6 reveal several noteworthy differences between the high ratio zinc silicate specimens with uncoated and coated cathodes. The specimens with the coated bottom steel (cathodes) showed currents that were significantly lower in magnitude than the uncoated specimens. The coated macrocells, Figures 5.2, 5.4 and 5.6, showed maximum corrosion currents between -0.10 and -0.15 mA and the curves were comparatively smooth. The long term increases in corrosion current magnitudes were very small and the rates did not appear to increase as the cycles continued.

In contrast, the macrocells with uncoated cathode steel demonstrated much greater corrosion activity . Figures 5.1, 5,3, and 5.5 show maximum corrosion current magnitudes of about -0.4 mA. Differences between peak values at the end of the wet and dry periods of the exposure cycles were considerably greater than in the macrocells with coated bottom bars.

The difference in corrosion performance may be explained in terms of the anode/cathode ratio. In a corrosion cell, the cathode functions only as the site of an electron-consuming reaction. The coated bottom steel in the macrocells provided a more resistive surface than the uncoated steel, effectively shrinking the size of the available cathode. With smaller cathodes, identical anodes and equivalent exposure conditions, the samples with coated bottom steel had a much larger anode/cathode ratio than the uncoated samples. Less corrosion damage would be expected in the cells with the coated bottom bars, due to this higher anode/cathode ratio.

Finally with respect to the zinc silicate samples, very few differences may be seen between the three coating conditions. The unrepaired, wire-brushed and repaired, and grit-blasted and repaired showed very similar corrosion current patterns.

Epoxy-Coated Top Steel: The epoxy-coated samples showed a much longer time to corrosion than the zinc-based coatings, requiring a minimum of 200 days for corrosion to initiate (see Figure 5.7). The longer delay resulted from the inactive nature of the epoxy coatings. The time to corrosion was the time required for water and chlorides to both diffuse to the level of the top steel and penetrate the epoxy barrier. No barrier penetration was necessary to produce corrosion currents in the case of the zinc-based coatings.

The epoxy-coated samples showed very low corrosion currents (about 1%) compared with the other coating schemes. (Note that the scale used in Figure 5.7 is 1/100 of the scale used in all other figures.) This current was produced solely by the corrosion of the steel; there was no sacrificial metal in the epoxy coating to provide additional currents.

Corrosion of epoxy-coated steel has only been known to occur where breaks occur in the coating, and the coatings used in these macrocells showed no visible damage prior to concrete placement. Therefore, the lower currents were expected.

Galvanized Top Steel: Overall, the galvanized samples (Figs. 5.8 and 5.9) demonstrated similar corrosion current behavior to the high ratio zinc silicate samples. The cells with uncoated bottom steel showed more activity than the samples with the coated bottom steel. However, the corrosion current magnitudes were significantly lower in the galvanized samples than in the zinc silicate samples. Also, the galvanized-bar corrosion currents did not appear to increase with time on the same scale as the zinc silicate specimens. Less corrosion appeared to take place in the galvanized macrocells.

An anomaly did occur with the galvanized specimens after approximately 250 days of exposure. In both the GB and the GC macrocells, the currents became erratic and fluctuated between negative and positive. The top steel in some of the macrocells became cathodic to the bottom steel. This behavior corresponded approximately with the appearance of corrosion products and cracking on the top surface of the macrocells.

When the bars were inspected, it was discovered that some corrosion was taking place on the bottom steel within the concrete. It would therefore seem that as the zinc in the galvanized coatings became depleted, the top steel was not able to protect the bottom steel from corrosion as chlorides began to reach the level of the cathodes. Anodic dissolution then began to take place on both the top and bottom steel, disturbing the corrosion potentials.

5.3 CHARGE FLOW DATA

5.3.1 Plots

Figures 5.10 -5.18 are presented below, and give the plots of total charge flow as a function of time for all the macrocells. Values were computed by integrating the current vs. time graphs in section 5.2.1, using a trapezoidal approximation. The total charge flow indicates the number of electrons that have participated in macrocell corrosion. High negative values therefore indicate high predicted corrosion damage.

5.3.2 Analysis of Charge Flow Data

High Ratio Zinc Silicate-Coated Anodes: The charge flow plots in Figures 5.10-5.15 indicate that more corrosion took place in the macrocells using uncoated cathodes than the cells with coated cathodes. The specimens with uncoated cathodes (Figures 5.10, 5.12, and 5.14) gave average total charge values about 2.5 to 3 times the values for the coated specimens (Figures 5.11, 5.13, and 5.15). Based on the total charge flow, the specimens with uncoated bottom steel may have experienced about 2.5 times the corrosion damage of the specimens with coated bottom steel. The specimens with uncoated cathodes appeared to corrode at increasing rates, while the corrosion rates of the coated cathode specimens

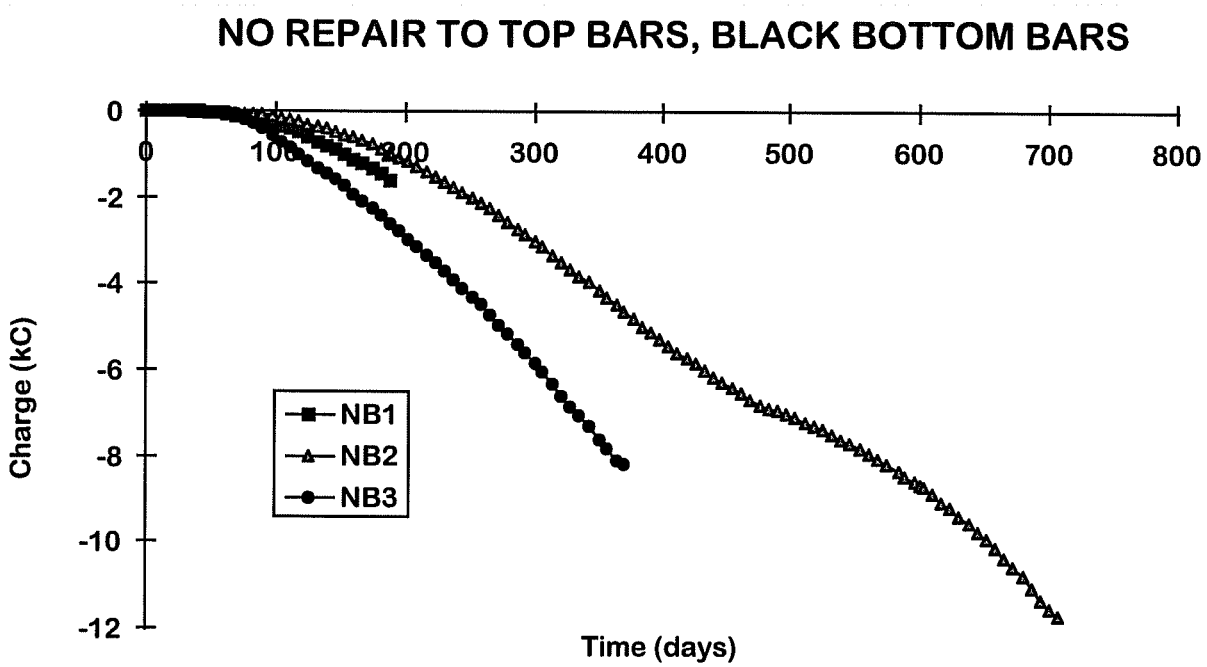

Figure 5- 10 Cumulative charge flow/damage: Group 1

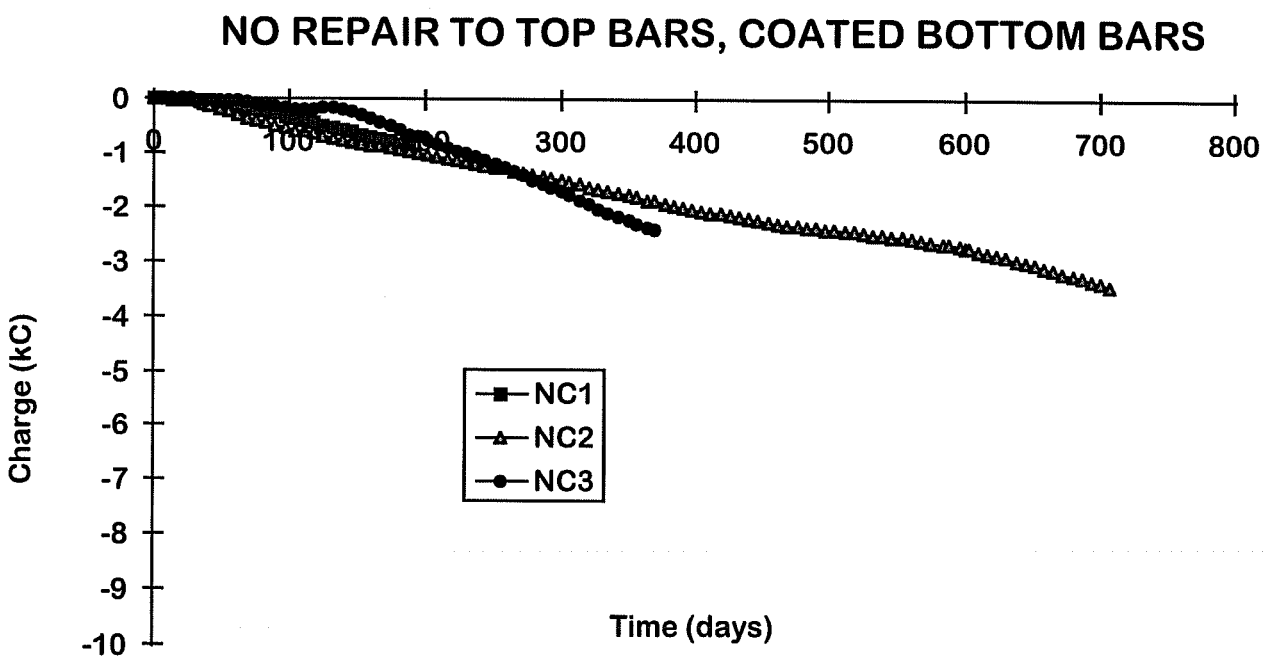

Figure 5- 11 Cumulative charge flow/damage: Group 2

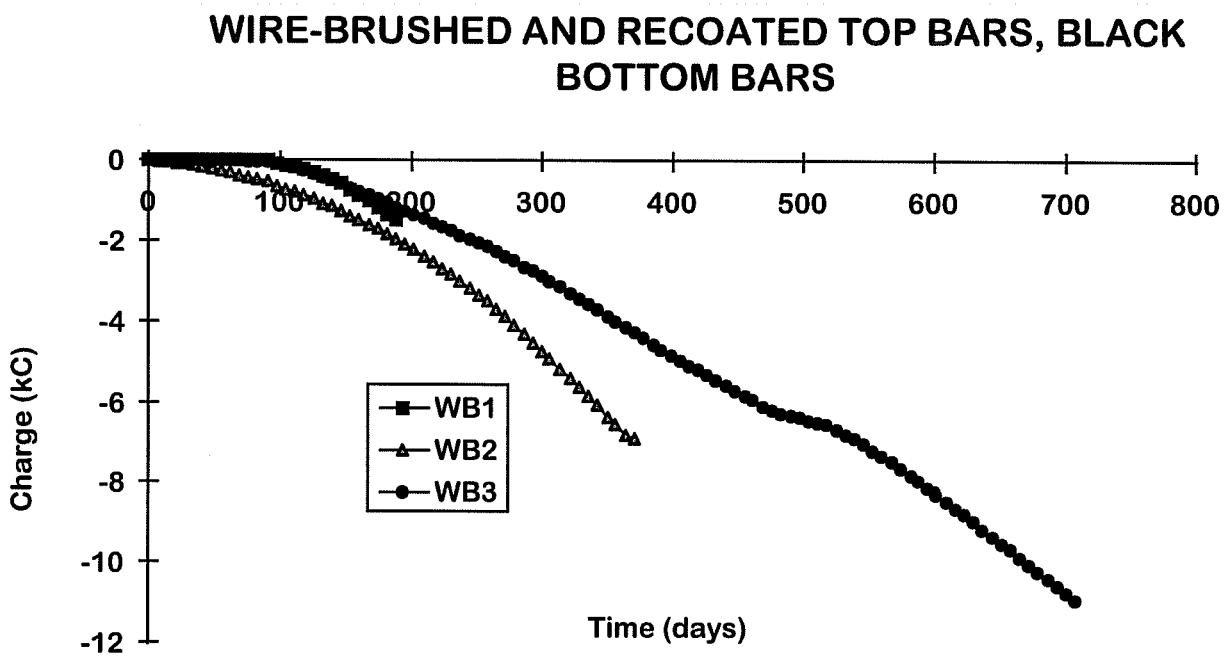

Figure 5- 12 Cumulative charge flow/damage: Group 3

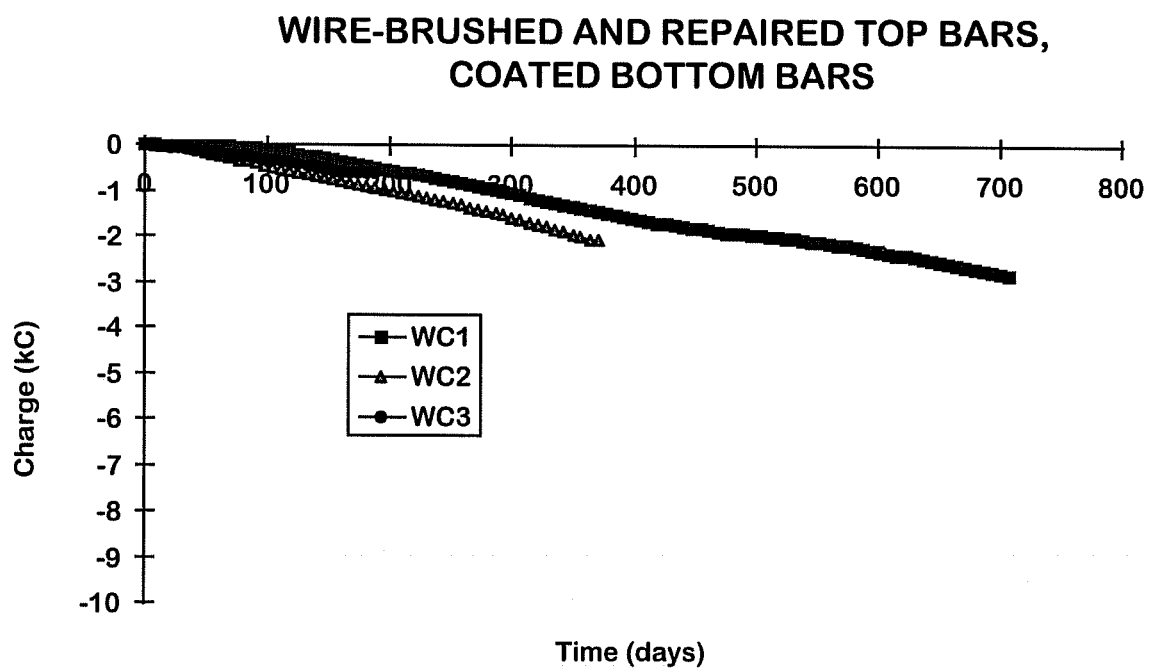

Figure 5- 13 Cumulative charge flow/damage: Group 4

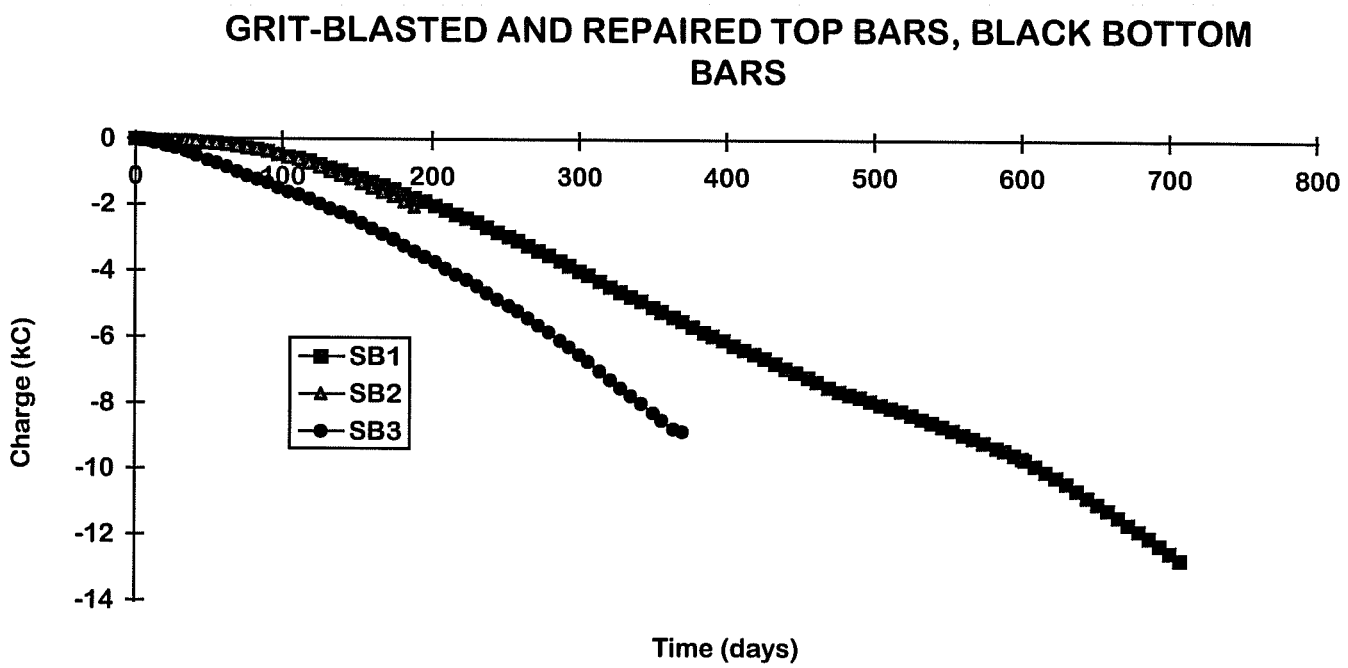

Figure 5- 14 Cumulative charge flow/damage: Group 5

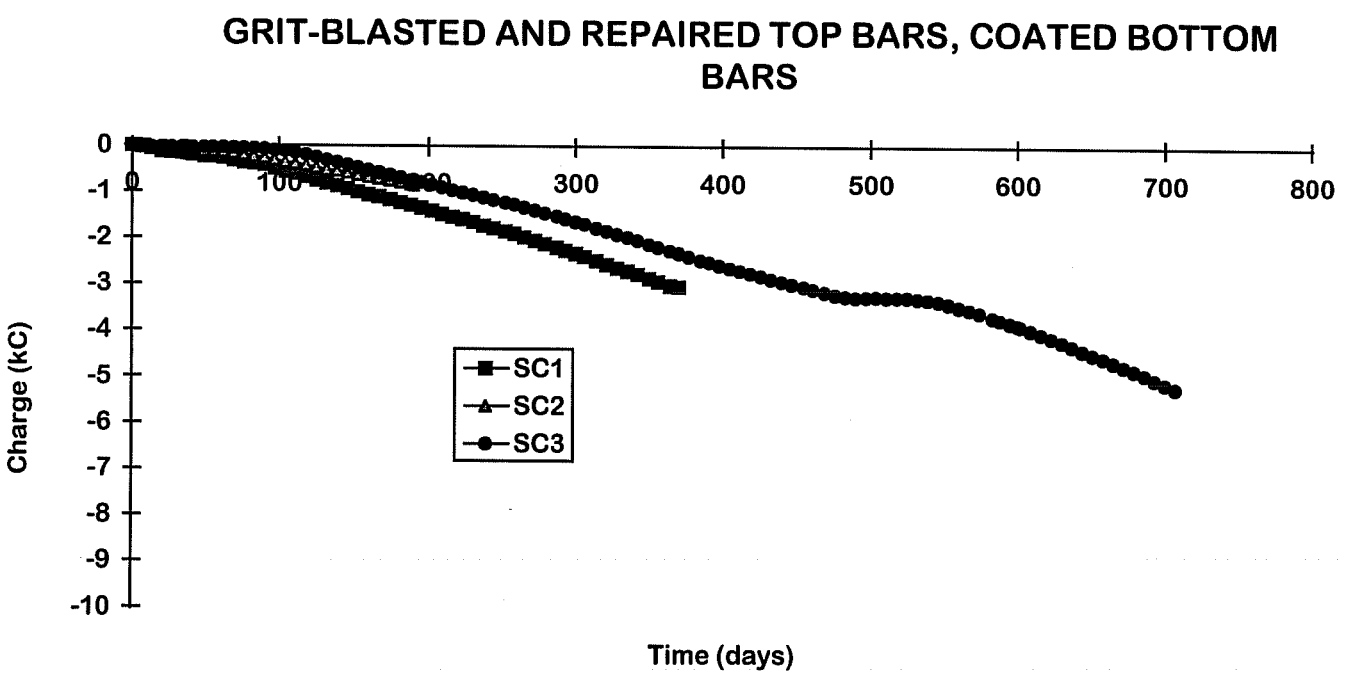

Figure 5- 15 Cumulative charge flow/damage: Group 6

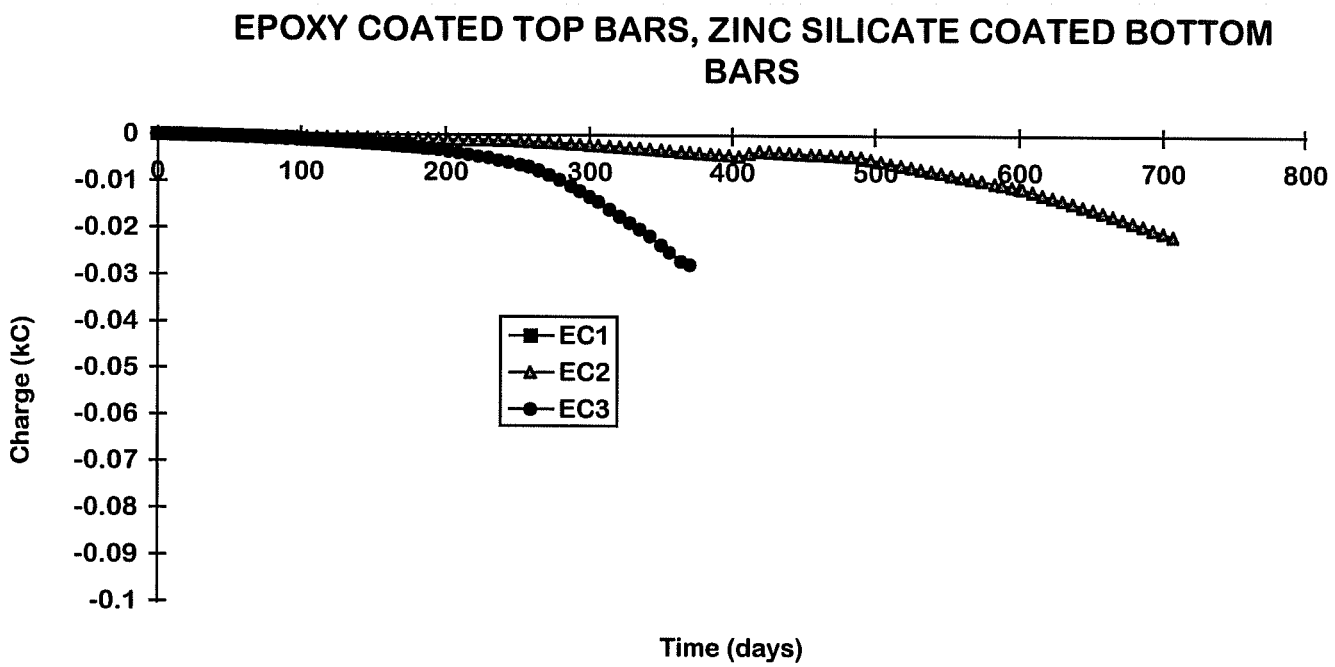

Figure 5- 16 Cumulative charge flow/damage: Group 7

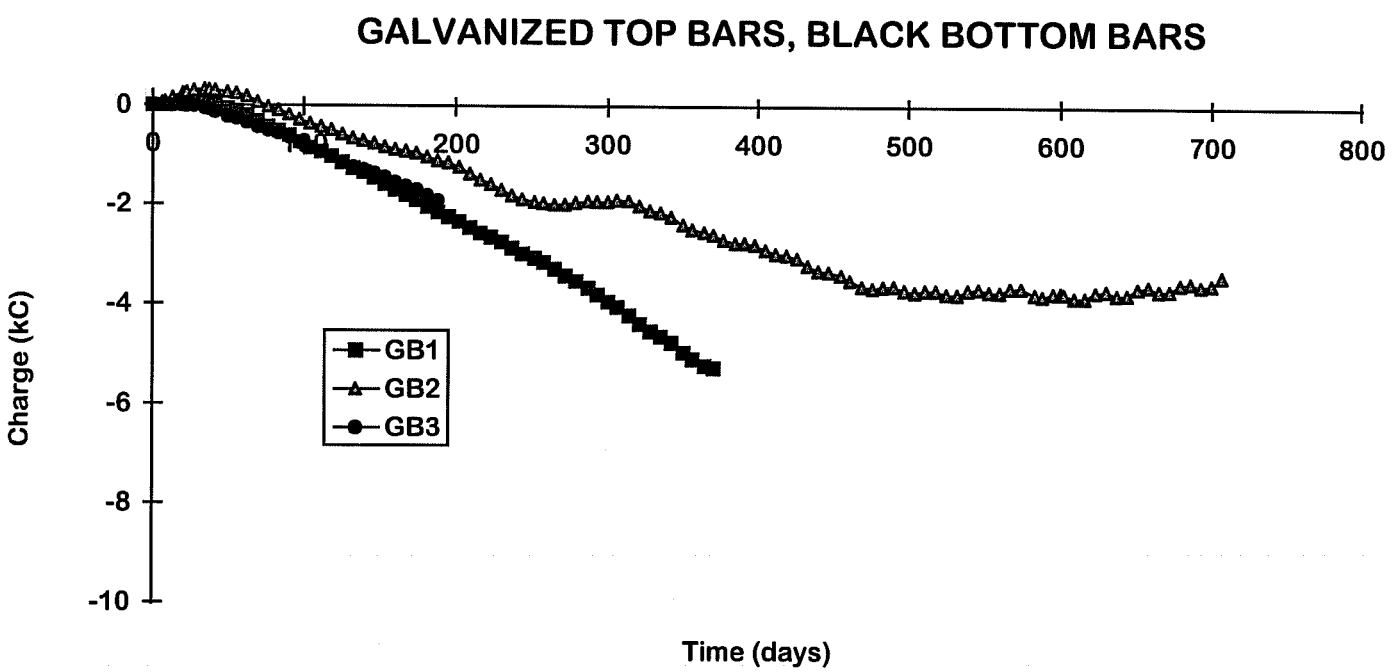

Figure 5- 17 Cumulative charge flow/damage: Group 8

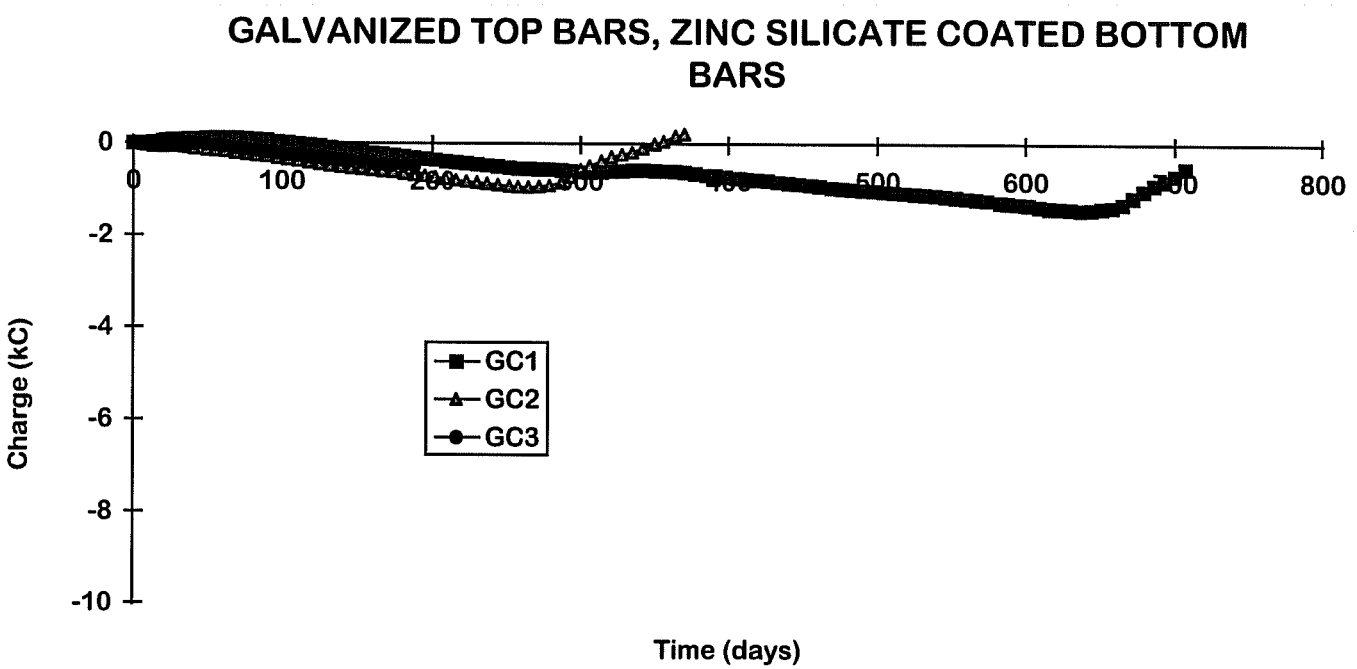

Figure 5- 18 Cumulative charge flow/damage: Group 9

remained comparatively constant. Visual inspection (Sec. 5.4) confirmed this trend. The difference in degree of corrosion of the coated cathode specimens and the uncoated cathode specimens was greater at 24 months than at 13 months and greater at 13 months than at 7 months.

Epoxy-Coated Anodes: Figure 5.16 describes the macrocells with epoxy-coated anodes and high ratio zinc silicate-coated cathodes. The average total charge flow value for this group of specimens is approximately 100 times lower than the zinc silicate specimens with coated cathodes. The epoxy specimens showed no significant corrosion.

Galvanized Anodes: The galvanized samples (Figs. 5.17 and 5.18) showed the same corrosion patterns as the high ratio zinc specimens. The cells with coated cathodes indicated lower predicted damage and fairly constant corrosion rates, while the cells with uncoated cathodes showed higher values of charge flux and generally increasing corrosion rates. Based on charge flow, the galvanized bars would appear to have corroded less than the zinc silicate samples, however this was not found to be the case on inspection.

Positive corrosion currents caused the graphs for specimens GB2, GC1, and GC2 to fluctuate and curve upward, indicating a shifting of the anode/cathode relationship. As mentioned, it appeared as if anodic dissolution was taking place on the bottom steel. On further inspection, a small amount of corrosion was found on the cathode steel within the concrete.

Summary: Comparison of Damage Predictions: The damage predictions have been summarized below in Table 5.1 for the specimens removed after 13 and 24 months. The macrocells have been listed in order of increasing damage, as predicted by charge flux at 13 months. Only one charge flow changed position between 13 and 24 months. It is evident from table 5.1 that both the epoxy and galvanized specmens would be expected to show less damage than the corresponding high ratio zinc silicate specimens

considering only the charge flow. The specimens with coated cathodes would be expected to exhibit less corrosion than those with uncoated bottoms bars. The bars that were grit-blasted and repaired were predicted to have the most corrosion damage.

Table 5- 1 *Summary of total charge flux values in order of increasing damage prection*

MACROCELL	DESCRIPTION	CHARGE FLOW (kC)	
		13 months	24 months
EC2	Epoxy-Coated Anodes; Coated Cathodes	-.020	-0.02
GC1	Galvanized Anodes; Coated Cathodes	-.11	-0.52
WC1	Wire-Brushed and Repaired Anodes; Coated Cathodes	-1.8	-2.8
NC2	Unrepaired Anodes; Coated Cathodes	-2.1	-3.4
SC3	Grit-Blasted and Repaired Cathodes; Coated Anodes	-2.8	-5.2
GB2	Galvanized Anodes; Uncoated Cathodes	-4.6	-3.4
WB3	Wire-Brushed and Repaired Anodes; Uncoated Cathodes	-5.9	-10.9
NB2	Unrepaired Anodes; Uncoated Cathodes	-7.1	-11.7
SB1	Grit-Blasted and Repaired Anodes; Uncoated Cathodes	-7.7	-12.7

5.4 *INSPECTION AFTER EXPOSURE*

5.4.1 Corrosion Locations

7-Month Inspection

In the case of all the high ratio zinc silicate specimens, corrosion was concentrated primarily in a zone extending 3 inches from the front faces of the macrocells. Corrosion was not specific to the resistor or non-resistor side, with three of the six samples showing more corrosion on the bar leg without the connection to the cathode steel. In earlier tests, [12] and in the galvanized specimens, corrosion was concentrated around the bend on the resistor side of the bars, reflecting a distance effect and macrocell action. The same mechanism did not appear be present in these tests with the zinc silicate specimens. Very little widespread corrosion was observed around the bends of the bars. Corrosion was the most severe near the front face, and in areas where voids in the concrete came into contact with the bars. Severe attack was observed in some cases at these void locations. Figure 5.19 is indicative of the corrosion found on the high ratio zinc silicate specimens.

The prominence of corrosion at the front-face locations indicates that the corrosion mechanism in the specimens during the first six months of exposure was likely the result of the test specimen geometry and was the result of microcell, rather than macrocell, action. Corrosion was concentrated in the areas highest in oxygen content, both in the specimens with uncoated cathodes and in the specimens with zinc silicate-coated cathodes. Oxygen affects corrosion primarily through the cathodic reaction, suggesting that both anodic and cathodic reactions were taking place on the top steel coated with the high ratio zinc silicate. Microcell corrosion near the front face was the initial governing mechanism with the new zinc silicate specimens.

Figure 5- 19 Corrosion locations typical of high ratio zinc silicate specimens

The galvanized specimens did not show similar patterns of corrosion. The most severe corrosion was around the bends of the bars. Corrosion was more uniform and widespread over the galvanized bar surface area, indicating macrocell behavior.

13-Month Inspection

Consistent with the 7-month Inspection, the high ratio zinc specimens opened after 13 months all showed corrosion in the first 1-3 inches from the front face of the macrocells. The additional vapor barrier applied after 8 months of exposure did not appear to halt corrosion in this area. No definite preference was shown for the resistor or the non-resistor ends of the bars. This corrosion damage again indicated microcell action, governed by the higher levels of oxygen near the face of the cells where the bars protruded.

In addition to the above observed pattern of corrosion, corrosion was noted over the straight and bent portions of the bars in 2 high ratio zinc specimens (SB3 and NB3), especially on the underside of the bars. This corrosion damage indicated that as more zinc coating became depleted, macrocell action was initiated.

Corrosion on galvanized bars after 13 months was similar to that occurred after 7 months but with increased deterioration. In contrast to high ratio zinc bars, the most severe corrosion on galvanized bars occurred around the bends of the bars. The galvanized bar corrosion was uniform and widespread over the bar surface area, indicating macrocell behavior.

Severe, localized corrosion was observed in both high ratio zinc and galvanized specimens in locations where voids in the concrete contacted the bar surface. For example, sample WB2 showed an isolated area of corrosion at a void, even though the surrounding coating was in very good condition and should have been controlled by sacrificial action. Severe local exposure appeared to overwhelm the galvanic capabilities of the coating in this instance. In contrast, there were other voids along the same bar that produced no corrosion. A high chloride concrete environment therefore appears to be able to limit the local effectiveness of galvanic action under some conditions - even when galvanic action in a global sense is taking place.

High ratio specimens demonstrated a slight tendency to corrode more on the underside of the anode bars than on the top surfaces. In every instance where there was a significant difference in corrosion between the top and bottom of the bar, the bottom was more heavily corroded. This pattern was observed in 4 of the 6 high ratio specimens. All three specimens with uncoated cathodes were in this group. Figures 5.20 and 5.21 illustrate the higher levels of corrosion on the underside of the bars.

In contrast, the galvanized specimens were seen to corrode most severely on the top surfaces of the bars. Higher levels of corrosion in the galvanized specimens caused the concrete to crack, bringing more oxygen into contact with the tops of the anodes. It is expected that this crack-driven corrosion caused the galvanized bars to corrode more heavily on the top surfaces. Figure 5.22 shows the pattern of galvanized bar corrosion.

24-Month Inspection

Specimens examined after 24 months of exposure exhibited many of the corrosion patterns previously observed after 7 and 13 months of exposure. Rust appeared in the first 1-3 inches from the front face of the macrocells. No corrosion preferential was observed for the resistor or the non-resistor ends of the

Figure 5- 20 Corrosion: Top surface of NB3

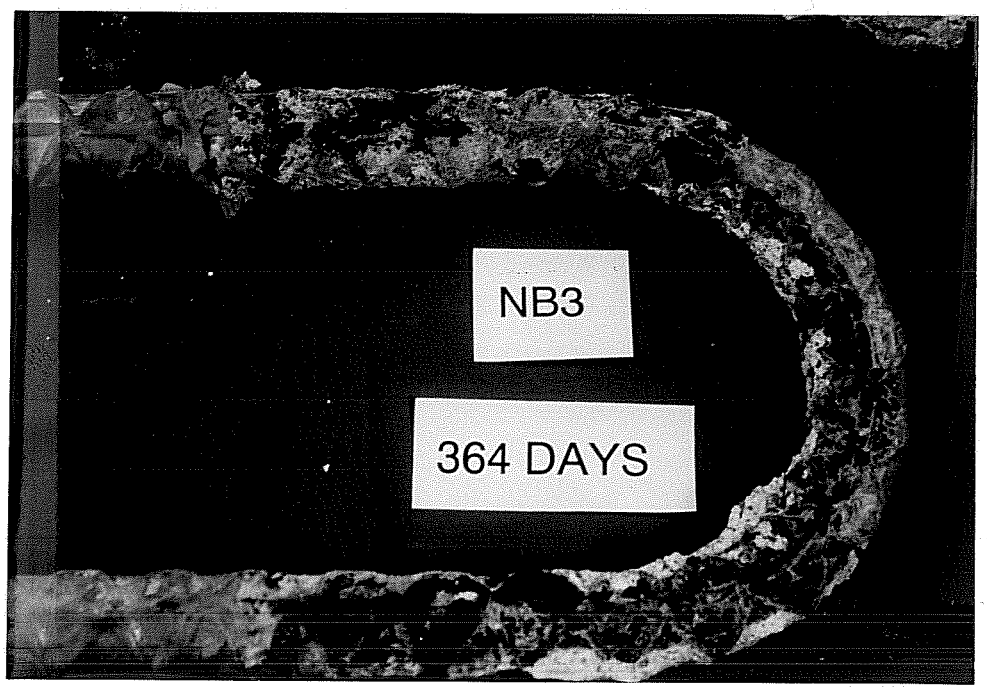

Figure 5- 21 Corrosion: Bottom surface of NB3

Figure 5- 22 Galvanized bar corrosion

bars. Severe, localized corrosion appeared in the vicinity of voids in the concrete. Figures 5.23 and 5.24 show all high ratio zinc silicate bars after 24 months of exposure.

In addition to the similarities with previously observed specimens, there were other corrosion trends for 24-month specimens: On 4 high ratio specimens, there was a pronounced tendency to corrode more on the underside of the anode bars than on the top surfaces. This includes all three specimens with uncoated cathodes (Fig. 5.23) and the specimen with non-repaired anode and coated cathode (NC bar in Fig. 5.24). Repaired specimens (wire-brushed and grit-blasted) with coated cathodes showed only slightly more corrosion on the underside of the anode bars than on the top sides (WC and SC bars in Fig. 5.24).

When corrosion on the bottom bar surfaces was much greater than that on the top bar surfaces, rust on the bottom surface was more evenly distributed around the bent and straight zones, while corrosion on the top surface was more localized on isolated spots on both straight and bent zones (Figure 5.23).

When corrosion on the bottom bar surfaces was only slightly greater than that on the top bar surfaces, corrosion on both top and bottom surfaces occurred in the form of isolated rust spots concentrated mainly on the straight zones close to the front concrete surface (WC and SC bars in Fig. 5.24).

After 24 months of exposure galvanized specimens showed the same trends as noted previously, but with increased corrosion deterioration. Concrete top surfaces had wide cracks along the rebar locations and showed extensive rust staining. Corrosion was uniform and widespread over the bar surface area. As with the high ratio bars, localized corrosion occurred in locations in direct contact with voids in the concrete. In contrast to high ratio bars, galvanized bars corroded more severely on the top surfaces of the bars than on their undersides.

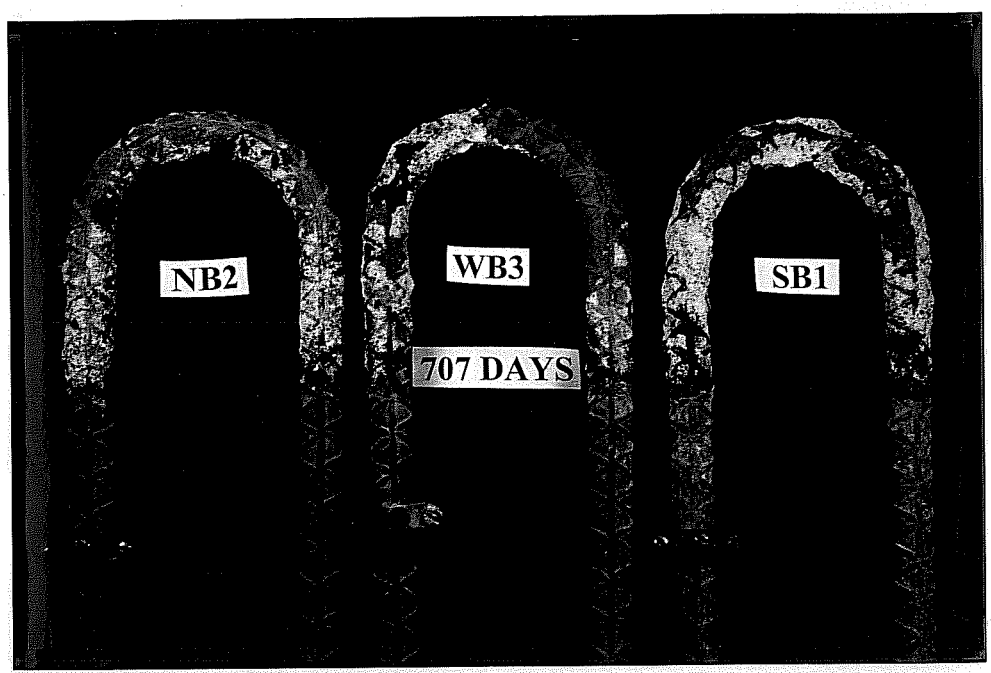

(a) Top surfaces

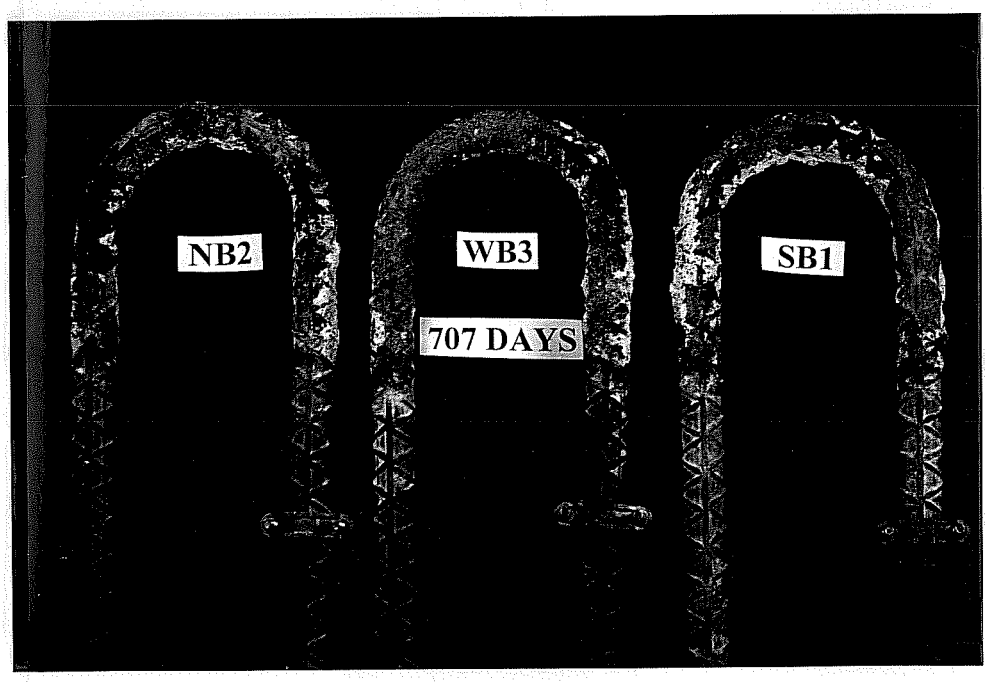

(b) Bottom surfaces

Figure 5- 23 Uncoated-cathode, high ratio zinc silicate bars after 707 days of exposure

5.4.2 Coating Adhesion to Concrete

7-Month Inspection

The high ratio zinc silicate coating was found to adhere slightly to the concrete in the macrocells. In all of the specimens opened, some of the coating was observed to stick to the surrounding concrete when the bars were removed. Figure 5.25 shows zinc silicate coating remaining on the concrete after the steel is removed from the macrocell. The coating tended to pull away from the bar, leaving a thin gray residue on the bar surface. More coating pulled away from the zinc silicate bars that had been repaired than from the bars that were left unrepaired. The repaired bars had a thicker coating, permitting more zinc silicate to adhere to the concrete.

The concrete-to-coating adhesion did not seem to be as strong as in the first generation of high ratio zinc silicate tested. Concrete adhesion seemed to be a critical factor in the failure of the earlier coating, and it was therefore a goal in the development of the second-generation zinc silicate to obtain a coating that

Figure 5- 25 Adhesion of high ratio zinc silicate coating to surrounding concrete

did not demonstrate such adhesion problems. Coating adhesion to concrete has not been eliminated in the current generation of coatings, but improved performance is evident. Figure 5.25, below, illustrates the coating adhesion to the concrete observed after 7 months of exposure.

In Figure 5.25, the concrete immediately adjacent to the high ratio zinc silicate coated bars was significantly darker than the surrounding material. A close examination of the concrete revealed a sponge-like texture and pin-hole sized voids along the concrete/steel interface. The change in color and the presence of voids suggests that chemical reactions between the coating and the moist concrete may have produced gas bubbles and discoloration.

13-Month Inspection

A particular point of interest in reference to coating adhesion was the question of behavior over time, i.e., whether the bond of the coating to the high ratio coated steel would change as a result of chemical reactions between the coating and concrete environment. No consistent pattern of changes in adhesion and coating delamination were observed. In one case, more of the coating adhered to the concrete after 13 months than after 7, while in another case, less adhesion was observed after 13 months. In other cases, no differences were observed. It was possible that differences in coating adhesion resulted from initial surface preparation and coating thickness, and were not induced by reaction with the concrete.

After thirteen months, the three methods of coating application seemed to produce different performance and loss of coating. More coating was found to pull away from the wire-brushed and recoated steel upon removal from the concrete than with the grit-blasted and repaired samples. The lowest loss of coating was observed with the unrepaired specimens.

Again, these differences were attributed to surface preparation between coats. The grit-blasted steel was given an ideal surface preparation, while the wire-brushed steel was not prepared as well prior to application of the repair coat. Poorer second coat adhesion probably caused more of the coating on the wire-brushed surface to pull away from the bars when removed from the concrete. Very little coating loss was observed with the unrepaired specimens because far less of the coating was left on the bars.

However, the different adhesion and pull-off characteristics did not appear to affect corrosion performance. Corrosion was not generally observed in areas where the coating pulled away from the steel. Also, the wire-brushed specimens showed somewhat less corrosion than the grit-blasted specimens, even though more coating was observed to pull away from the wire-brushed bars.

In all high ratio zinc silicate specimens, there were clean differences in adhesion between the top and bottom surfaces of the bars. The coating pulled away from the top surfaces of the steel more than from the bottom surfaces. The texture of the bottom surfaces was also crusty, with small fragments of concrete still attached to the coating, in contrast with the smoother texture of the top surfaces. Figures 5.26 and 5.27 illustrate these differences.

24-Month Inspection

At the time of examination after 24 months of exposure, concrete from most of previously opened specimens was not available. This made it difficult to obtain a complete figure of the behavior over time. Comparison of the two only available specimens (SB2 and SC2, both opened after 7 months) with their companion 24-month specimens seems to confirm that there were not consistent pattern of changes in coating adhesion to concrete over time. For SB specimens, on the one hand, more of the coating adhered to the concrete after 24 months than after 7 months. For SC specimens, on the other hand, more of the concrete adhered to the concrete after 7 months than after 24 months.

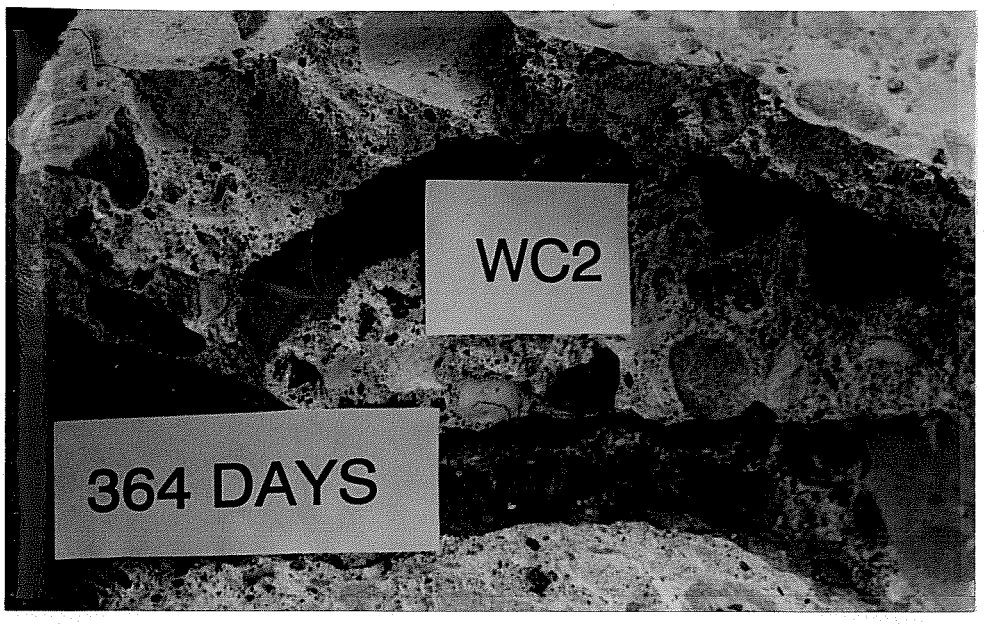

Figure 5- 26 Adhesion to top and bottom surfaces: zinc silicate

Figure 5- 27 Difference in texture — top and bottom surfaces

Comparing methods of coating application, more of the coating adhered to the concrete on the WC specimen than on the WB, SC, and SB specimens. It seems that slightly more coating adhered to concrete on the SC specimen than on the WB and SB specimens, but the difference is not appreciable. These findings partially support the previous notion that more coating pulls away from the wire-brushed bars than from grit-blasted bars. Like specimens inspected at 13 months, both NB and NC specimens showed almost no coating adhered to concrete after 24 months of exposure.

As was observed after 13-months, the differences in coating adhesion and pull-off characteristics of high ratio zinc bars did not appear to affect corrosion performance after 24 months. Areas where coating pulled away from the steel did exhibit corrosion. For instance, specimen WC, which showed the most coating adhesion to concrete, experienced the least corrosion. Adhesion of coating to the concrete was not felt to be a determining factor in corrosion behavior.

After 24 months, high ratio zinc bars also showed clear differences in coating adhesion between the top and bottom surfaces of the bars. More coating pulled away from the top surfaces of the bars than from the bottom surfaces. Likewise, the texture of the bar bottom surfaces was also crusty while the bar top surfaces showed a smoother texture. The differences in adhesion and texture may have been due to chemical reactions between the coating and the fresh concrete that produced small amounts of gas. The gas may have been trapped against the underside of the bars, resulting in tiny air pockets and weakening bond between the bar and the concrete. This phenomenon would explain the propensity for corrosion along the bottom surfaces of the steel, the lower adhesion, and the sponge-like texture of the concrete along the interface.

5.4.3 Comparison of Corrosion Behavior

7-Month Inspection

The most significant differences in the high ratio zinc silicate specimens were between the cells with coated and uncoated bottom steel. There was less corrosion on the specimens with zinc silicate-coated bottom steel than on the specimens with uncoated bottom steel. The charge flux data gave similar results. Figures 5.28 and 5.29, show the zinc silicate-coated steel with coated and uncoated cathodes examined in the 7-month Inspection.

Figures 5.28 and 5.29 show the high ratio bars, and further illustrates that after seven months of exposure, the state of the zinc silicate coating prior to concrete placement did not significantly affect corrosion performance. There were only small differences between the unrepaired bars and the bars that were recoated, or between the bars repaired by different techniques. The only significant differences resulted from coating the cathodes. Galvanic action did take place with the zinc silicate coatings. Without galvanic protection the more heavily damaged anodes would have shown more corrosion than the bars with repaired coatings.

It was also observed that the galvanized specimens showed significantly more corrosion than the corresponding high ratio zinc silicate specimens. This result was surprising, as the charge flux data indicated lower currents with the galvanized specimens than with any of the zinc silicate specimens with similar cathodes.

Figures 5.30 and 5.31 show the results with the galvanized and zinc silicate anodes. Corrosion of the galvanized bars was more widespread than on the bars coated with high ratio zinc silicate, and was located primarily around the bends, where the steel had yielded. Corrosion of the zinc silicate bars was

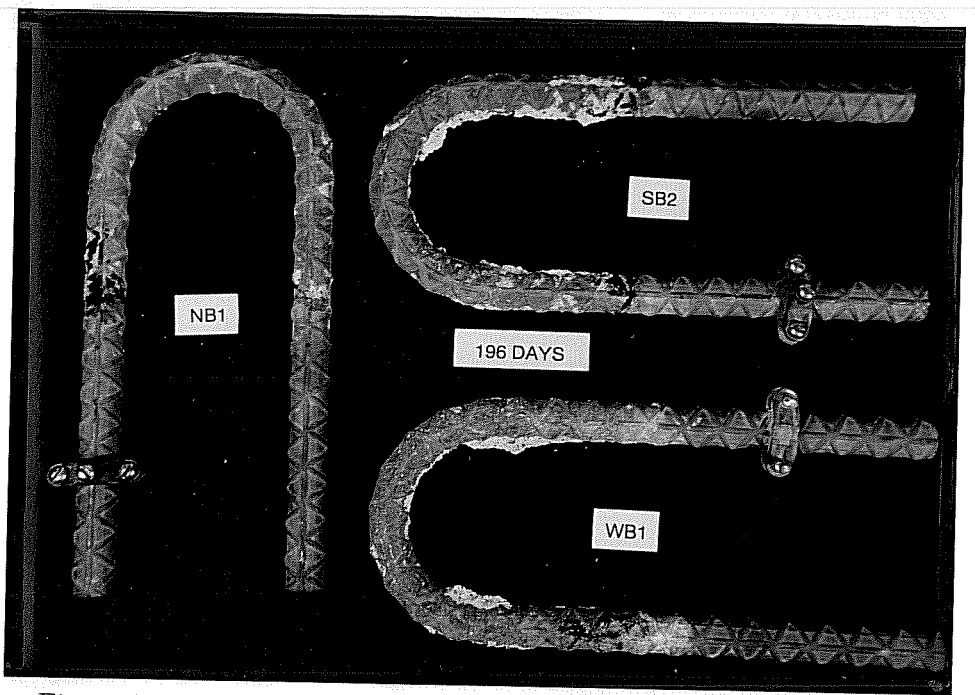

Figure 5- 28 High ratio zinc silicate anodes with uncoated bottom steel

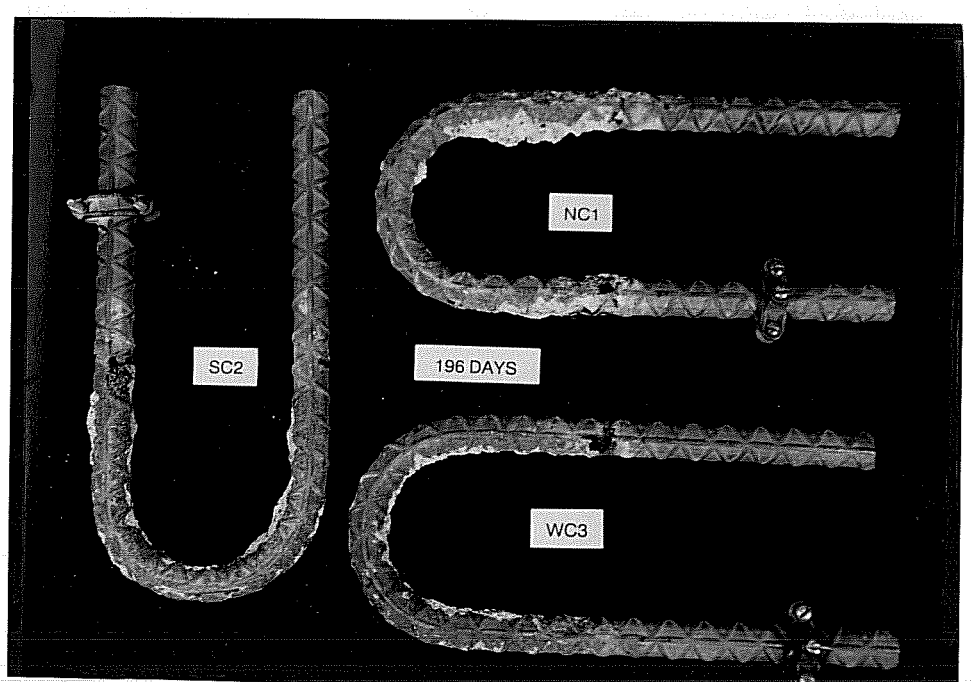

Figure 5- 29 High ratio zinc silicate anodes with coated bottom steel

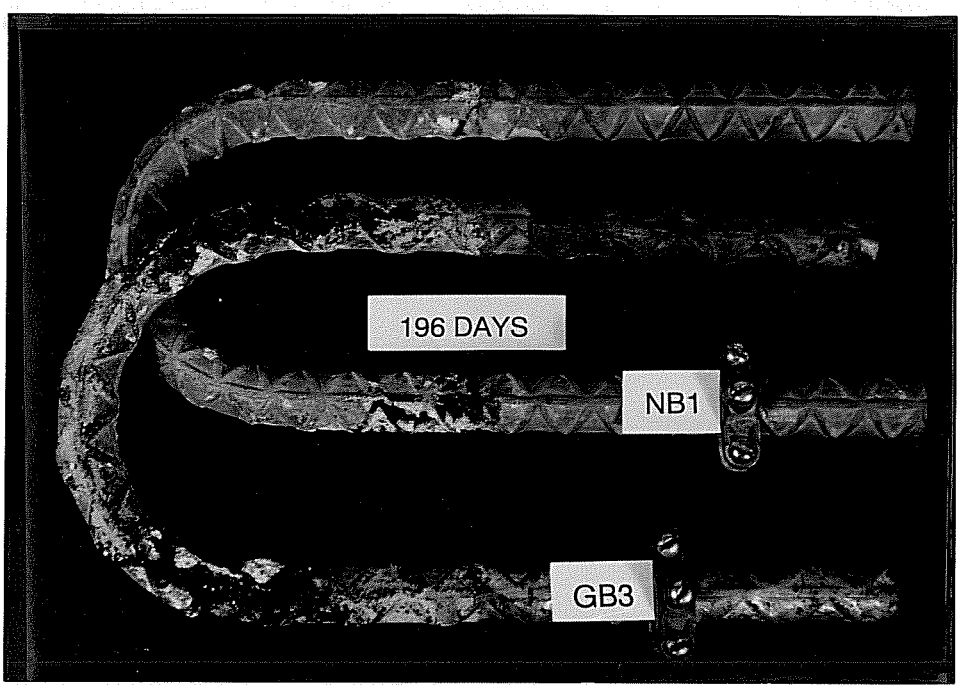

Figure 5- 30 Comparison between galvanized and zinc silicate anodes

Figure 5- 31 Galvanized and high ratio zinc silicate anodes

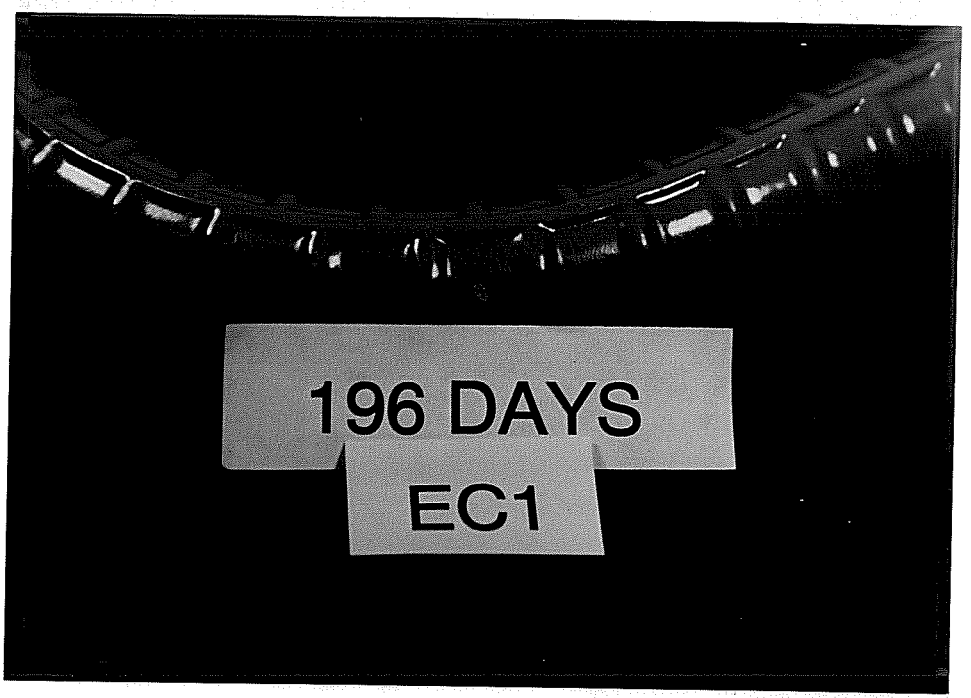

Figure 5- 32 Epoxy-coated anode

located on the bar legs, near the face of the macrocells. As mentioned, the galvanized specimens experienced primarily macrocell corrosion, while the zinc silicate specimens initially experienced microcell corrosion. Regardless of the mechanism, though, the galvanized specimens did not perform nearly as well as the zinc silicate specimens.

Figure 5.32 shows the epoxy-coated anode after removal from the macrocell. There was no visible corrosion on the bar, which appeared to be in pristine condition. The epoxy specimen demonstrated the least corrosion of all the specimens opened. This behavior was reflected accurately by the charge flux data.

13-Month Inspection

As observed in the specimens inspected at 7 months, the specimens with coated cathodes performed better than the specimens with uncoated cathodes. In each group of macrocells, less corrosion was observed in the cells with coated bottom steel. NB3, for example, corroded more than the corresponding coated-cathode sample, NC3. Figure 5.33 shows a comparison between NB3 and NC3.

The differences produced by using the coated cathodes were more pronounced after 13 months than after 7 months. The increasing disparity was caused by the fact that very little deterioration took place in the high ratio coated-cathode specimens between 7 and 13 months. The coatings were essentially in the same condition. In fact, the unrepaired group (NC) showed slightly less corrosion at 364 days than at 196 days. Figure 5.34, below, illustrates this observation.

In contrast, the uncoated-cathode, high ratio zinc silicate specimens deteriorated significantly between 7 and 13 months. Corrosion spread from the front-face regions to the bends in the steel. Severe localized corrosion was also observed at concrete voids, although some voids did not produce corrosion.

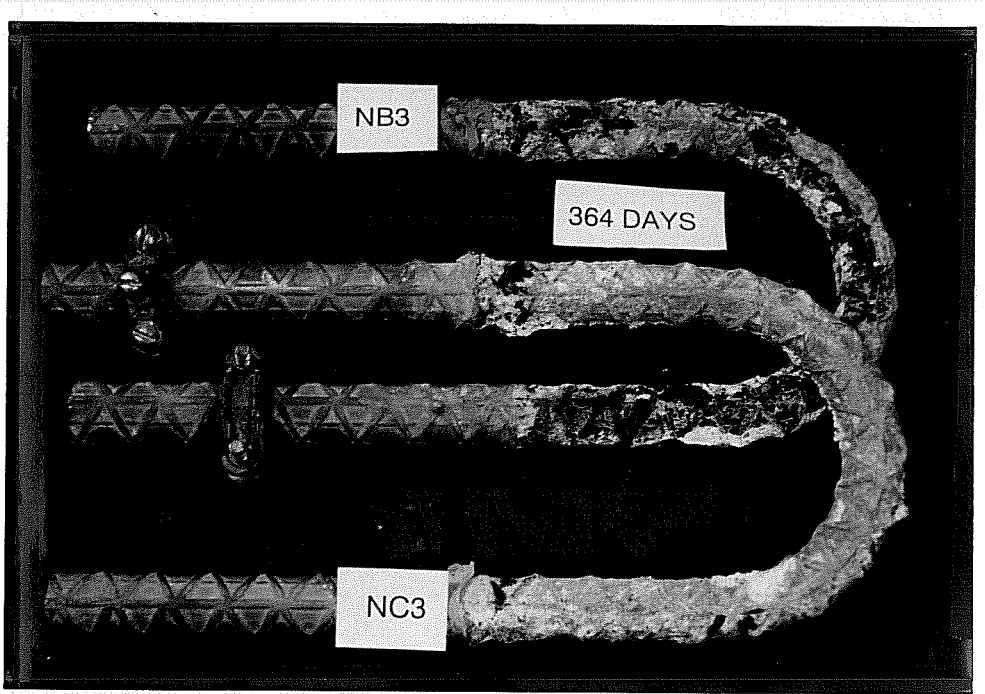

Figure 5- 33 Corrosion with coated and uncoated cathodes

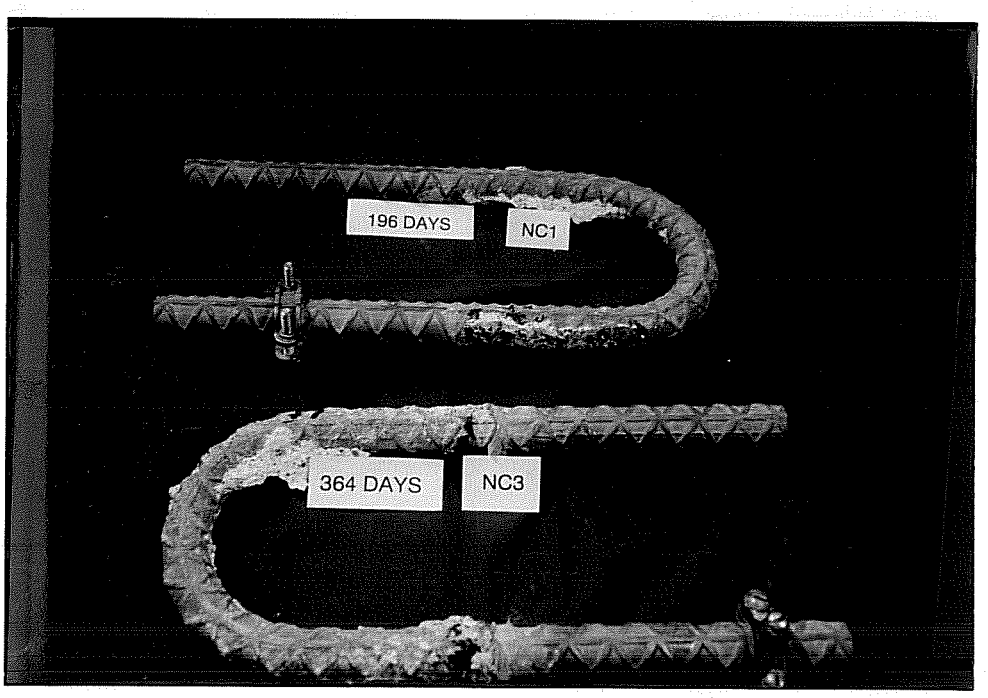

Figure 5- 34 Corrosion of unrepaired bars at 196 and 354 days

Coating damage impacted the corrosion performance of the high ratio samples with uncoated cathodes. While similar corrosion damage was found on samples SB3 and WB2, sample NB3 was corroded over a much larger area. Moderate corrosion was observed over a large portion of the underside of the bar. See Figure 5.21 for an illustration of corrosion to NB3.

Both galvanized specimens opened after 13 months demonstrated much more corrosion than any of the high ratio zinc silicate bars. These specimens were also much more corroded than the galvanized specimens opened after 7 months. Corrosion appeared to have accelerated during this time period.

The galvanized steel was corroded over much of the bar surface area, with noticeable area reduction. Severe attack was observed near the site of cracks in the concrete. Figure 5.35 shows the galvanized bars. The photograph was taken after the black and green corrosion products changed to rust color.

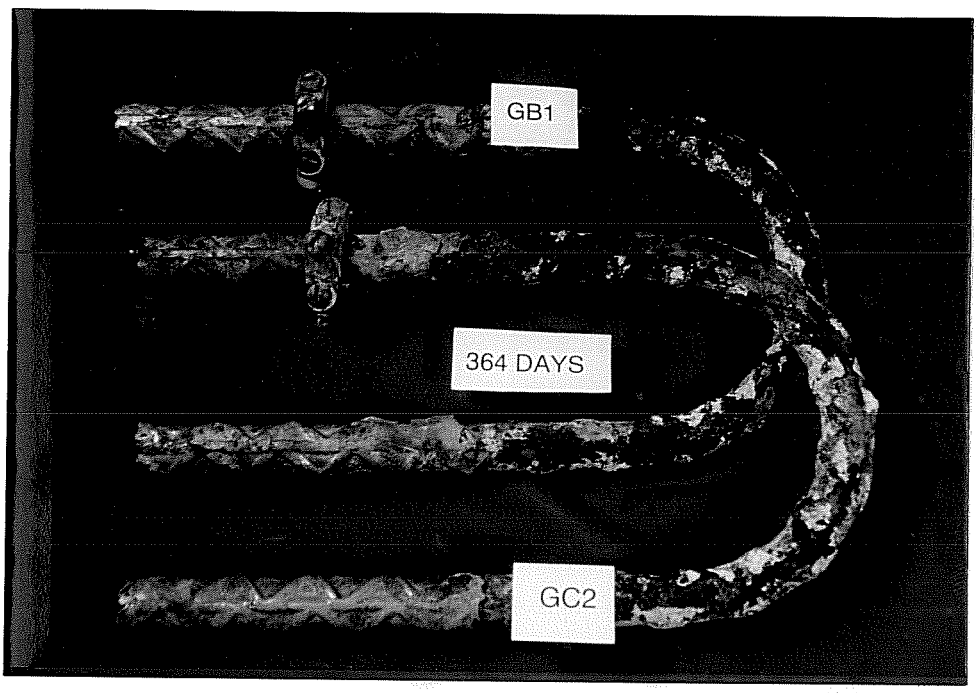

Figure 5- 35 Galvanized bars after 13 months of exposure

The epoxy-coated bar exhibited no corrosion after 13 months of exposure. The coating preserved its shiny and pristine condition. This behavior was in close agreement with corrosion current and charge flow charts.

24-Month Inspection

As was previously observed in the specimens opened at 7 and 13 months, specimens with coated cathodes consistently showed less corrosion damage than those having uncoated cathodes. This behavior was well reflected in the corrosion current and charge flow charts. Figure 5.36 illustrates the diffeence for specimens WB3 and WC1.

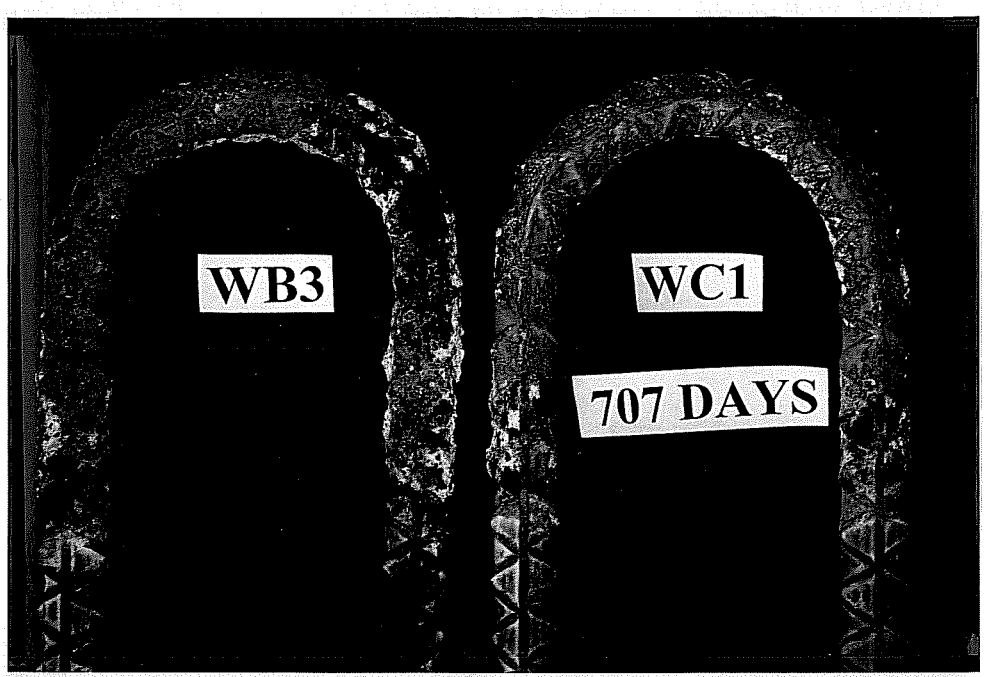

Figure 5- 36 Corrosion with uncoated and coated cathodes after 707 days

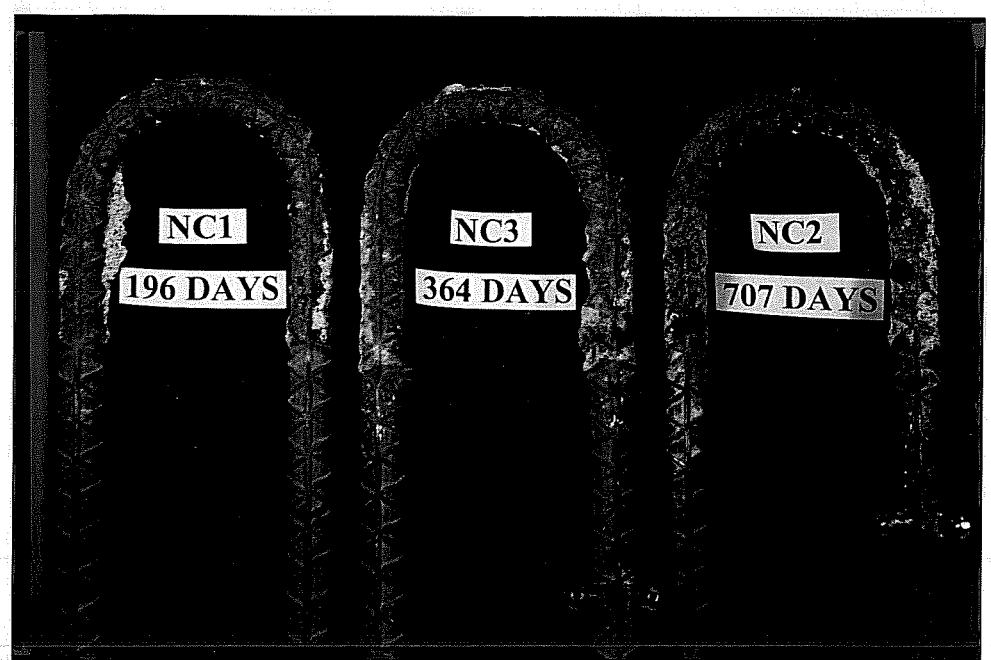

Figure 5- 37 Corrosion of unrepaired bars from specimens with coated cathodes at 196, 364, and 707 days

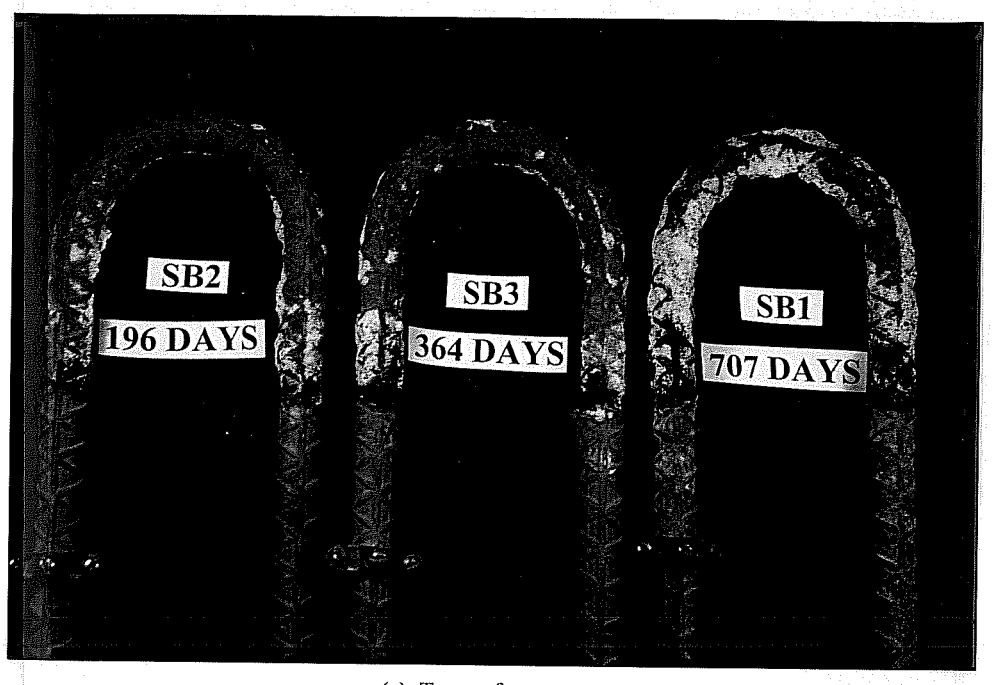

(a) Top surface

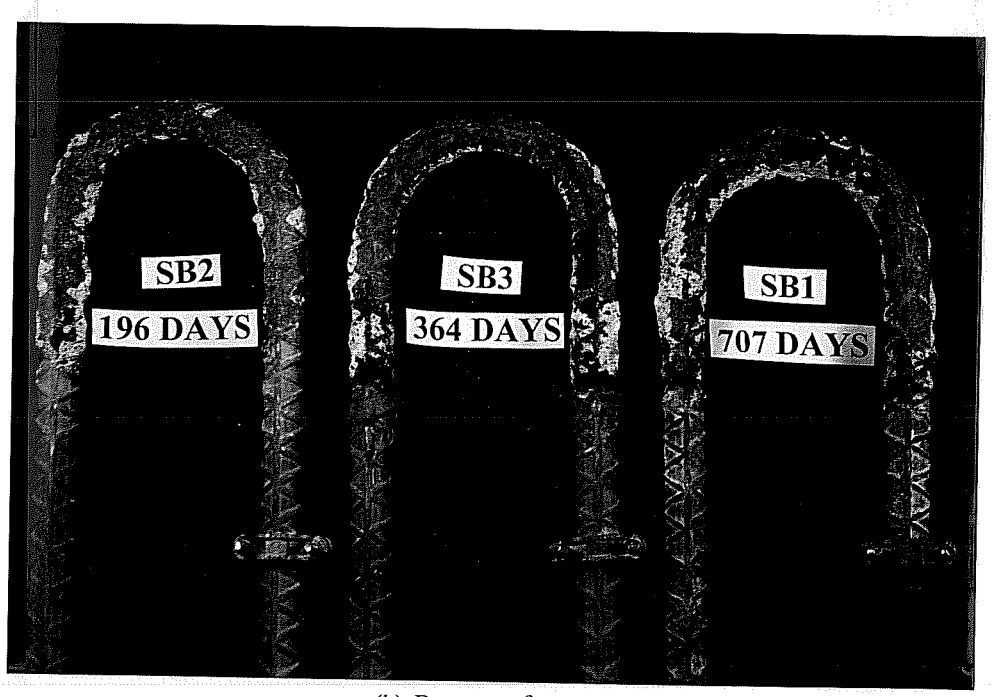

(b) Bottom surface

Figure 5- 38 Corrosion of grit-blasted and recoated bars from uncoated-cathode specimens after 196, 364 and 707 days

The differences produced by using coated cathodes were more pronounced after 24 months than after 13 and 7 months. The only exception was for non-repaired specimens, were such differences were more remarkable after 13 months than after 7 months, but less pronounced after 24 months than after 13 months. This was due to an increased deterioration in the high ratio coated cathode specimen between 13 and 24 months. Figure 5.37 illustrates this observation.

Coated-cathode high ratio specimens were able to maintain good protection throughout 24 months of severe exposure. Virtually all corrosion of these samples was restricted to the front-face regions, and was not severe. Protection was maintained around the bends and at voids in the concrete. The only exception was the non-repaired sample NC2, where corrosion on the bottom surface occurred on both straight and bent zones and was more evenly distributed, as can be seen in Fig. 5.24(b).

High ratio zinc specimens with uncoated cathodes further deteriorated between 13 and 24 months. Figures 5.38 and 5.39 show the corrosion progression with time of grit-blasted bars and wire brushed bars on their top and bottom surfaces. As shown in the figures, the increase in corrosion with time was more prominent on the bottom surfaces of the bars than on the top surfaces. It is possible that the higher conductivity of the uncoated cathodes and resulting higher rates of corrosion depleted the zinc in the high ratio coatings, decreasing their galvanic protection capability. It is also possible that chlorides penetrated to the depth of the bottom steel, forcing the top steel coatings to sacrifice for both mats of steel. Clearly, the uncoated-cathode specimens showed signs of increasing distress.

Up to 13 months, the corrosion performance of all the high ratio specimens using coated cathodes was fairly uniform. Consistent with the 7-month inspection, the wire-brushed specimen showed slightly less corrosion than both the grit-blasted specimen and the unrepaired specimen, but the differences were slight. After 24 months, however, corrosion performance among coated cathode specimens was less uniform and some differences started to occur. The non-repaired specimen started to corrode much more than both the wire-brushed and grit-blasted specimens [See Fig. 5.24(b)]. The grit-blasted specimen showed slightly more corrosion than the wire-brushed specimen, but in general, both specimens exhibited good surface condition after 24 months. Figure 5.24(b) illustrates the above observations. It may be concluded, therefore, that when repaired specimens with coated cathodes were used, the zinc silicate coatings functioned well for at least 24 months of exposure.

As for the 1-year specimens, coating damage influenced the corrosion performance of the high ratio zinc samples with uncoated cathodes after two years. However, corrosion kept progressing in repaired and recoated bars. Although the unrepaired sample still exhibited more corrosion than both the wire-brushed and grit-blasted samples, the repaired and recoated bars experienced more corrosion spread over a larger area as compared to one year of exposure, as can be seen on Fig. 5.23(b).

It is therefore evident that as the high ratio zinc silicate coatings were depleted sacrificially, damage levels to the coatings became significant for both coated and uncoated cathode specimens. Clearly, it is important to repair coating damage where possible.

Similar to 7 and 13-month specimens, galvanized bar specimens showed considerably more corrosion than all of the high ratio zinc silicate bars. Galvanized rebars corroded throughout their entire length. Attack was particularly severe at concrete crack locations on the bar top surfaces. Large volume accumulation of corrosion products was observed at such locations.

The galvanized specimen with coated cathodes demonstrated less corrosion than the specimen with uncoated cathodes, but the difference was less pronounced than with the high ratio specimens. The use of coated cathodes in the galvanized cells did not retard corrosion to the same extent.

This behavior suggests a synergistic interaction between steel with the same coating. The high ratio zinc silicate coating prevented corrosion most effectively when all of the steel was coated with the high ratio coating. It may therefore be concluded that the high ratio zinc silicate coating should be used on all steel to provide maximum corrosion protection.

As in the 7 and 13-month autopsies, the epoxy specimen showed no visible signs of corrosion after 24 months of exposure. The epoxy coating consistently provided the best corrosion protection to the reinforcing steel out of the coatings investigated in this study. It must be underscored, however, that the epoxy was completely undamaged prior to concrete placement. Epoxy coatings provide exceptional protection when the coatings are free from defects. It may be difficult to achieve this standard in practice.

5.4.4 Reliability of Damage Predictions

A comparison was made between the corrosion damage predicted by total charge flux and the actual damage as observed visually after 24 months. For the visual inspection, a ranking of 10 was awarded to the most heavily damaged bar, and a ranking of 1 was awarded to the bar with the least observed corrosion. The remaining bars were ranked in order of relative damage. Damage was assessed according to corroded surface area and depth of penetration.

In terms of charge flux, a value of 10 was awarded to the specimen with the highest flux, and a 1 was awarded to the bar with the lowest flux. Liner interpolation between these two extremes was used to assign rankings to the remaining bars.

The results of the damage rankings are presented below, in Table 5.2.

Observed damage to high ratio zinc silicate coating specimens after 24 months of exposure did not always correlate with charge flux data. In both coated and uncoated cathode groups, grist-blasted specimens were expected to corrode the most based on charge flux readings. However, visual

Table 5- 2 Predicted and observed damage rankings for zinc-silicate coated bars

MACROCELL	RATING BASED ON OBSERVED DAMAGE [10=WORST; 1=BEST]	RATING BASED ON CHARGE FLUX [10=WORST; 1=BEST]
WC1	1	1
NC2	2.4	1.1
SC3	1.2	1.6
WB3	3.2	2.9
NB2	4.0	3.1
SB1	3.0	3.3

examination revealed that grit-blasted specimens experienced less corrosion damage than unrepaired specimens and their damage was comparable to that of wire-brushed specimens. Charge flux readings successfully predicted that uncoated cathode specimens would experience more corrosion deterioration than coated cathode specimens. Likewise, charge flux data accurately predicted that the epoxy coated specimens would experience very little or no corrosion damage. For galvanized bars, charge flux readings completely failed to predict damage (Not shown on Table 5.2)

It may be concluded that corrosion potentials and charge flux calculations will approximate the relative performance of high ratio zinc silicate coatings in a macrocell model. Charge flux clearly illustrated the benefits of coating the bottom steel.

5.5 CORROSION PRODUCTS

The most prominent corrosion products visible on the zinc silicate samples were black. Small areas of dark green and rust-color were also observed. Upon exposure to the atmosphere, the black and dark green substances changed to rust-color within minutes. The fact that all of the products changed to rust-color indicates that iron was the primary material in the corrosion product.

Other research has found zinc to produce zinc oxide (no), zinc hydroxychloride ($ZnCl_2*4Zn(OH)_2$), and zinc hydroxychloride II ($Zn_5(OH)_8*H_2O$) during corrosion. [13] Zinc oxide is white in color and could have been mistaken for fragments of concrete in the Inspection. Neither zinc hydroxychloride nor zinc hydroxychloride II were observed on the steel bars.

The black corrosion products were expected to be black magnetite (Fe_3O_4). Black magnetite is known to react with oxygen to form red brown iron (III) oxide, $2Fe_2O_3*H_2O$, accounting for the observed transformation to rust-color.

The dark green products appeared to be a complex chloride compound. Other researchers have observed dark green products to form during the chloride corrosion of steel in concrete, changing to rust-color upon exposure to the atmosphere. [1] These phenomena correspond well with the behavior observed during inspection.

5.6 CHLORIDE DATA

5.6.1 Inspection Results

The chloride concentrations at a depth of 1-2 inches were measured prior to inspection for each macrocell opened. The results are given in Figures 5.40

Examination of the figures yields several observations. For each inspection, the chloride concentrations measured at the depth of the top reinforcing steel were fairly consistent. The readings taken after 196 days gave a mean value of 0.17% and a standard deviation that was 17.2% of the mean. The 364-day readings gave a mean value of 0.20% and a standard deviation of 21.7% of the mean. Readings after 707 days showed a mean value of 0.38% and a standard deviation of 9.9% of the mean (specimen NC2 was excluded from mean calculation because of suspect test result).

The scatter observed was probably due, for the most part, to lack of homogeneity in the concrete. In addition, the depth range sampled was larger than recommended. The scatter would also be reduced if more samples had been taken from each specimen.

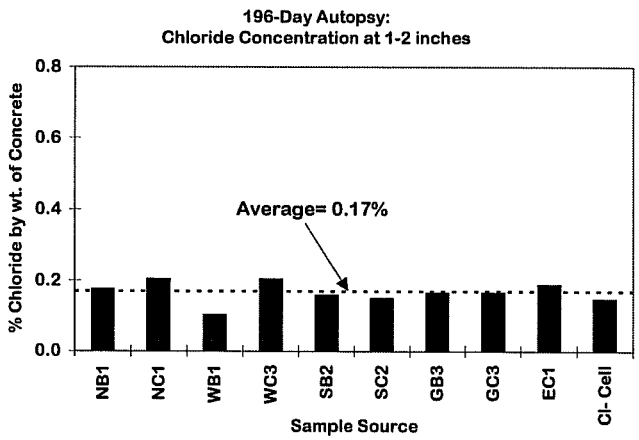

(a) After 196 days of exposure

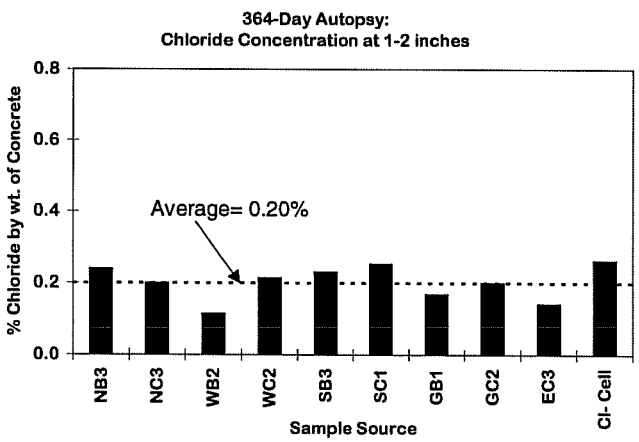

(b) After 364 days of exposure

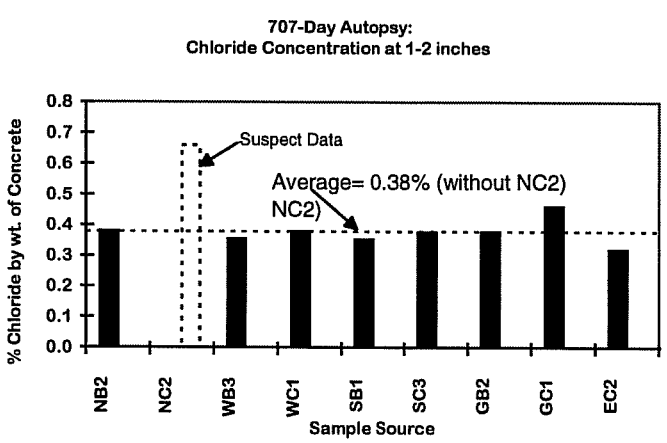

(c) After 707 days of exposure

Figure 5- 40 Chloride concentrations

Based on these results, the chloride measurements provided a good indication of chloride levels in the concrete. However, chloride levels can not be used to predict levels of corrosion, particularly when corrosion protection systems are employed. No correlation was found between measured chloride concentration and the differences in corrosion performance of the specimens.

Average chloride concentrations at the depth of the top steel between 196 and 364 days of exposure increased from 0.17% to 0.20%. Exposure conditions remained largely the same during that period.; however, between 364 and 707 days of exposure, the mean chloride concentration increased significantly from 0.20% to 0.38%.

Post-mortem examination after 707 days of exposure revealed that although most of the specimens continued to experience corrosion progression, the overall condition of those specimens had not significantly changed as might have been expected for the high chloride concentrations measured. Only the non-repaired specimen with coated cathode showed a sudden increase in the corrosion rate after 2 years. It is noteworthy that repaired and recoated specimens with coated cathodes remained in very good condition despite the severity of the exposure during the second year.

5.6.2 Changes in Chloride Concentration Over Time

Figure 5.41 shows the chloride concentration measured at a depth of 1.375 inches from the exposed face of the chloride cells as a function of time. Such depth is about equal to that of the top anode rebars in the macrocells.

The following graph shows a steady increase in chloride levels in the first year of exposure. However, from 364 to 500 days there was a sharp increase in the chloride concentration (from 0.17% to 0.39% by weight of concrete). After 500 days, chloride levels showed a more erratic trend but seemed to keep

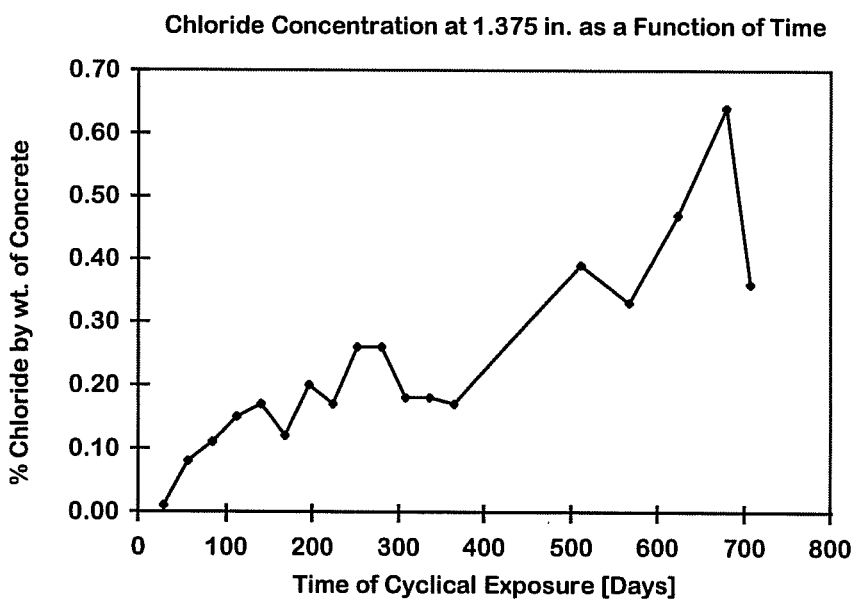

Figure 5- 41 Chloride concentrations at the level of the top steel over the life of the experiment

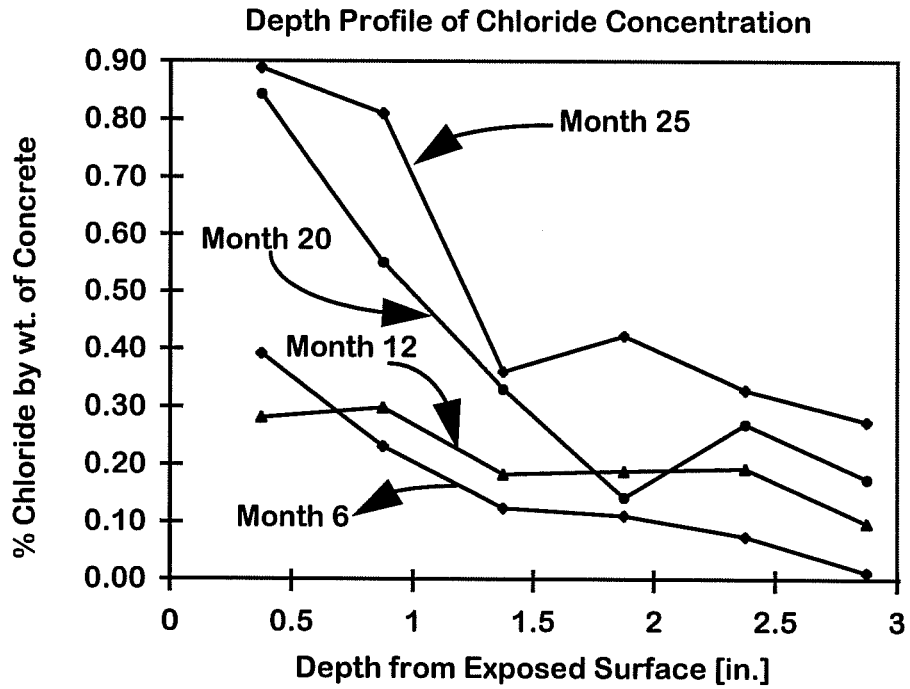

Figure 5- 42 Chloride depth profiles showing chloride diffusion over time

increasing. Disregarding the highest peak value at 680 days, the average chloride level for the second year was 0.39% by weight of concrete.

Chloride concentrations at the level of the top steel reached 0.08% after two exposure cycles. Chloride concentration guidelines suggest that corrosion initiates at chloride concentrations of approximately 0.05% by weight of concrete. [22] The exposure conditions were therefore severe over virtually the entire life of the experiment.

Chloride concentration depth profiles obtained from the chloride samples at 6, 12, 20, and 25 months have been plotted on the same scale in Figure 5.42. Up to the first year of exposure, the graphs show a maximum chloride concentration of approximately 0.40% by weight of concrete. This maximum was reached at a depth of 0.375 inches. For the second year of exposure, chloride levels were as high as 0.80% to 0.90% by weight of concrete at a depth of 0.375 inches. It can be observed that the chloride profiles for the second year exhibited steep gradients and chloride concentration sharply decreased with depth. However, the lowest chloride-content levels at deeper layers were of the same order as the highest chloride levels at shallow depths for the first year of exposure.

CHAPTER 6

SUMMARY AND CONCLUSIONS

6.1 SUMMARY

Corrosion current data and visual inspection produced the following results:

1. The macrocells with coated bottom steel experienced less corrosion activity than the cells with uncoated bottom steel. This was found to be true with both the high ratio zinc silicate and the galvanized specimens.

2. The high ratio zinc silicate specimens with coated bottom steel demonstrated only small levels of corrosion after 13 months, with minimal increases in visible corrosion damage between 7 and 13 months. Coating damage and repair techniques did not seem to affect observed corrosion performance. However, corrosion significantly increased between 13 and 24 months for the unrepaired bars while repaired-recoated bars remained in good condition.

3. The high ratio zinc silicate specimens with uncoated bottom steel showed light corrosion damage after 7 months, but deteriorated considerably between 7 and 13 months, and between 13 and 24 months. Coating damage was found to affect corrosion performance, with more corrosion occurring on the unrepaired bars.

4. The wire-brushed and repaired zinc silicate bars produced slightly lower corrosion currents than the grit-blasted and repaired bars. Corrosion damage on both wire-brushed and grit-blasted bars was similar.

5. The second-generation high ratio zinc silicate coating was found to have different concrete adhesion characteristics than the first-generation that was tested in a similar fashion earlier. Although some adhesion and pull-off was observed with the second-generation, debonding was less severe and more localized than with the first-generation. Also, corrosion did not tend to occur in areas where the coating pulled away from the steel.

6. In the high ratio zinc silicate samples, a better bond to the concrete was observed along the top surfaces of the bars than along the bottom surfaces.

7. Corrosion on high-ratio zinc silicate bars was almost always more severe on the bottom surface than on the top. The differences were likely due to the availability of oxygen and chlorides at air pockets and voids which were more prominent on the underside of the bars.

8. Corrosion current data erroneously predicted more corrosion damage in the high ratio zinc silicate specimens than in the galvanized specimens. It was found in the 7, 13 and 24-month autopsies that the galvanized top bars corroded significantly more than the high ratio zinc silicate top bars.

9. The epoxy bars experienced no visible corrosion after 24 months of exposure.

10. Chloride concentration data revealed that severe conditions were present during the first year and even more severe during the second year of testing. Chloride levels at the depth of the top steel were high enough to promote corrosion after only 2 months of exposure.

6.2 CONCLUSIONS

The test results allowed the following conclusions to be made:

1. The high ratio zinc silicate coating examined in this round of tests demonstrated superior corrosion performance to the high ratio zinc silicate formulation studied earlier. Less corrosion was observed on the steel protected with the new coating after 7 months of exposure, and corrosion damage was more localized. The new coating gave evidence of galvanic protection, preventing corrosion in areas of damage while zinc remained in the coating. The first generation coating did not appear to provide sacrificial protection.

2. The high ratio zinc silicate coating outperformed the galvanized coating investigated in these tests. All inspections revealed more corrosion on the galvanized bars than on the corresponding high ratio bars. However, the condition of the galvanized bars prior to casting was poor, and may not have represented a state-of-the-art galvanized coating.

3. The epoxy coating provided the most effective corrosion protection of the coatings investigated. The epoxy coating was undamaged prior to casting. More corrosion might have occurred on the epoxy bars if the coating had been damaged and the cathode not coated, given the passive nature of epoxy coatings.

4. Coating adhesion/bonding to the concrete was not a dominant factor in the corrosion performance of the high ratio zinc silicate coating. No correlation was observed between areas where large amounts of the coating were removed from the steel when the concrete was demolished for inspection, and areas of corrosion damage.

5. Corrosion was concentrated in areas rich in oxygen near the surface where the bars protruded from the concrete and at voids that formed around the bar during concrete placement. As corrosion progressed and the zinc in the coating became depleted, corrosion activity spread to locations of coating damage.

6. Corrosion performance was dramatically improved by coating the cathode steel, in addition to the anode steel, with the high ratio zinc silicate. The high ratio zinc silicate coating provided good corrosion protection to the steel embedded in concrete when all the steel was coated in this fashion.

7. Repairing coating damage improved corrosion performance, especially after long periods of exposure.

8. Optimum protection was achieved by coating all layers of reinforcement and repairing damage to coating before concrete was placed.

BIBLIOGRAPHY

1. "ACI Forum: Influence of Cholorides in Reinforced Concrete," Corrosion, Concrete, and Chlorides: Steel Corrosion in Concrete: Causes and Restraints. Detroit: American Concrete Institute, 1987.

2. Baker, E., Money, K., Sanborn, C. "Marine Corrosion Behavior of Bare and Metallic-Coated Steel Reinforcing Rods in Concrete," Chloride Corrosion of Steel in Concrete. Philadelphia: American Society for Testing and Materials, 1977.

3. Cady, P. "Corrosion of Reinforcing Steel in Concrete - A General Overview of the Problem," Chloride Corrosion of Steel in Concrete. Philadelphia: American Society for Testing and Materials, 1977.

4. Cook, A., Radtke, S. "Recent Research on Galvanized Steel for Reinforcement of Concrete," Chloride Corrosion of Steel in Concrete. Philadelphia: American Society for Testing and Materials, 1977.

5. Cook, H., McCoy, W. "Influence of Chloride in Reinforced Concrete," Chloride Corrosion of Steel in Concrete. Philadelphia: American Society for Testing and Materials, 1977.

6. Cornet, I., Bresler, B. "Corrosion of Steel and Galvanized Steel in Concrete," Materials Protection, April, 1966.

7. Delahunt, J., Nakachi, N. "Long Term Economic Protection with One-Coat of Inorganic Zinc-Rich," Journal of Protective Coatings and Linings, Vol. 6, no. 2, February, 1989.

8. Erlin, B., Hime, W. "Chloride-Induced Corrosion," Corrosion, Concrete, and Chlorides: Steel Corrosion in Concrete: Causes and Restraints. Detroit: American Concrete Institute, 1987.

9. Erlin, B., Hime, W. "Some Chemical and Physical Aspects of Phenomena Associated with Chloride-Induced Corrosion" Corrosion, Concrete, and Chlorides: Steel Corrosion in Concrete: Causes and Restraints. Detroit: American Concrete Institute, 1987.

10. Fontana, M. G. Corrosion Engineering. USA: McGraw Hill, Inc., 1986.

11. Fraczek, J. "A Review of Electrochemical Principles as Applied to Corrosion of Steel in a Concrete or Grout Environment," Corrosion, Concrete, and Chlorides: Steel Corrosion in Concrete: Causes and Restraints. Detroit: American Concrete Institute, 1987.

12. Frosch, R. "Performance of Reinforcing Steel Coated with a High Ratio Zinc Silicate," Master's Thesis. Austin: University of Texas at Austin, 1992.

13. Hime, W., Machin, M. "Performance Variances of Galvanized Steel in Mortar and Concrete," Corrosion Engineering, Vol. 49, No. 10, 1993.

14. Holm, J. "Comparison of the Corrosion Potential of Calcium Chloride and a Calcium Nitrate Based Non-Chloride Accelerator - A Macrocell Approach," Corrosion, Concrete, and Chlorides: Steel Corrosion in Concrete: Causes and Restraints. Detroit: American Concrete Institute, 1987.

15. Lehmann, J. "Cathodic Protection (Corrosion Control) of Reinforced Concrete Structures Using Conductive Coatings," Corrosion, Concrete, and Chlorides: Steel Corrosion in Concrete: Causes and Restraints. Detroit: American Concrete Institute, 1987.

16. McGlothlin, Q., Curtis, E., Cox, J. "Self-Curing Inorganic Zinc Coatings," Materials Protection, February, 1966.

17. Mehta, P. "Effect of Cement Composition on Corrosion of Reinforcing Steel in Concrete," Chloride Corrosion of Steel in Concrete. Philadelphia: American Society for Testing and Materials, 1977.

18. Munger, C. G. "Inorganic Zinc Coatings: A Review," Journal of Protective Coatings and Linings, June, 1987.

19. Munger, C. G. "VOC-Compliant Inorganic Zinc Coatings," Materials Protection, October, 1990.

20. Munger, C. G. Corrosion Prevention by Protective Coatings. Houston: National Association of Corrosion Engineers, 1984.

21. Munger, C. G. "Surfaces, Adhesion, Coatings," Anaheim, CA: National Association of Corrosion Engineers, Presented During *Corrosion/83*, 1983.

22. Peterson, C. G. "RCT Profile Grinding Kit for In-Situ Evaluation of the Chloride Diffusion Coefficient and the Remaining Service Life of a Reinforced Concrete Structure," Sweden: Presented at the *Chloride Ingress in Concrete Structures Symposium*, January, 1993.

23. Sanjurjo, S., Hettiarachchi, K., Wood, B., Cox, P. "Development of Metallic Coatings for Corrosion Protection of Steel Rebars," Washington: Strategic Highway Research Program, 1993.

24. Szokolik, A. "Evaluating Single-Coat, Inorganic Zinc Silicates for Oil and Gas Production Facilities in Marine Environments," Journal of Protective Coatings and Linings, March 1992.

25. Waldrip, H. "Testing Zinc-Rich Coatings for Protecting Steel," Materials Protection, May, 1966.

26. Weyers, R. and Cady, P. "Deterioration of Concrete Bridge Decks from Corrosion of Reinforcing Steel," Concrete International, Vol. 9, No. 1, January, 1987.

27. Yeomans, S., "A Conceptual Model for the Corrosion of Galvanized Steel Reinforcement in Concrete," Unofficial report released by the University College, University of New South Wales, Australia, 1993.